ISSN 1881-7831 Online ISSN 1881-784X

DD&T

Drug Discoveries & Therapeutics

Volume 12, Number 1
February, 2018

IRCA BSSA

IACMHR

www.ddtjournal.com

DD&T
Drug Discoveries & Therapeutics

ISSN: 1881-7831
Online ISSN: 1881-784X
CODEN: DDTRBX
Issues/Year: 6
Language: English
Publisher: IACMHR Co., Ltd.

Drug Discoveries & Therapeutics is one of a series of peer-reviewed journals of the International Research and Cooperation Association for Bio & Socio-Sciences Advancement (IRCA-BSSA) Group and is published bimonthly by the International Advancement Center for Medicine & Health Research Co., Ltd. (IACMHR Co., Ltd.) and supported by the IRCA-BSSA and Shandong University China-Japan Cooperation Center for Drug Discovery & Screening (SDU-DDSC).

Drug Discoveries & Therapeutics publishes contributions in all fields of pharmaceutical and therapeutic research such as medicinal chemistry, pharmacology, pharmaceutical analysis, pharmaceutics, pharmaceutical administration, and experimental and clinical studies of effects, mechanisms, or uses of various treatments. Studies in drug-related fields such as biology, biochemistry, physiology, microbiology, and immunology are also within the scope of this journal.

Drug Discoveries & Therapeutics publishes Original Articles, Brief Reports, Reviews, Policy Forum articles, Case Reports, News, and Letters on all aspects of the field of pharmaceutical research. All contributions should seek to promote international collaboration in pharmaceutical science.

Editorial Board

Editorial and Head Office:

Pearl City Koishikawa 603,
2-4-5 Kasuga, Bunkyo-ku,
Tokyo 112-0003, Japan
Tel.: +81-3-5840-9697
Fax: +81-3-5840-9698
E-mail: office@ddtjournal.com

Drug Discoveries & Therapeutics

Editorial and Head Office

Pearl City Koishikawa 603, 2-4-5 Kasuga, Bunkyo-ku,
Tokyo 112-0003, Japan

Tel: +81-3-5840-9697, Fax: +81-3-5840-9698
E-mail: office@ddtjournal.com
URL: www.ddtjournal.com

Editorial Board Members

CONTENTS

Volume 12, Number 1, 2018

Review

Original Article

Brief Report

CONTENTS (*Continued*)

Case Report

Guide for Authors

Copyright

Review

DOI: 10.5582/ddt.2017.01064

China's achievements and challenges in improving health insurance coverage

Cuirong Zhao[1], Chao Wang[2], Chengwu Shen[1], Qian Wang[1,*]

[1] *Department of Pharmacy, Shandong Provincial Hospital affiliated to Shandong University, Ji'nan, China;*
[2] *Department of Rehabilitation medicine, Shandong Provincial Hospital affiliated to Shandong University, Ji'nan, China.*

Summary **China has undertaken waves of healthcare reforms to keep pace with its rapid economic growth. By 2011, universal health insurance coverage was successfully achieved through the creation of a basic social medical insurance system. Growing economic power, extensive government subsidies, and strategies for program implementation are critical to that achievement. However, the breadth and depth of coverage varies considerably across insurance schemes and localities. The disjointed insurance scheme led to inequality in coverage, accessibility, and affordability of medical services, lopsided allocation of health resources, and increasing medical expenditures, and these remain crucial challenges for healthcare insurance coverage. This paper describes societal conditions, polices, achievements and challenges in improving health insurance coverage in China. Thailand's experience in universal health insurance coverage and its implications for China's new medical reform are also discussed. Solutions including sustainable increases in government investment, transformation of payment methods, reinforcement of primary health care delivery and the referral system, and standardization of benefits packages are strongly recommended to address challenges in China's long-running medical reform.**

Keywords: Health insurance, universal coverage, healthcare reform, China

1. Introduction

China has made remarkable advances in economic growth during the past several decades. However, the health care system in China has not kept pace with economic growth (*1,2*). Many residents still have difficulty obtaining access to healthcare when ill. Health insurance coverage for the population declined and has remained very low for a number of years (*3*). The outbreak of severe acute respiratory syndrome (SARS) in 2003 sounded a wake-up call for Chinese leaders who had failed to pay close attention to the public's concerns (*4,5*). In 2007, China's health system was ranked 144th in terms of quality and access out of 190 countries by the World Health Organization (WHO), far below poorer countries like Haiti (*6*). The enormous discrepancy between health system development and economic advancement motivated the Chinese government to implement a system-wide Healthcare Reform Plan (*3*). The central government of China has started to focus more on the reform of health insurance to sustain economic development and is committed to providing universal health insurance coverage to 1.3 billion people (*4*). Although China faced great challenges in making health insurance more accessible and affordable, marked changes have been made in China's health system over the past three decades (*4,7*).

2. China's achievement of universal health insurance coverage

2.1. *Societal conditions for improving health insurance coverage*

In the early decades after the founding of the People's Republic of China, China's health insurance system was revered by other countries because of its extensive coverage (*8*). In urban areas of China, the Labor

**Address correspondence to:*
Dr. Qian Wang, Department of Pharmacy, Shandong Provincial Hospital affiliated with Shandong University, No. 324, Jing Wu Road, Jinan, 250021, China.
E-mail: wangqian.9186@163.com

Table 1. Summary of China's three public insurance schemes in 2011 (*4*).

Items	UEBMI	URBMI	NRCMS
Year initiated	1998	2007	2003
Individuals covered	Urban employees	Urban unemployed, elderly, children, students, and disabled	Rural residents
Nature of employment	Mandatory	Voluntary	Voluntary
Unit of enrollment	Individuals	Individuals	Households
Risk-pooling unit	City	City	Country
Enrollment rate (%)	92	93	97
Number of enrollees (million)	252	221	832
Premium per person per year (US$)	240	21	24
Including government subsidy (US$)	0	18	18
Benefit coverage			
Inpatient reimbursement rate (%)	68	48	44
% of counties or cities covering general outpatient care	100	58	79
Predominant payment method	FFS	FFS	FFS

Insurance Scheme for employers was started in 1951 as an employment-based health insurance scheme (*4*). In 1952, a public insurance scheme called the Government Insurance System was launched for government employees, their dependents, and college students (4). Almost all urban residents were covered by health insurance plans until the late 1970s (*9*). In rural areas of China, the Cooperative Medical Scheme was launched in the late 1950s (*4*). Each rural commune organized its own commune-based medical scheme and provided medical services to its members and their families with minimum charges (*8*). Approximately 90 percent of rural residents were insured through the scheme in the mid-70s, representing the vast majority of the rural population (*8,10*).

However, the aforementioned health insurance schemes disappeared, and insurance coverage surprisingly decreased as economic reforms were initiated in 1978 (*3*). In the countryside, the collective farming mechanisms were replaced by a new "household responsibility system", leading to the collapse of the commune-based Cooperative Medical Scheme (*11*). Consequently, rural residents had no health insurance and paid all medical expenses themselves, resulting in a high risk of suffering illness-induced poverty (*12*). A study reported that health insurance coverage for the rural population declined to 12% in 1993 and to 9% in 1998 (*13*). Similarly, in urban area, health insurance schemes for employees also gradually disappeared due to rising health care costs and inefficiency of state-owned enterprises (*4,14*). Privatization efforts in the public health care sector led to overuse and decreased the quality and affordability of health care (*3*). Moreover, market-oriented economic reforms and privatization caused millions of employees to lose their jobs, as well as their health insurance coverage, in the 1990s (*15*). Insurance coverage for urban residents decreased to 53% in 1993 and to 42% in 1998 (*13,14*).

A point worth noting is that these data indicate that inequities in health care between urban and rural areas grew as insurance coverage decreased. The inequities were exacerbated by the increased income gap between rural and urban areas (*16*). People in rural areas had less ability to pay and a higher likelihood of having limited access to health care due to financial reasons than urban residents. Deteriorating insurance coverage and the rapid increase in health care costs led to health care affordability becoming a leading public concern (*17*). However, the extent of coverage did not truly alarm Chinese leaders until the outbreak of severe acute respiratory syndrome (SARS) in 2003, which strongly impacted China's health-care system and economy (*5*). Chinese leaders became aware of underinvestment in the health care system and the urgent need to implement fundamental reform. A number of policies and interventions were introduced to enhance the health insurance system in order to provide universal coverage by 2020 (*18*).

2.2. *Policies and achievements in improving health insurance coverage*

To promote insurance coverage, the Chinese government implemented systematic schemes (as shown in Table 1) (*4*), including the New Rural Cooperative Medical Scheme (NRCMS) in rural areas and the Urban Employee Basic Medical Insurance (UEBMI) and Urban Resident Basic Medical Insurance (URBMI) in urban areas. Together, these three insurance schemes constituted China's basic social medical insurance system and rapidly expanded the extent of coverage so that 95% of the total Chinese population was insured by 2011 (*19*).

NRCMS, a government-led voluntary insurance scheme, was initiated in 2003 to improve access to health insurance for rural residents (*20*). Unlike mandatory insurance, the NRCMS is operated and organized by county. The central government linked allocation of its subsidies to the extent of the population covered in each country, giving local governments a strong incentive to expand the extent of coverage. Enrollment in the NRCMS is usually based on households rather than individuals, which is as one of

the most effective approaches for rapid expansion of coverage (*20,21*). Funds for the NRCMS are jointly provided by the central government, local governments, and rural households, with a ratio of contribution of 2:2:1 (*i.e.*, 80% from the government and 20% from rural residents) (*20,22*). Government has continuously increased subsidies for the NRCMS, which is crucial to expanding coverage. By 2011, government subsidies accounted for 75% of premiums for the NRCMS (*23*). The average annual flat-rate premium per capita of the NRCMS was 113 RMB in 2009 (*24*), and that amount increased to 246 RMB in 2011 and to 500 RMB in 2015 (*25*). The benefits package and reimbursement of medical expenses for enrollees in the NRCMS were decided by county governments based on their financial status. In the first five years, the NRCMS prioritized coverage of inpatient medical care throughout the country. A study reported that the effective inpatient reimbursement rate was around 44% in 2011 (*4*). Coverage of outpatient services coverage was expanded gradually, and more funding has been allocated to cover outpatient services in most counties (*20*). According to statistics, 79% of counties covered general outpatient care and 89% of counties covered outpatient care for major and chronic diseases in 2011 (4). In addition to the policies and schemes mentioned earlier, other approaches, including simplification of procedures for enrollment and reimbursement and public service campaigns touting benefits from the NRCMS, were adopted to attract enrollment and expand coverage (*20*). As government subsidies increased and the scheme's benefits improved, enrollment in the NRCMS gradually increased from 21% in 2003 to 97% in 2011, so more than 830 million people are covered (*19*).

To improve health insurance coverage in urban China, the UEBMI was implemented in 1998 to cover the urban employed and the URBMI was implemented in 2007 to cover urban residents (*19*). The UEBMI scheme, which was intended to cover urban employees and retirees but not their families, was launched in two medium-sized cities (Zhenjiang and Jiujiang) in 1994 and spread nationally in 1998 (*7*). UEBMI premiums, paid jointly by employers and employees, are equivalent to 8 percent of an employee's monthly pay, with 6 percent from the employer and 2 percent contributed by the employee (*7*). The premium for retired workers was paid by their former employers. Enrollment in the UEBMI is based on individuals and local governments are responsible for operating the UEBMI, with flexibility to adjust policies regarding implementation and reimbursement. The benefits packages of the UEBMI are designed to cover not only inpatient medical care but also outpatient services, including medical services for major and chronic diseases (*4*). A study reported that the effective inpatient reimbursement rate for the UEBMI was about 68% in 2011 (*4*). Thus far, the UEBMI has been the most generous public insurance scheme, with premiums per person per year as high as 240 US$ (equivalent to about 1,500 RMB) and coverage extending to 92% of eligible individuals in 2010 (*4*).

The URBMI was launched with substantial government subsidies and is highly similar to NRCMS in design. Its chief enrollees include children, elderly, college students, and unemployed urban residents not covered by the UEBMI scheme (*26*). Enrollment in the URBMI is voluntary and it is based on individuals. URBMI premiums are also jointly financed by the individual and central and local governments. The government contribution accounted for 85% of premiums for the URBMI by 2011 (*23*), so the insurance scheme has become a very attractive investment option. Local health insurance bureaus are responsible for determining financing levels from the government, which vary depending on the financial status of the region and the individual. The premium per person per year was about 21 US$, with 18 US$ from government subsidies, in 2011 (*4*). When the URBMI started, its benefits packages covered only inpatient services. A study reported that the effective inpatient reimbursement rate for the URBMI was 48% in 2011 (*4*). Outpatient care was gradually covered, with 58 % of cities covering general outpatient care and 83% of cities covering outpatient care for major and chronic diseases by 2011 (*4*). As government subsidies increased, coverage reached 93% in 2010 (*23*).

3. Challenges in and prospects for improving health insurance coverage

Although the achievement of extensive health insurance coverage is remarkable, a number of challenges have hindered progress in providing universal healthcare coverage. The inequality in coverage, accessibility, and affordability of medical services is a major challenge for healthcare insurance coverage and a significant public concern (*27,28*). The disjointed insurance scheme for residents in urban and rural areas has become a main driver of inequity in healthcare insurance coverage (*29*), which varies considerably in breadth and depth across insurance schemes and localities (*28*). As mentioned in 2.2, the NRCMS and the URBMI have much lower premiums, a lower inpatient reimbursement rate, and smaller benefits packages than the UEBMI has, though the benefits are relatively modest. These three schemes reduced the burden of medical expenses on individuals and households to some extent. Since medical expenses have increased, the proportion of out-of pocket payments for healthcare services remains high, and this is especially true for the rural population (*27*). According to statistics, the proportion of out-of-pocket expenditures to total national health expenditures decreased dramatically from 60% in 2001 to 35% in 2011 at the national level (*4*). In contrast, the proportion of out-of-pocket payments as a share of average annual

Table 2. Attributes of main heath insurance schemes in Thailand during achievement of UC (2002) (*33*).

Items	CSMBS	SSS	UC
Year initiated	1963	1990	2001
Individuals covered	Government employees, retirees, and dependents	Private sector employees	Remaining Thais
Financing sources	General taxpayers	Employers, employees, and government (1.5% contribution by each) to payroll	General taxpayers
Nature of employment	Fringe benefits	Mandatory	Social welfare
Risk pooling	National	National	National
Benefit coverage	Outpatient and inpatient services, health prevention	Same as CSMBS	Same as CSMBS
Predominant payment method	FFS	Capitation	Capitation for outpatient services Global budget plus DRGs for inpatient services

household living expenses for rural residents increased from 5.2% in 2000 to 8.4% in 2011 (*30*). Moreover, a large number of migrants have very limited access to health insurance due to locality-based benefits from the NRCMS and the household registration system (*31*). When seeking medical services, migrants must pay the full cost of services and receive reimbursement when they return to their hometowns (*20*). Information technology has helped the government develop a portable NRCMS. However, the limited coverage of NRCMS benefits means that migrants cannot afford health care costs in cities, leading to a greater financial burden for migrants and inequity in health care (*4*). Fee-for-service (FFS) is the prevailing method of payment in the UEBMI, the URBMI, and the NRCMS, and in government-run medical insurance involving purchasers and third-party payers. Profits give providers strong incentives to over-provide services, leading to over-use of health services and rising costs (*32*).

To address these issues, the government has been working to increase investment and reimbursements in health care insurance. Other payment methods, such as capitation, global budgets, and diagnosis-related groups (DRGs), are conductive to cost containment and have been attempted in some cities (*33*). The integration of the UEBMI, the URBMI, the NRCMS, and medical assistance programs, a promising strategy to develop a uniform standard health insurance system for urban and rural residents, is proceeding along with China's new medical reform, though it faces a variety of challenges (*27,29*). With increased attention from the government and the development of health information technology, the UEBMI, the URBMI, and the NRCMS were basically linked in 2013 to 2014. This also involved merging health insurance for special groups including migrant workers and farmers with no land to cultivate. Pursuant to opinions of the State Council, the URBMI and the NRCMS were integrated and a basic medical insurance system was created for urban and rural residents in each province of the country from 2014 to 2017 (*34*). The UEBMI and the basic medical insurance system for urban and rural residents will presumably be integrated to constitute national health insurance and supplementary medical insurance before 2020 (*35*). National health insurance intends to provide basic medical insurance for all members of the public and to guarantee basic medical services. Supplementary medical insurance will cover a higher level of health care needs (*35*).

4. Thailand's experience

In Thailand, there are three major public health insurance schemes (as shown in Table 2), namely the Civil Servant Medical Benefit Scheme (CSMBS), the Social Security Scheme (SSS), and the universal coverage (UC) scheme (*36*). The CSMBS was initiated in 1963 to cover the government and the SSS was initiated in 1990 to cover the private sector (36). The remaining 30% or so of Thais were left without any medical insurance coverage until the introduction of the UC scheme in 2001. The UC scheme, a tax-funded health insurance scheme, rapidly provided almost universal coverage to the entire population of Thailand by early 2002 (*33,36*). Sustainable tax-funded health financing was found to play a vital complementary role in providing universal coverage and equitable access in Thailand, which is a country in transition that is still developing with a large informal sector (*36*). This pragmatic approach provides a useful reference for another developing country with a massive rural population and urban unemployed residents like China. Unlike China's other insurance schemes, the benefits package of the UC scheme covers outpatient, inpatient, and preventive health services (*33,36*). The comprehensive benefits package was designed to be standardized across the UC, the CSMBS, and the SSS to ensure equity. The UC scheme uses capitation for outpatient services, while it uses global budgets and DRGs for inpatient services to control health expenditures (*33,36*). These methods of payment can be adopted in Chinese cities depending on the fiscal status of local governments. The UC scheme adopted a capitation contract model mandating that enrollees

seek care at designated and contracted district health centers or hospitals (*33,36*). Beneficiaries were required to purchase health services from a primary contractor first and were entitled to receive free care at registered providers. Individuals who failed to purchase services from a primary contractor must pay the full cost of services received. This useful approach to cost containment (*37*) was buttressed by the strength of health care infrastructure supported by shifting health care budgets from urban to rural facilities (*34*), the requirement that new medical graduates being employed providing health services in rural areas for three years (*38*), and services from community and village nurses and health care volunteers (*39*). These policies resulted in extensive coverage for Thailand and are a useful model for China's new medical reform. Reinforcing primary health care delivery and the referral system is critical to implementing a hierarchical medical system and reducing geographical disparities in health care.

5. Conclusion

China has successfully provided universal coverage to 1.3 billion people, representing the largest expansion in insurance coverage in human history. This impressive achievement is attributed to renewed political commitment by top leaders, strong public support, extensive government subsidies, strategies for program implementation, and growing economic power, affording the government the unprecedented opportunity to increase investment in health care (*4*). Nonetheless, there are many challenges to providing universal insurance coverage, including lopsided allocation of health resources, increasing medical expenditures, inequitable health service utilization, and large disparities between urban and rural areas of China (*27,28*). Potential solutions to these challenges include sustainable increases in government investment, transformation of payment methods to control medical costs (*33*), reinforcement of primary health care delivery and the referral system, and standardization of benefits packages through integration of the UEBMI, the URBMI, and the NRCMS (*29*). Thailand's experience in improving the equity and efficiency of its health system and providing universal coverage is a valuable reference for China (*33*). China's political philosophy and its government are committed to improving the well-being of its citizens.

References

1. Tang S, Meng Q, Chen L, Bekedam H, Evans T, Whitehead M. Tackling the challenges to health equity in China. Lancet. 2008; 372:1493-1501.
2. Hu S, Tang S, Liu Y, Zhao Y, Escobar ML, de Ferranti D. Reform of how health care is paid for in China: Challenges and opportunities. Lancet. 2008; 372:1846-1853.
3. Blumenthal D, Hsiao W. Privatization and its discontents: The evolving Chinese health care system. N Engl J Med. 2005; 353:1165-1170.
4. Yu H. Universal health insurance coverage for 1.3 billion people: What accounts for China's success? Health Policy. 2015; 119:1145-1152.
5. Shaw K. The 2003 SARS outbreak and its impact on infection control practices. Public Health. 2006; 120:8-14.
6. Wang T. China takes a stab at universal healthcare. www.forbes.com Available at *http://www.forbes.com/2009/01/22/china-health-care-marketsecon-cx_twdd_0122markets04.html* (accessed July 14, 2016).
7. Xu HW, Short SE. Health insurance coverage rates in 9 provinces in China doubled to 49 percent from 1997-2006, with a dramatic rural upswing. Health Aff (Millwood). 2011; 30:2419-2426.
8. Hsiao W. Transformation of health-care in China. N Engl J Med. 1984; 310:932-936.
9. Hsiao WCL. The Chinese health care system: Lessons for other nations. Soc Sci Med. 1995; 41:1047-1055.
10. Bogg L, Dong H, Wang K, Cai W, Vinod D. The cost of coverage: Rural health insurance in China. Health Policy Plan. 1996; 13:238-252.
11. Liu Y. Development of the rural health insurance system in China. Health Policy Plan. 2004; 19:159-165.
12. Liu Y, Hsiao W, Li Q, Liu X, Ren M. Transformation of China rural health care financing. Soc Sci Med. 1995; 41:1085-1093.
13. Liu Y, Rao K, Hu S. Towards establishment of a health protection system in rural China. Beijing: Asian Development Bank; 2003.
14. Ma J, Lu M, Quan H. From a national, centrally planned health system to a system based on the market: Lessons from China. Health Aff. 2008; 27:937-948.
15. Du J. Economic reforms and health insurance in China. Soc Sci Med. 2009; 69:387-395.
16. Liu Y, Hsiao WC, Eggleston K. Equity in health and health care: The Chinese experience. Soc Sci Med. 1999; 49:1349-1356.
17. Fan M. Health care tops list of concerns in China. Washington Post, USA, January 10, 2008; p. 7.
18. Communist Party of China Central Committee. State Council. Opinions of the Communist Party of China Central Committee and the State Council on Deepening the Health Care System Reform. Beijing: Government of the People's Republic of China, 2009.
19. Fang K, Shia B, Ma S. Health insurance coverage and impact: A survey in three cities in China. PloS One. 2012; 7:e39157.
20. Meng Q, Xu K. Progress and challenges of the rural cooperative medical scheme in China. Bull World Health Organ. 2014; 92:447-451.
21. You X, Kobayashi Y. The new cooperative medical scheme in China. Health Policy. 2009; 91:1-9.
22. Zhang D, Shi L, Tian F, Zhang L. Care utilization with China's new Rural Cooperative Medical Scheme: Updated evidence from the China Health and Retirement Longitudinal Study 2011-2012. Int J Behav Med. 2016; 23:655-663.
23. Yip WC-M, Hsiao WC, Chen W, Hu S, Ma J, Maynard A. Early appraisal of China's huge and complex health-care reforms. The Lancet. 2012; 379:833-842.
24. Meng W. Medical security system and medicine reimbursement policy in China. Bhuket, Thailand: in International Society for Pharmacoeconomics and

Outcomes Research Asia-Pacific Conference; 2010.
25. Ma J, Xu J, Zhang Z, Wang J. New cooperative medical scheme decreased financial burden but expanded the gap of income-related inequity: Evidence from three provinces in rural China. Int J Equity Health. 2016; 15:72.
26. Barber SL, Yao L. Health insurance systems in China – A briefing note. Geneva: World Health Organization; 2010. *http://www.who.int/healthsystems/topics/financing/healthreport/37ChinaB_YFINAL.pdf* (accessed February 2, 2018).
27. Wang X, Zheng A, He X, Jiang H. Integration of rural and urban healthcare insurance schemes in China: An empirical research. BMC Health Serv Res. 2014; 14:142.
28. Flatø H, Zhang H. Inequity in level of healthcare utilization before and after universal health coverage reforms in China: Evidence from household surveys in Sichuan Province. Int J Equity Health. 2016; 15:96.
29. Pan XF, Xu J, Meng Q. Integrating social health insurance systems in China. Lancet. 2016; 387:1274-1275.
30. Long Q, Xu L, Bekedam H, Tang S. Changes in health expenditures in China in 2000s: Has the health system reform improved affordability. Int J Equity Health. 2013; 12:40.
31. Zhao Y, Kang B, Liu Y, Li Y, Shi G, Shen T, Jiang Y, Zhang M, Zhou M, Wang L. Health insurance coverage and its impact on medical cost: Observations from the floating population in China. PLoS One. 2014; 9:e111555.
32. Yip W, Hsiao WC, Meng Q, Chen W, Sun X. Realignment of incentives for health-care providers in China. Lancet. 2010; 375:1120-1130.
33. Li C, Yu X, Butler JR, Yiengprugsawan V, Yu M. Moving towards universal health insurance in China: Performance, issues and lessons from Thailand. Soc Sci Med. 2011; 73:359-366.
34. Yang LP, Chen F. Discussion on integration of medical insurance system for urban and rural residents in China. Yi Xue Yu She Hui. 2017; 30:18-21. (in Chinese)
35. Sun CX, Zhang LQ, Xing W, Li L, Zhao XF, Zhao X, Weng RM. Research on the integration and optimization design of universal health care system in China. China Planning Press, Beijing, China, 2016; pp. 81-84.
36. Tangcharoensathien V, Prakongsai P, Limwattananon S, Patcharanarumol S, Jongudomsuk P. Achieving universal coverage in Thailand: What lessons do we learn? Research Report of the Health System Knowledge Network. 2007.
37. Ros CC, Groenewegen PP, Delnoij DM. All rights reserved, or can we just copy? Cost sharing arrangements and characteristics of health care systems. Health Policy. 2000; 52:1-13.
38. Pachanee C, Wibulpolprasert S. Incoherent policies on universal coverage of health insurance and promotion of international trade in health services in Thailand. Health Policy Plan. 2006; 21:310-318.
39. Hanucharurnkul S. Nurses in primary care and the nurse practitioner role in Thailand. Contemp Nurse. 2007; 26:83-93.

(November 20, 2017; Revised February 24, 2018; Accepted February 26, 2018)

Original Article

DOI: 10.5582/ddt.2018.01004

Construction of a simple evaluation system for the intestinal absorption of an orally administered medicine using *Bombyx mori* larvae

Fumika Ichino[1], Hidemasa Bono[2], Takeru Nakazato[2], Atsushi Toyoda[3], Asao Fujiyama[3], Kikuo Iwabuchi[1], Ryoichi Sato[4], Hiroko Tabunoki[1,*]

[1] *Department of Science of Biological Production, Graduate School of Agriculture, Tokyo University of Agriculture and Technology, Tokyo, Japan;*
[2] *Database Center for Life Science (DBCLS), Joint Support-Center for Data Science Research, Research Organization of Information and Systems (ROIS), Mishima, Shizuoka, Japan;*
[3] *Center for Information Biology, National Institute of Genetics, Mishima, Shizuoka, Japan;*
[4] *Graduate School of Bio-Applications and Systems Engineering (BASE), Tokyo University of Agriculture and Technology, Tokyo, Japan.*

Summary **Human intestinal absorption is estimated using a human colon carcinoma cell line (Caco-2) cells from human colorectal adenocarcinoma, intestinal perfusion, or a mammalian model. These current evaluation systems are limited in their ability to estimate human intestinal absorption. In addition, *in vivo* evaluation systems using laboratory animals such as mice and rats entail animal ethics problems, and it is difficult to screen compounds on a large scale at the drug discovery stage. Thus, we propose the use of *Bombyx mori* larvae for evaluation of intestinal absorption of compounds as an alternative system in this study. First, to compare the characteristics among Caco-2 cells, human intestine, and *B. mori* larval midgut, we analyzed their RNA-seq data, and we found 26 drug transporters common to humans and *B. mori*. Next, we quantitatively developed an oral administration technique in *B. mori* and established a method using silkworm *B. mori* larvae that can easily estimate the intestinal permeability of compounds. Consequently, we could determine the dose and technique for oral administration in *B. mori* larvae. We also developed a *B. mori* model to evaluate the intestinal permeability of orally administered. Our constructed evaluation system will be useful for evaluating intestinal permeability in medical drug development.**

Keywords: Intestinal permeability, transporters, next-generation sequencing, *B. mori*

1. Introduction

Although drug discovery can be genome-based, many candidate compounds are rejected in clinical trials for pharmaceutical products. A major reason for such as rejection is poor pharmacokinetics; in particular, poor intestinal absorption of candidate compounds. As a screening method using a human colon carcinoma cell line (Caco-2) for predicting the intestinal absorption of a compound, the Caco-2 cell culture system is derived from high-throughput screening and *in situ* perfusion systems (Figure 1) (*1-3*). However, these current evaluation systems cannot be used to evaluate the intestinal absorption of any compound, maintaining the villus structure and function of the small intestinal epithelium (*4*). In addition, *in vivo* evaluation systems have problems related to time, expense, and the ethics of using laboratory animals, such as mice and rats. For these reasons, it is difficult to screen compounds on a large scale. Therefore, we need to construct a new evaluation method for the intestinal absorption of candidate compounds for large scale screening.

The silkworm *Bombyx mori* is a lepidopteran insect that is used as a model organism in agricultural research. Their genome sequence is almost completely

**Address correspondence to:*
Dr. Hiroko Tabunoki, Department of Science of Biological Production, Graduate School of Agriculture, Tokyo University of Agriculture and Technology, 3-5-8 Saiwai-cho, Fuchu, Tokyo 183-8509, Japan.
E-mail: h_tabuno@cc.tuat.ac.jp

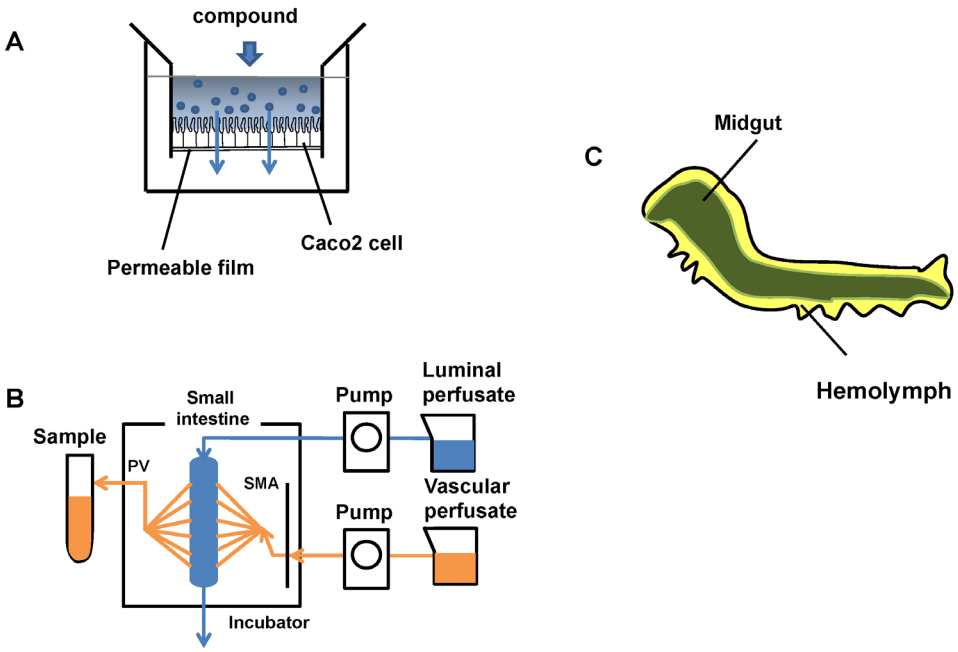

Figure 1. Evaluation of model systems for intestinal permeability and the internal structure of *B. mori* larva. (A) Caco-2 cell system. The cells are cultured on a permeable film, and the objective compound is dissolved into the culture medium. The compound passes through the permeable film and into a lower culture dish. **(B)** Intestinal perfusion system. A modification by Ishihara *et al*. (2001) (*2*). The small intestine was dissected from mice and set into an incubator filled with buffer (37°C). A solvent containing the objective compound was perfused by a pump into the small intestine. SMA: superior mesenteric artery; PV: portal vein. **(C)** Internal structure of *B. mori* larva. Most of the body is occupied by the midgut (green), and its surroundings are filled with hemolymph (yellow).

characterized, various spontaneous genetic mutants are available, and the silkworm is amenable to transgenics, genome editing, and transcriptome analysis (*5-10*). Moreover, the larval body size is bigger than that of *Drosophila melanogaster*: their gastrointestinal tract occupies ≥ 80% of the whole larval body and is structurally similar to the human small intestine (*11*); however, *B. mori* has never been used as an evaluation model for the absorption of a compound. Hamamoto *et al*. (*12*) investigated the pharmacokinetics (absorption, distribution, metabolism, excretion) of some drugs by using silkworm larvae and showed that most of the data were consistent with those of the mouse model (*13,14*). Drugs are metabolized by P450 enzymes and are then processed in a conjugation reaction. These metabolic processes and excretion of compounds are similar to those of mammalian models (*12*); for example, the effective dose of antibiotics in the bacterial infection model using silkworm larvae was consistent with that in the mammalian model (*15*). These results indicate the possibility that silkworms can be used as a substitute for mammals.

In addition, current intestinal permeability systems cannot adequately predict the intestinal absorption of compounds at the pharmaceutical investigation stage. To evaluate pharmacokinetics without laboratory animals at the preliminary developmental stage, an evaluation system that can easily predict absorption from the small intestine of an orally administered compound is required. Such a system not only has economic advantages, such as reduced time and cost, but also improved animal ethics at the preliminary developmental stage; however, there is still no suitable screening method available. We therefore propose the use of *B. mori* larvae for the evaluation of intestinal permeability. This model can easily and conveniently predict the intestinal absorption of compounds; thus, we quantitatively developed oral administration techniques in *B. mori* and established a method using *B. mori* larvae that can rapidly measure the intestinal permeability of compounds.

2. Materials and Methods

2.1. *Insects*

The *B. mori* larvae used in the study were supplied by Ueda-Sha Co. Ltd. (Ueda-shi, Nagano, Japan). Silkworm larvae were reared on an artificial diet of Silkmate 2S (Nosan, Tsukuba-shi, Ibaraki, Japan). Insects were maintained at 25°C with a 12-h light/dark cycle. Day 3 fifth-instar *B. mori* larvae were used for the evaluation of intestinal absorption. The *B. mori* strain o751 (wild-type) used in the RNA-seq analysis was obtained from the Institute of Genetic Resources, Faculty of Agriculture, Kyushu University (NBRP silkworm database: *http://silkworm.nbrp.jp/index_en.html*).

2.2. *RNA-seq analysis*

Total RNA was isolated from the midgut of day 3 fifth-instar *B. mori* larvae of *B. mori* o751 wild-type by using a PureLink® RNA extraction kit (Thermo Fisher Scientific Inc., Valencia, CA, USA) according to the manufacturer's protocol. The RNA quality was assessed by using an Agilent Bio-analyzer 2100 (Agilent Technologies, Santa Clara, CA, USA). Paired-end sequencing cDNA libraries were constructed with 4 μg of total RNA from o751 wild-type samples (n = 3) by using a TruSeq RNA Sample Preparation Kit Set A (Illumina Inc., San Diego, CA, USA) according to the manufacturer's protocol. RNA-seq was performed by using a HiSeq 2500 system (Illumina Inc.). The data quality of the fastq files was verified by using the FastQC tool (Babraham Bioinformatics, *http://www.bioinformatics.babraham.ac.uk/projects/fastqc/*). The around 43-M paired-end reads (2 × 150 bp) were mapped to the reference *B. mori* genome available from the Ensembl Genome database (*16*) using the Bowtie2 program version 2.3.2 with default parameters (*17*). RNA-Seq by Expectation-Maximization software version 1.3.0 was used for the calculation of expression values in transcripts per million (TPM) (*18*).

The gene expression data for Caco-2 cells and human small intestine was obtained from the Reference Expression Dataset (*19*). Data used for the comparative analysis were "Processed expression data of all samples for CAGE human PRJDB3010 (FANTOM5)" (doi: 10.6084/m9.figshare.4028613.v4) downloaded from *https://doi.org/10.6084/m9.figshare.4028613.v4.*

2.3. *Identification of B. mori human transporter homologs by systematic BLAST search*

To identify the human transporter homolog in the silkworm, genes that were homologous to human genes were identified by performing a systematic basic local alignment search tool (BLAST) search (tblastx) with a cutoff E-value of significant homology at 10^{-10} (query: human transporter cDNA sequence; database: whole silkworm cDNA sequence set from the Ensembl database).

2.4. *Determination of dose for oral administration to B. mori larvae*

To determine the dose for oral administration, we injected several amounts of water into day 3 fifth-instar *B. mori* larvae *via* their mouthparts by using a disposable syringe (Terumo, Shibuya-ku, Tokyo, Japan) with a modified TSK 30G needle (Tochigi-seiko Co. Ltd., Utsunomiya-shi, Tochigi, Japan) as an oral probe. The tip of the 30G needle was filed by using sand paper, and the edge of the needle tip was removed for oral administration. The silkworm larvae were not fed for 24 h before the administration of the compounds. The body weights of day 3 fifth-instar *B. mori* larvae were 2.88 ± 0.16 g (mean ± SD). In this experiment, we defined "success" as survival of the larvae the day following the oral administration (for 24 h), and there were no problems in the oral injection into the larva; whereas "failure" was defined as death or other problems occurring in the course of the oral injection into the larva. We statistically calculated a correlation coefficient for the relationship between dose and larval body weight by using Microsoft Excel. In this experiment, we denoted "success" as 1 and "failure" as 0.

2.5. *Determination of the LD_{50} of theophylline, tetracycline hydrochloride, and chloramphenicol in day 3 fifth-instar B. mori larvae*

Theophylline, tetracycline hydrochloride, and chloramphenicol were purchased from Wako Pure Chemical Industries, Ltd. (Chuo-ku, Tokyo, Japan). To determine the 50% of lethal dose (LD_{50}) in day 3 fifth-instar *B. mori* larvae, we orally injected theophylline, tetracycline hydrochloride, and chloramphenicol by using the modified oral probe mentioned above. Theophylline was dissolved in 20% dimethyl sulfoxide (Wako Pure Chemical Industries, Co., Ltd.) at 0 (control), 1, 1.25, 1.50, 1.75, and 2.00 mg/g and injected at a volume of 0.18 mL/g body weight. Tetracycline hydrochloride was dissolved in distilled water (Otsuka Pharmaceutical Co., Ltd., Naruto-shi, Tokushima, Japan) at 0 (control), 1, 1.25, 1.50, 1.75, 2.00, 2.25, and 2.50 mg/g and injected at a volume of 0.18 mL/g body weight. Chloramphenicol was dissolved in 100% ethanol (Wako Pure Chemical Industries, Co., Ltd.) at 0 (control), 0.2, 0.4, 0.6, 0.7, 0.8, and 1.0 mg/g and injected at a volume of 0.18 mL/g body weight. Each of the control groups was injected with their respective undiluted solvent.

The number of dead silkworms after 24 h was counted and the mortality rate was calculated using the formula mortality rate (%) = (X/Y) × 100, where X = dead larvae in the group and Y = total larvae in the group. To calculate the LD50, larval mortality rates were analyzed by using the Probit Analysis (*20*) option of the JMP 10.0 software package (SAS Institute Japan Ltd., Minato-ku, Tokyo, Japan). After obtaining these results, we determined the LD_{50} values of theophylline, tetracycline hydrochloride, and chloramphenicol for administration to *B. mori* larvae.

Theophylline, tetracycline hydrochloride, and chloramphenicol, prepared at 1.25, 1.5, and 0.6 mg/g in each solvent, respectively, were injected into 10 larvae at a volume of 0.18 mL/g body weight. After 0.5, 1, 1.5, 2, 3, 4.5, 6, and 9 h, intact hemolymph was collected from each compound-treated larva without a reducing agent and immediately frozen at −80°C until use.

2.6. *Sample preparation for evaluation of intestinal permeability*

To remove protein components, one volume of methanol (Wako Pure Chemical Industries, Co., Ltd.) was added to the collected hemolymph. This was mixed well by using a vortex mixer and kept on ice for 15 min and then centrifuged at 1,000g for 15 min at 4°C. The supernatant was transferred to a new tube and filtered by using a 0.45-μm filter (ADVANTECH Co., Ltd., Bunkyo-ku, Tokyo, Japan). Finally, the adjusted sample was added to seven volumes of methanol for the analysis of intestinal permeability by high-performance liquid chromatography (HPLC).

2.7. *Determination of HPLC detection conditions*

The following equipment was used for the detection of intestinal permeability by HPLC analysis: an intelligent pump (JascoPU.2080Plus; JASCO Co., Ltd. Hachioji-shi, Tokyo, Japan), ultraviolet detector (UV.2077Plus, Mx.2080.31, DG, 2080.53; JASCO Co., Ltd.), and an octa decyl silyl (ODS) 18 column (25 cm × 4.6 mm I.D.; GL Science, Shinjyuku-ku, Tokyo, Japan), and a step-wise gradient mode (flow rate; 0.7 mL/min). The mobile phase used the following conditions: 5% MeOH containing 0.2% acetic acid, 100% Methanol, 100:0→60:40 for 0-15 min, and 60:40→60:40 for 15-30 min. All analyses were performed at room temperature (25°C). Chromato-PRO software (Run Time Co., Ltd., Hachioji-shi, Tokyo, Japan) was used in data processing. The elution was monitored at 273 nm (theophylline) or 275 nm (tetracycline hydrochloride and chloramphenicol).

3. Results

3.1. *Identification of common drug transporters in the human intestine and B. mori larval midgut*

To compare the characteristics among Caco-2 cells, the human small intestine, and the *B. mori* larval midgut, we analyzed the *B. mori* larval midgut RNA-seq data to identify the homologs of the human drug transporters expressed in the small intestine. As a result, we found 26 drug transporter homologs that were common in the *B. mori* larval midgut and human intestine. In contrast, the ATP-Binding Cassette (ABC) Subfamily A Member 13 (*ABCA13*) and *ABCB4* were expressed only in the human intestine. Moreover, Solute Carrier Family (SLC) 22 Member 15 (*SLC22A15*), *ABCA5*, *ABCB1*, *ABCG2*, and Solute Carrier Organic (*SLCO*) Anion Transporter Family Member 4 A1 (*SLCO4A1*) were not expressed in the *B. mori* larval midgut. *ABCC8*, *ABCG1*, *ABCG4*, *ABCG5*, *ABCG8*, *SLCO3A1*, *SLCO5A1*, and SV2-Related Protein (*SVOP*) were not expressed in the Caco-2 cells.

Table 1. Human transporter homologs expressed in the *B. mori* larval midgut

Gene symbol	Caco-2 (CAGE value)	Human (CAGE value)	*B. mori* (TPM value)
ABCA3	2.4	2.2	81.5
ABCA5	0.8	4.2	0
ABCA13	0	0.2	0
ABCB1	2.7	5.3	0
ABCB4	0	0.8	0
ABCB5	0	0.5	13.6
ABCB6	2.5	1.8	8.8
ABCB7	3.1	3.2	1.4
ABCB8	2.6	2.8	1.7
ABCB10	2.9	3.2	2.9
ABCC1	2.4	2.2	0.1
ABCC3	3.2	4.6	0.2
ABCC4	3.7	2.5	40.3
ABCC8	0	0.8	0.4
ABCC10	2.4	2.6	0.2
ABCD3	3.6	3.6	0.5
ABCG1	0	3.7	2.3
ABCG2	2.8	5.2	0
ABCG4	0	0.2	1.2
ABCG5	0	4.5	0.8
ABCG8	0	4.7	0.1
SLC2A8	4.2	3.2	2.4
SLC15A1	2.1	5.9	0.4
SLC15A2	0.5	0.1	17.4
SLC22A1	0	0	0.2
SLC22A3	0.2	1.5	6.2
SLC22A4	0.5	2.7	9.2
SLC22A5	2.2	3.8	1.3
SLC22A6	0	0	220.8
SLC22A12	0	0	6.0
SLC22A13	0	0.1	6.8
SLC22A15	0.1	0.8	0
SLC22A16	0	0	0.2
SLCO3A1	0	1.7	0.1
SLCO4A1	1.6	2.1	0
SLCO5A1	0	0.2	0.8
SVOP	0	0.3	0.2

Additionally, *SLC22A1*, *SLC22A6*, *SLC22A12*, *SLC22A13*, and *SLC22A16* were expressed only in the *B. mori* larval midgut (Table 1). Therefore, there were few differences in the expressed genes among *B. mori*, Caco-2, and human small intestine.

The RNA-seq reads supporting the conclusions of this article are available in the Sequence Read Archive with the following accession numbers: DRR095108, DRR095109, and DRR095110.

3.2. *Evaluation of the LD_{50} values of theophylline, tetracycline hydrochloride, and chloramphenicol*

To determine the dose for oral administration, we injected various amounts of water into day 3 fifth-instar *B. mori* larvae by oral administration. In this experiment, we defined success as survival of the larvae surviving until the following day and failure as death or a problem occurring in the oral injection to the larvae. We then, calculated the relationship between the amount of water and larval body weight (Figure 2, Table 2), selecting 0.18

mL/g as injection dose. All oral administration doses were set at 0.18 mL/g in this study.

Next, we evaluated the LD50 of theophylline, tetracycline hydrochloride, and chloramphenicol, which are used as predictors of intestinal absorption in mammalian models and humans. Thus, we determined the LD50 in day 3 fifth-instar *B. mori* larvae to be 1.49 mg/g (95% confidence interval; CI, 1.37-1.60) for theophylline, 1.95 mg/g (95% CI, 1.83-2.05) for tetracycline hydrochloride, and 0.74 mg/g (95% CI, 0.69-0.80) for chloramphenicol.

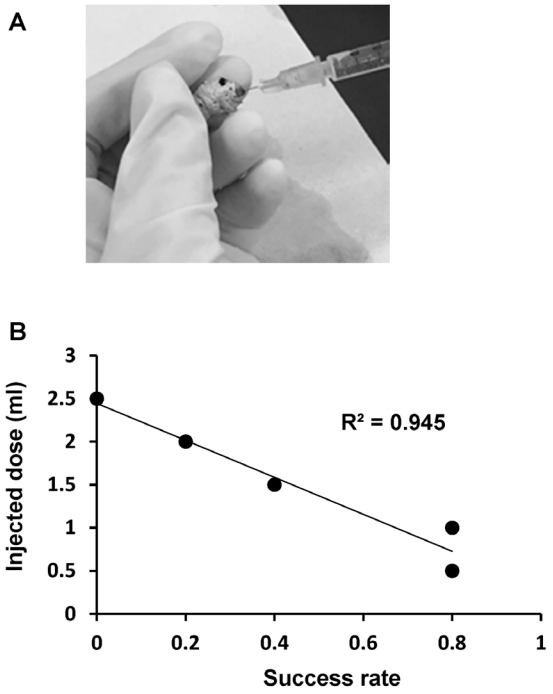

Figure 2. Relationship between success rate and injection dose. (A) Oral administration to *B. mori* larvae. **(B)** Relationship between success rate and injection dose of oral administration in *B. mori* larvae. R2 indicates the correlation coefficient.

3.3. *Construction of the B. mori model to evaluate the intestinal permeability of compounds by oral administration*

To easily evaluate the intestinal permeability of theophylline, tetracycline hydrochloride, and chloramphenicol, we assessed their intestinal permeability by using *B. mori* larvae. First, we investigated the conditions for HPLC analysis by using each compound, and the flow rate and composition of the solvent were determined. Retention times were as follows: approximately 23 min for theophylline, approximately 25 min for tetracycline hydrochloride, and 35 min for chloramphenicol. Subsequently, theophylline, tetracycline hydrochloride, and chloramphenicol were

Table 2. Relationship between success rate and injection dose

Success rate (%)	Injection dose (mL) per individual	Injection dose (mL) per body weight
80	0.73	0.25
90	0.51	0.18
95	0.40	0.14

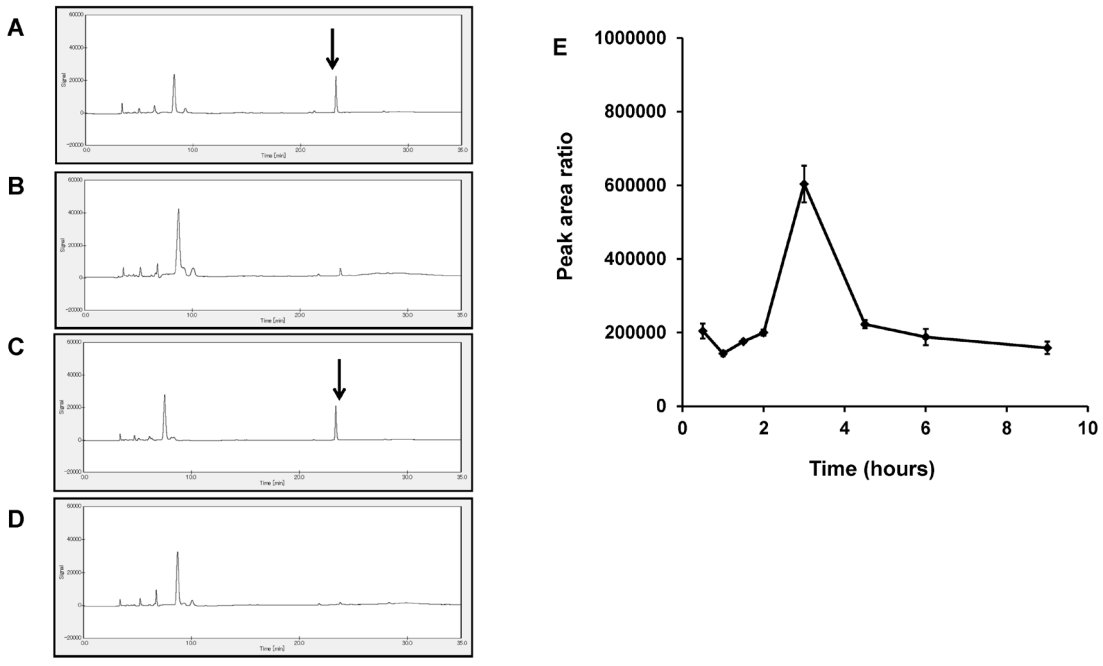

Figure 3. Determination of the intestinal permeability of theophylline by HPLC analysis. (A) Oral administration of theophylline after 30 min. **(B)** Oral administration of the solvent after 30 min. **(C)** Oral administration of theophylline after 1.5 h. **(D)** Oral administration of the solvent after 1.5 h. **(E)** Time course of the detection of intestinal permeability of theophylline by HPLC analysis. The peak area ratio was calculated by using Chromato-pro software.

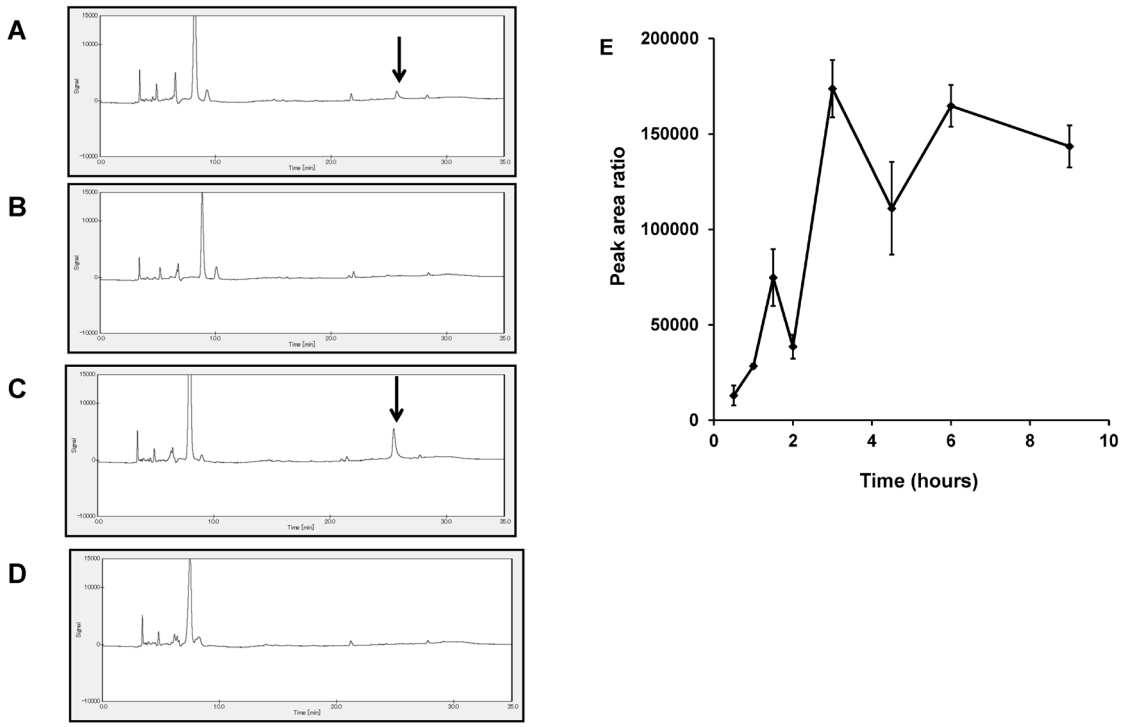

Figure 4. Detection of the intestinal permeability of tetracycline hydrochloride by HPLC analysis. (A) Oral administration of tetracycline hydrochloride after 30 min. **(B)** Oral administration of the solvent after 30 min. **(C)** Oral administration of tetracycline hydrochloride after 1.5 h. **(D)** Oral administration of the solvent after 1.5 h. **(E)** Time course of the detection of intestinal permeability of tetracycline hydrochloride by HPLC analysis. The peak area ratio was calculated by using Chromato-pro software.

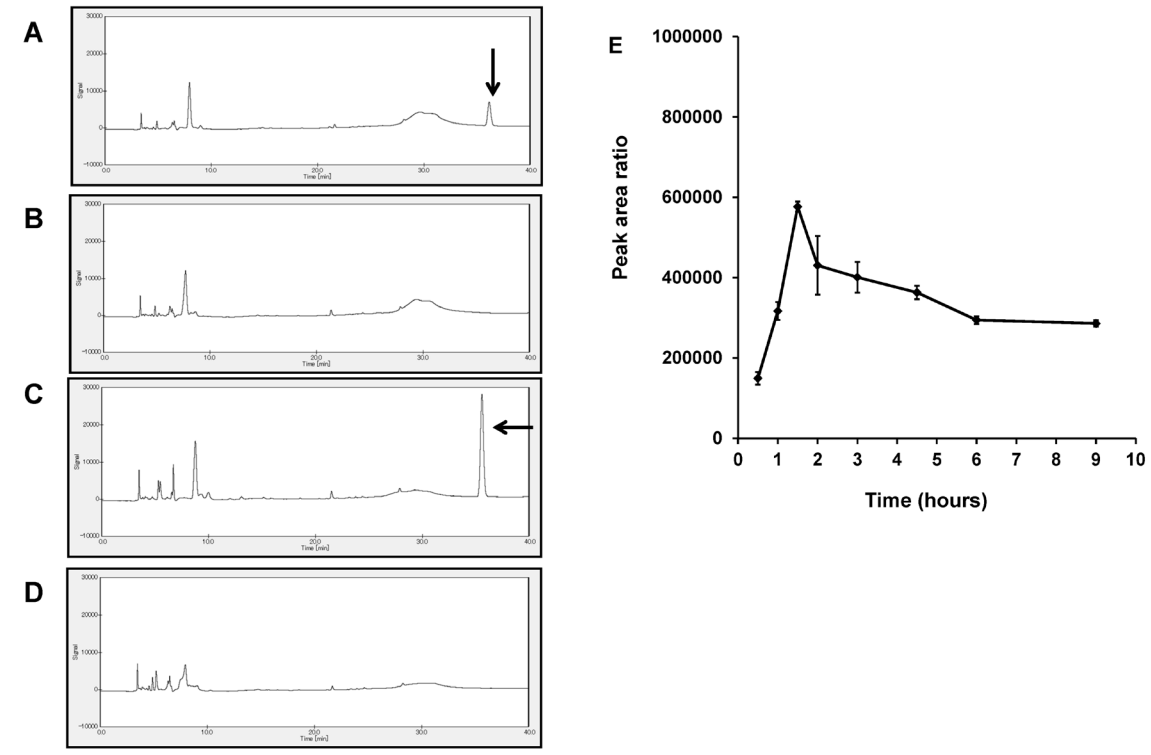

Figure 5. Detection of the intestinal permeability of chloramphenicol by HPLC analysis. (A) Oral administration of chloramphenicol after 30 min. **(B)** Oral administration of the solvent after 30 min. **(C)** Oral administration of chloramphenicol after 1.5 h. **(D)** Oral administration of the solvent after 1.5 h. **(E)** Time course of the detection of intestinal permeability of chloramphenicol by HPLC analysis. The peak area ratio was calculated by using Chromato-pro software.

injected orally into the *B. mori* larvae. Theophylline was injected at 1.25 mg/g body weight of *B. mori* at a volume of 0.18 mL, and the hemolymph was collected after 30 min. We detected the peak that indicates theophylline by HPLC (Figures 3A and 3C, indicated by arrow). Furthermore, the peak confirmed that theophylline was absorbed from the midgut 30 min after administration. The peak reached its maximum intensity at 3 h, and then gradually decreased (Figure 3E).

Similarly, tetracycline hydrochloride was injected at 1.5 mg/g body weight of *B. mori* at a volume of 0.18 mL, and the peak indicating that the tetracycline hydrochloride penetrated the hemolymph from the midgut was detected from 30 min to 9 h after administration (Figures 4A and 4C, indicated by arrow). The peak reached its maximum intensity at 3 h and then decreased (Figure 4E).

Chloramphenicol was injected at 0.6 mg/g body weight of *B. mori* at a volume of 0.18 mL, and the peak indicating that the chloramphenicol penetrated the hemolymph from the midgut was detected from 30 min to 9 h after administration (Figures 5A and 5C, indicated by arrow). Interestingly, chloramphenicol had the largest peak area in the collected hemolymph at 1.5 h after administration (Figure 5C). When the amount of chloramphenicol absorbed from the midgut was examined, the maximum concentration of the drug occurred at 1.5 h after the administration and then gradually decreased (Figure 5E).

Retention times were 23.5 ± 0.17 min (mean ± SD) for theophylline, 25.7 ± 0.02 min for tetracycline hydrochloride, and 36.4 ± 0.42 min for chloramphenicol. Thus, theophylline, tetracycline hydrochloride, and chloramphenicol permeated through the midgut to the hemolymph 30 min after administration (Figures 3A, 4A, and 5A). No remarkable peak was detected in each control solvent (Figures 3B, 3D, 4B, 4D, 5B, and 5D). Hence, the intestinal permeabilities of theophylline, tetracycline hydrochloride, and chloramphenicol could be evaluated by using the *B. mori* model.

4. Discussion

First, we analyzed the RNA-seq data of the day 3 fifth-instar *B. mori* larval midgut to compare the characteristics between the human small intestine and *B. mori* larval midgut. Interestingly, 16 ABC transporters and 7 SLC transporter genes were commonly expressed in the *B. mori* larval midgut and human intestine. The ABCG transporter genes were well-conserved between *B. mori* and human; however, Caco-2 cells did not express ABCG transporters. Although 11 SLC transporter genes were identified in the *B. mori* larval midgut, SLC transporter genes and their function have not been analyzed in *B. mori*.

Fifty-one ABC transporter genes have been identified in *B. mori* and are categorized into eight classes (*21*). However, the function of most ABC transporter genes has not been analyzed without the *B. mori* ABC transporter subfamily C member 2 (*BmABCC2*), which relays transported Cry toxins from *Bacillus thuringiensis* (*22*). Additionally, a single amino acid mutation of *BmABCC2* causes a resistance to Cry toxin in *B. mori* (23). BmABCC2 has high homology with the human *ABCC4*, also known as multi-drug resistance protein 4, which is involved in organic anion transport and drug resistance. The midgut RNA-seq data showed that *BmABCC2* mRNA expression was greater than that of the other transporters in day 3 fifth-instar *B. mori* larvae; also, human *ABCC4* was expressed in the small intestine in the public RNA-seq data that we employed. Thus, human *ABCC4* and *BmABCC2* might share with similar function.

While the dietary amount increases from day 3 to day 5 in fifth-instar *B. mori* larvae in *B. mori*, their body size is also increases from day 3 to day 5 (*24*). Thus, in this study, day 3 fifth-instar *B. mori* larvae would be appropriate for evaluation of the intestinal permeability of compounds. It is suggested that the functions of the *B. mori* larval midgut and the human small intestine are similar in terms of intestinal permeability of compounds.

Next, we developed an oral administration method for day 3 fifth-instar *B. mori* larvae without damaging the oral cavity and gastrointestinal tract. In addition, we used a relatively large *B. mori* strain, Kinshu × Showa, which remained fasting for 24 h, so we could easily inject *via* oral administration. We could thus determine the dose per weight.

Then, we used *B. mori* larvae to examine the intestinal absorption of three compounds with clear intestinal absorption in humans. Theophylline, tetracycline hydrochloride, and chloramphenicol were examined for their intestinal permeability (*http://www.genome.jp/kegg/drug/*) because these compounds showed clear dose-response curves in *B. mori* larva. In humans, the time of maximum concentration (T_{max}) of theophylline has been reported as 24 h, whereas those of tetracycline hydrochloride and chloramphenicol have been reported as 2 and 3 h, respectively (*http://www.genome.jp/kegg/drug/*). In this study, the T_{max} values of theophylline, tetracycline hydrochloride, and chloramphenicol for *B. mori* correlated with the human T_{max} values.

The LD_{50} values in *B. mori* for tetracycline and chloramphenicol were comparable to those in mice. According to the material safety data sheet (MSDS), the LD_{50} is 0.24 mg/g for theophylline, 2.8 mg/g for tetracycline hydrochloride, and 1.5 mg/g for chloramphenicol with oral administration in mice. However, the LD_{50} for theophylline did not agreed with that in mice data in this study. Thus, LD_{50} does not necessarily need to match with mice data in the transition of the plasma concentration of theophylline

because the transition of the plasma concentration of theophylline in *B. mori* was similar to that in humans. The lethal dose and intestinal permeability can be considered to be different factors in drug characterization. Furthermore, the peaks that indicated the absorption of these compounds from the midgut could be detected by HPLC analysis approximately 30 min after oral administration.

Although theophylline and tetracycline might be substrates of some transporters, such as *SLC22A6*, *SLC22A7*, *SLC22A8*, *SLC22A9* (*25*), it is unclear if these transporters are responsible for elimination of theophylline and tetracycline from the small intestine. *SLC22A6* is related to transport of tetracycline. *SLC22A6* is involved in the excretion of substrates in human. Additionally, *SLC22A6* was highly expressed in *B. mori*, but, it was not expressed in the small intestine of the human. Thus, differences in the expression of drug transporters may cause differences in drug absorption. However, the T_{max} of tetracycline in *B. mori* was consistent with that through the human small intestine. This result indicated that tetracycline could be evaluated by using a *B. mori* model without effects of *SLC22A6*. However, we only examined the expression of human homolog transporters in *B. mori* by using midgut RNA-seq data. In the future studies, it will be necessary to clarify where these transporters are expressed and how they are involved in drug absorption in the midgut cells in *B.mori*.

In addition, the absorption of these compounds might be affected by the peritrophic membrane in *B. mori* larvae. Pesticides with molecular weights of 50-450 have shown oral toxicity in insects (*26*); thus, compounds with molecular weights of ≤ 500 may be easily absorbed from the *B. mori* larval midgut. Using the isolated *B. mori* larval midgut, Hamamoto *et al*. (*12*) reported that the relationship between the polarity and molecular weight of a compound determines their intestinal permeability. In this experiment, we showed that membrane permeation in the midgut was induced by compounds that are more hydrophobic than hydrophilic and that membrane permeation was more likely induced by compounds of smaller molecular weight. Furthermore, Hamamoto *et al*. (*12*) mentioned that the isolated midgut of the *B. mori* model has similar intestinal permeability to those in humans and mice.

The human small intestine has a pH of 5-7 in the upper part and 7-8 in the lower part (*27*), whereas the *B. mori* larval midgut has a pH of approximately 11 (*28*). Differences in pH may cause structural changes in some compounds when it passes through the midgut. For this reason, when administering a compound, we should consider suitable solvents and adjust the pH inside the midgut to be equal to that of the human small intestine.

The method for evaluating the intestinal absorption of a compound used in this study is much simpler than the pre-existing intestinal perfusion system. Furthermore, the prediction of intestinal absorption of a compound *via* transporters would be more appropriate than existing methods because whole bodies were used in this study. As an advantage, *B. mori* can be maintained throughout the year by using an artificial diet, and large numbers of genetically homogeneous individuals can be kept in a narrow space at low cost. In addition, there are no animal ethics problems.

Prediction of the intestinal permeability of some compounds in humans is difficult because of species differences and bioavailability. If we can produce transgenic silkworms that express human drug transporters in the midgut, we will be able to solve this problem; therefore, *B. mori* larva is considered helpful for evaluation of the intestinal permeability of a compound at the screening stage. In sum, we propose the use of *B. mori* larvae to evaluate intestinal absorption of compounds. This system will be useful for evaluation of intestinal permeability in medical drug development.

Acknowledgements

The wild type silkworm strain o751 was obtained from the National Bio Resource Project KAIKO (NBRP KAIKO) at the Center of Genetic Resources at Kyushu University. Computations were partially performed on the NIG supercomputer at the ROIS National Institute of Genetics.

This work was supported by JSPS KAKENHI grant number JP26450465 to HT, grant number JP15H02483 to KiI and HT, and grant number JP15H02837 to RS and HT. This work was also supported by the NIG Collaborative Research Program (2014-A171 and 2015-A155). This work was also supported by the National Bioscience Database Center (NBDC) of the Japan Science and Technology Agency (JST) to HB and TN.

References

1. Griffin B, O'Driscoll C. Models of the Small Intestine. In: *In Situ* Drug Absorption Studies: *In Situ*, *In Vitro* and *In Silico* Models: VII (Biotechnology: Pharmaceutical Aspects) (Ehrhardt C, Kim KJ, eds.). Springer, 2007; pp. 34-76.
2. Barthe L, Woodley J, Houin G. Gastrointestinal absorption of drugs: Methods and studies. Fundam Clin Pharmacol. 1999; 13:154-168.
3. Ishihara E, Usami M, Miura T, Tanigawa K. Glucose absorption from the small intestine in GK rats: A study of the isolated perfused intestine. J Jpn Diabetes Soc. 2001; 44:191-196.
4. Lennernäs H, Palm K, Fagerholm U, Artursson P. Comparison between active and passive drug transport in human intestinal epithelial (caco-2) cells *in vitro* and human jejunum *in vivo*. Int J Pharm. 1996; 127:103-107.
5. Mita K, Kasahara M, Sasaki S, *et al*. The genome sequence of silkworm, *Bombyx mori*. DNA Res. 2004;

11:27-35.
6. Xia Q, Zhou Z, Lu C, *et al*. A draft sequence for the genome of the domesticated silkworm (*Bombyx mori*). Science. 2004; 306:1937-1940.
7. Suetsugu Y, Futahashi R, Kanamori H, *et al*. Large scale full-length cDNA sequencing reveals a unique genomic landscape in a lepidopteran model insect, *Bombyx mori*. G3 (Bethesda). 2013; 9:1481-1492.
8. Tomita M. Transgenic silkworms that weave recombinant proteins into silk cocoons. Biotechnol Lett. 2011; 33:645-654.
9. Wang F, Ma S, Xu H, Duan J, Wang Y, Ding H, Liu Y, Wang X, Zhao P, Xia Q. High-efficiency system for construction and evaluation of customized TALENs for silkworm genome editing. Mol Genet Genomics. 2013; 288:683-690.
10. Xia Q, Cheng D, Duan J, *et al*. Microarray-based gene expression profiles in multiple tissues of the domesticated silkworm, *Bombyx mori*. Genome Biol. 2007; 8:R162.
11. Kobayashi M. Fine structure of the basal granular cell in the midgut epitherium of the silkworm, *Bombyx mori*. J Seric Sci Jpn. 1971; 40:101-106.
12. Hamamoto H, Kurokawa K, Kaito C, *et al*. Quantitative evaluation of the therapeutic effects of antibiotics using silkworms infected with human pathogenic microorganisms. Antimicrob Agents Chemother. 2004; 48:774-779.
13. Hamamoto H, Kamura K, Razanajatovo IM, Murakami K, Santa T, Sekimizu K. Effects of molecular mass and hydrophobicity on transport rates through non-specific pathways of the silkworm larva midgut. Int J Antimicrob Agents. 2005; 26:38-42.
14. Hamamoto H, Tonoike A, Narushima K, Horie R, Sekimizu K. Silkworm as a model animal to evaluate drug candidate toxicity and metabolism. Comp Biochem Physiol C Toxicol Pharmacol. 2009; 149:334-339.
15. Kaito C, Akimitsu N, Watanabe H, Sekimizu K. Silkworm larvae as an animal model of bacterial infection pathogenic to humans. Microb Pathog. 2002; 32:183-190.
16. Kersey PJ, Allen JE, Armean I, *et al.* Ensembl genomes 2016 more genomes, more complexity. Nucleic Acids Res. 2015; 44:D574-D580.
17. Langmead B, Salzberg S. Fast gapped-read alignment with Bowtie 2. Nat Methods. 2012; 9:357-359.
18. Li B, Dewey CN. RSEM: Accurate transcript quantification from RNA-Seq data with or without a reference genome. BMC Bioinformatics. 2011; 12:323.
19. Ono H, Ogasawara O, Okubo K, Bono H. RefEx, a reference gene expression dataset as a web tool for the functional analysis of genes. Sci Data. 2017; 4:170105.
20. Finny DJ. Quantal response and the dosage response curve. In: Probit Analysis: A Statistical Treatment of the Sigmoid Response Curve. Cambridge University Press, Cambridge, UK, 1947; pp. 8-19.
21. Liu S, Zhou S, Tian L, Guo E, Luan Y, Zhang J, Li S. Genome-wide identification and characterization of ATP-binding cassette transporters in the silkworm, *Bombyx mori*. BMC Genomics. 2011; 12:491.
22. Tanaka S, Miyamoto K, Noda H, Jurat-Fuentes JL, Yoshizawa Y, Endo H, Sato R. The ATP-binding cassette transporter subfamily C member 2 in *Bombyx mori* larvae is a functional receptor for Cry toxins from *Bacillus thuringiensis*. FEBS J. 2013; 280:1782-1794.
23. Atsumi S, Miyamoto K, Yamamoto K, *et al*. Single amino acid mutation in an ATP-binding cassette transporter gene causes resistance to Bt toxin Cry1Ab in the silkworm, *Bombyx mori*. Proc Natl Acad Sci U S A. 2012; 109:E1591- E1598.
24. Mukaiyama F, Ito T. Digestion experiments in the silkworm, *Bombyx mori*, by means of artificial diets. (I) Amount of food consumed, amount of food digested, and coefficient of digestibility. J Seric Sci Jpn. 1962; 31:317-322.
25. Russel FGM. Chapter 2, Transporters: Importance in drug absorption, distribution, and removal. In: Enzyme- and Transporter-Based Drug-Drug Interactions: Progress and Future Challenges (Pang, K. Sandy, Rodrigues, A. David, Peter, Raimund M. eds.), Springer, NY, U.S.A, 2010; pp. 27-49.
26. Ferrer I, Fernandez-Alba A, Zweigenbaum JA, Thurman EM. Exact-mass library for pesticides using a molecular-feature database. Rapid Commun Mass Spectrom. 2006; 20:3659-3668.
27. Soderind E, Dressman JB. Physiological factors affecting drug release and absorption in the gastrointestinal tract. In: Oral Drug Absorption: Prediction and Assessment (Dressman JB, Reppas C, eds.). CRC Press, NY, U.S.A, 2000; pp. 10-14.
28. Eguchi M, Kuriyama K, Daimon H. High alkalinity and function of proteases of digestive juice from the silkworm, *Bombyx mori*. J Seric Sci Jpn. 1986; 55:46-53.

(January 23, 2018; Revised February 10, 2018; Accepted February 21, 2018)

Original Article

DOI: 10.5582/ddt.2017.01073

Generic selection criteria for safety and patient benefit [VII]: Comparing the physicochemical and pharmaceutical properties of brand-name and generic terbinafine hydrochloride cream

Mitsuru Nozawa[1], Miho Goto[1], Yuko Wada[2], Miyuki Kumazawa[3], Ken-ichi Shimokawa[4], Fumiyoshi Ishii[2,*]

[1] *Triad Japan Co., Ltd., Kanagawa, Japan;*
[2] *Department of Self-medication and Health Care Sciences, Meiji Pharmaceutical University, Tokyo, Japan;*
[3] *Department of Mathematical Science, Meiji Pharmaceutical University, Tokyo, Japan;*
[4] *Department of Pharmaceutical Sciences, Meiji Pharmaceutical University, Tokyo, Japan.*

Summary **We measured and compared the physicochemical properties (pH, yield value, and squeeze force) of a drug for dermatomycosis, terbinafine hydrochloride-containing cream (brand-name product), and 12 generic products to clarify the characteristics of each product. On pH measurement, the pH value of the brand-name product, Lamisil, was 4.8, and those of the generic products ranged from 4.3 to 5.5, showing no marked difference. Furthermore, the yield value of Lamisil, as an index of cream ductility, was 122.2 dyn/cm^2, and those of the generic products ranged from 42.1 to 1,621.5 dyn/cm^2. In particular, the value of a generic product, Taiyo (42.1 dyn/cm^2), was significantly lower, whereas that of another one, Viras (1,621.0 dyn/cm^2), was significantly higher. In addition, the squeeze force was measured by attaching a HapLog® to the thumb and second finger. The value of Lamisil was 12.9 N, and those of the generic products ranged from 8.0 to 15.4 N. The values of generic products, Mylan (8.6 N), Tebinaceil (9.0 N), and Kelger (8.0 N), were significantly lower, whereas that of another one, Viras (15.4 N), was significantly higher. These results showed that there were marked differences in the pharmaceutical properties between the generic and brand-name products. The above pharmaceutical characteristics of drugs facilitated the presentation of reasons for differences in the sense of use, which characterizes external preparations, suggesting that products appropriate for individual patients can be recommended.**

Keywords: Cream, terbinafine hydrochloride, brand-name drug, generic drug, HapLog®

1. Introduction

In Japan, national health expenditure has annually increased, raising a serious social issue (*1*). To overcome this, a strategy to reduce health expenditure by promoting generic products was proposed (*2*). Concerning the promotion of generic drug usage, the quantity share of generic products is 56.2% as of September 2015. There was a cabinet decision in June 2015, and new target quantity shares in 2017 and in the early phase between 2018 and 2020 were established as ≥ 70 and ≥ 80%, respectively. At each pharmacy, generic product-promoting strategies have been positively attempted to achieve the above targets (*2*).

It is important for pharmacists to understand the equivalence of a generic product to a brand-name product or physicochemical properties and recommend a generic product based on an adequate triage from the viewpoint of national health maintenance and health expenditure reduction. However, there are no criteria for selecting generic products; therefore, it is not easy to select drugs appropriate for individual patients.

We previously reported that various patient needs could be met by clarifying the physicochemical and

Released online in J-STAGE as advance publication February 25, 2018.

**Address correspondence to:*
Dr. Fumiyoshi Ishii, Department of Self-medication and Health Care Sciences, Meiji Pharmaceutical University, 2-522-1, Noshio, Kiyose, Tokyo 204-8588, Japan.
E-mail: fishii@my-pharm.ac.jp

pharmaceutical properties of various dosage forms, primarily consisting of external preparations, which markedly differ in the sense of use: ointments, creams, lotions (*3,4*), ophthalmic liquids/solutions (*5*), nasal spray (*6*), and tapes (*7,8*). The appearance-based stability of a brand-name drug, Rinderon®-VG (principal components: betamethasone valerate, gentamicin sulfate), and 10 generic products (5 ointments, 3 creams, and 2 lotions) was evaluated, and their pH, viscosity, and contents were measured. There were marked differences in the rheology among the ointments, creams, and lotions (*3*). These results may have been related to differences in pharmaceutical techniques or additives in the process of manufacturing among various pharmaceutical companies. The sense of use or effects of each product may differ among patients. We concluded that caution was particularly needed when switching a brand-name drug to a generic product.

In this study, we summarized information for pharmacists to adequately select preparations in accordance with patient needs by comparing/evaluating the pharmaceutical properties of a drug for dermatomycosis, terbinafine hydrochloride-containing cream, and generic products.

2. Materials and Methods

2.1. *Materials*

Ethical pharmaceuticals of cream containing terbinafine hydrochloride (1 brand-name "Lamisil® cream 1%" and 12 generic products) were used in this study. Product name, abbreviated name, class, company name and lot number of these products are presented in Table 1.

2.2. *Measurement of pH*

Each cream preparation (1.0 g) was heated and dissolved by adding 10 mL of purified water. After cooling, it was measured using a Benchtop pH meter F-74 and ISFET pH electrode 0040-10D (HORIBA, Ltd., Kyoto, Japan). Measurement was performed 3 times at 25 ± 2°C, and the mean ± standard deviation (S.D.) was calculated.

2.3. *Measurement of ductility*

The spread diameter of each cream preparation was measured using a spread meter 419 (Rigo Co., Ltd., Tokyo). Measurement was conducted 3 times at room temperature (25 ± 2°C), and the mean value was calculated. The spread diameter was determined at 34 points between 5 and 1,800 seconds after the start of measurement. The spread diameter (cm) of each cream preparation was plotted on a longitudinal axis, and the time (seconds) was plotted on a transverse axis to prepare a semilog graph. The spread and viscosity of each cream preparation were calculated from the slope and y-intercept (*9,10*). Furthermore, the yield value was calculated using the following formula (*11*):

$$S_0 = \frac{48PVG}{\pi^2 D^5}$$

S_0: yield value (dyn/cm^2), P: weight of glass plate (g), V: amount of sample (cm^3)

G: gravitational acceleration (980 cm/sec^2), D: maximum spreading diameter (cm)

π: the ratio of the circumference of a circle to its diameter

2.4. *Measurement of squeeze force*

To assess the squeeze force to push out various preparations from a container, a wearable tactile sensor (Haptic Skill Logger (HapLog®), Kato Tech Co., Ltd., Kyoto, Japan) was used as a tool for evaluating the sense of touch (*12,13*). For measurement, the tactile sensors were attached to the right thumb and second finger, respectively, and the total force (thumb + second finger) required to squeeze 1 fingertip unit (FTU: volume of cream squeezed between the first joint and tip of the second finger) of cream while putting the center of the container between the thumb and second finger

Table 1. Cream products used in this experiment

Product name	Abbreviated name	Class	Company name	Lot numbers
Lamisil® Cream 1%	Lamisil	brand-name	Novartis Pharma K. K.	P0942
Viras® Cream	Viras	generic	Towa Pharm. Co., Ltd.	A199
Terbinafine Hydrochloride Cream 1% "Mylan"	Mylan	generic	Mylan Seiyaku Ltd.	013AKM
Terbinafine Hydrochloride Cream 1% "F"	F	generic	Fuji Pharma Co., Ltd.	2E01
Terbinafine Hydrochloride Cream 1% "Sandoz"	Sandoz	generic	Sandoz	212370
Tebinaceil® Cream 1%	Tebinaceil	generic	TOA Pharm. Co., Ltd.	T07TW
Terbinabine® Cream 1%	Terbinabine	generic	Nichi-Iko Pharm. Co., Ltd.	H1060
Ramitect® Cream*	Ramitect	generic	Sawai Pharm. Co., Ltd.	12X03
Tebeana® Cream 1%	Tebeana	generic	Iwaki Seiyaku Co., Ltd.	2E013
Terbinafine Hydrochloride Cream 1% "MEEK"	MEEK	generic	Kobayashi Kako Co., Ltd.	02SP21
Kelger® Cream	Kelger	generic	Maeda Pharm. Industry Co., Ltd.	2JC
Terbinafine Hydrochloride Cream 1% "Taiyo"	Taiyo	generic	Teva Takeda Pharma Ltd.	B11491
Terbinafine Hydrochloride Cream 1% "JG"	JG	generic	Nihon Generic Co., Ltd.	204100

*Currently, Ramitect® cream has its name changed to terbinafine hydrochloride cream 1% "Sawai".

was regarded as the squeeze force (N). These sensors facilitate the simultaneous assessment of the sensor-wearing person's finger contact force and sense of touch through the free sense of touch at the fingertip, whereas there are errors in the contact force related to individual differences in the attachment method or finger size. For this reason, the values were corrected in each person. Measurement was conducted 7 times per bottle of cream with the same lot number. In addition, concerning a product with different lot numbers, measurement was conducted for a total of 3 bottles. Subsequently, the mean of respective means was calculated, and adopted as the value of the product.

2.5. *Statistical analysis*

The values were compared using *Dunnett's* test. A *p*-value of 0.01 was regarded as significant.

3. Results

3.1. *Measurement of pH*

The influence of pH on the stability of drugs has been indicated. We measured the pH value of each preparation used in this experiment. The results are shown in Figure 1. The pH value of the brand-name drug, Lamisil, was 4.8, and the values of the generic products ranged from 4.3 to 5.5, showing no marked difference.

3.2. *Measurement of ductility*

When applying a cream preparation to the skin, the sense of use depends on its ductility and viscosity. We measured the spread diameter and time of each cream preparation using a spread meter. In addition, we prepared a semilog graph (longitudinal axis: spread diameter, transverse axis: time) to calculate the slope and y-intercept of each preparation. The results are shown in Figures 2 and 3. The slope of Lamisil was 0.24, whereas those of the generic products ranged from 0.02 to 0.36 (Figure 2). In particular, the value of a generic product, Viras (0.02), was significantly lower than that of Lamisil, and the value of another generic product, Taiyo (0.36), was significantly higher than that of Lamisil.

On the other hand, the y-intercept of Lamisil was 3.05, whereas the values of the generic products ranged from 2.55 to 3.33, as shown in Figure 3. In particular, the value of a generic product, Viras (2.55), was significantly

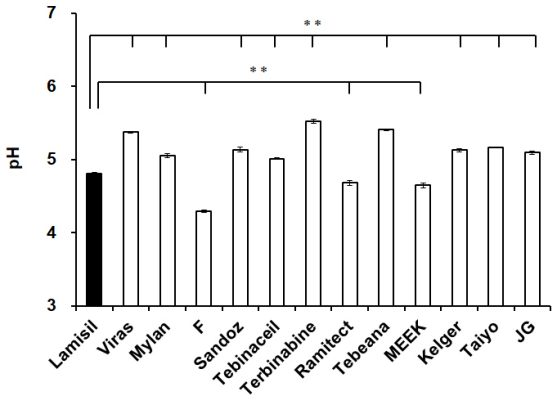

Figure 1. pH measurement of various preparations (*n* = 3). $^{**}p < 0.01$ (*vs*. Lamisil, *Dunnett*-test). ■: brand-name, □: generic.

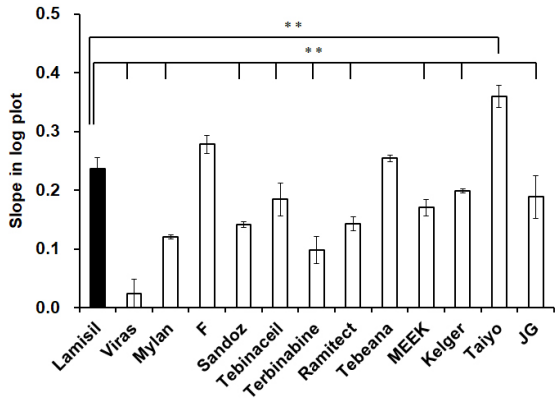

Figure 2. Slope measurement of various cream preparations (*n* = 3). $^{**}p < 0.01$ (*vs*. Lamisil, *Dunnett*-test). ■: brand-name, □: generic.

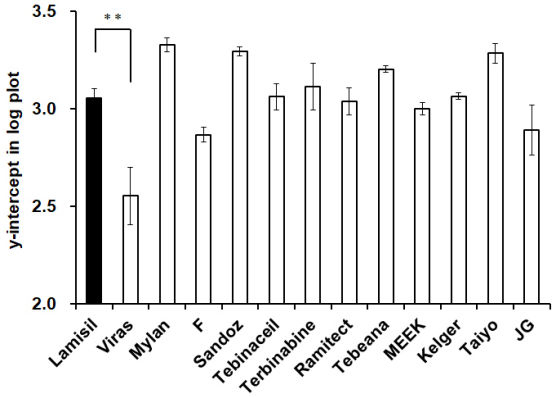

Figure 3. Y-intercept measurement of various cream preparations (*n* = 3). $^{**}p < 0.01$ (*vs*. Lamisil, *Dunnett*-test). ■: brand-name, □: generic.

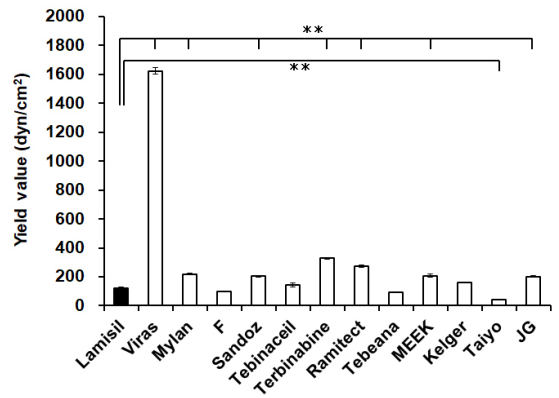

Figure 4. Yield value measurement of various cream preparation (*n* = 3). $^{**}p < 0.01$ (*vs*. Lamisil, *Dunnett*-test). ■: brand-name, □: generic.

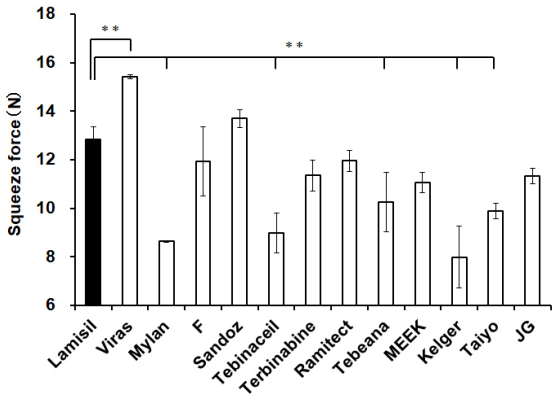

Figure 5. Squeeze force measurement of various cream preparations (n = 3). $^{**}p < 0.01$ (*vs*. Lamisil, *Dunnett*-test). ■: brand-name, □: generic.

lower than that of Lamisil, and the values of Mylan (3.33), Sandoz (3.29), and Taiyo (3.28) were higher than that of Lamisil.

The yield value is known as an index of cream ductility. As shown in Figure 4, the yield value of Lamisil was 122.2 dyn/cm^2, whereas the values of the generic products ranged from 42.1 to 1,621.0 dyn/cm^2. In particular, the value of a generic product, Taiyo (42.1 dyn/cm^2), was significantly lower, and that of Viras (1,621.0 dyn/cm^2) was significantly higher.

3.3. *Measurement of the squeeze force*

The squeeze force is expressed as a force required to push out a dose of each preparation. We measured the squeeze force by attaching a HapLog® to the right thumb and second finger, as shown in Figure 5. The squeeze force of Lamisil was 12.9 N, whereas the values of the generic products ranged from 8.0 to 15.4 N. In particular, the values of Mylan (8.6 N), Tebinaceil (9.0 N), and Kelger (8.0 N) were significantly lower, and that of Viras (15.4 N) was significantly higher.

4. Discussion

External preparations need to have adequate physiological/sensory properties, such as the sense of touch, ductility, color, and smell, in addition to pharmaceutical or pharmacological properties (*14*). As patients apply ointment or cream preparations to an affected site with their hands, low-ductility viscous preparations may be difficult to apply. A study suggested the necessity of improving a base, considering patients' availability or comfortableness (*15*).

For the use of an external preparation, a preparation with a pH similar to that of the skin surface should be selected. Non-stimulant preparations are recommended for affected sites. The pH of the epidermis is neutral, but that of the corneal layer is weakly acid. The pH of the skin surface ranges from 4.5 to 6.0 (*16*). Therefore, a pH of 4.5 to 6.0 may be optimal for external preparations, being similar to that of the skin surface. In particular, the use of an external preparation may deteriorate symptoms in sensitive-skin patients; a preparation with a pH similar to that of the skin surface should be selected to reduce the risk.

Based on the results of this experiment, the pH values of the generic products ranged from 4.3 to 5.5. Product F showed a slightly lower value (4.3), but the values of the other products were within the pH range of healthy skin (4.5 to 6.0). Therefore, there may have been no influence on the skin (Figure 1).

With respect to the ductility of various cream preparations, a semilog graph was prepared using a spread meter by plotting the spread diameter (cm) of each preparation on a longitudinal axis and the time (seconds) on a transverse axis. The linear expression of a logarithmic trendline for the plot was induced. The slope of this linear expression for Lamisil was 0.24, and the y-intercept was 3.05. Regarding these values as criteria, preparations with a greater slope can be evaluated as more ductile, and those with a higher y-intercept as less viscous (Figures 2 and 3). Initially, the ductility of a generic product (Taiyo) with a slope of 0.36, which was a maximum, was considered to be favorable, whereas that of Viras, with a slope of 0.02, which was a minimum, was considered to be unfavorable (Figure 2). On the other hand, generic products of which the y-intercept values were relatively high, Mylan (3.33), Sandoz (3.29), and Taiyo (3.28), were considered to be less viscous. These products may be spread with a weak force. Furthermore, the y-intercept value of Viras (2.55) was significantly lower; this preparation may be very viscous, requiring a strong force for spreading (Figure 3).

The yield value refers to a stress limiting the deformation/floating of semisolid substances, such as cream and ointment preparations; therefore, it is used as an index of easiness to apply. Preparations with a lower yield value may be more easily applied. A generic product of which the yield value was high (1,621.0 dyn/cm^2), Viras, was considered to be difficult to apply. The yield value of Taiyo (42.1 dyn/cm^2) was approximately 1/39 of that of Viras; therefore, Taiyo may be spread with a weak force (Figure 4). These results suggest that the sense of use markedly differs among the preparations.

The squeeze force of each cream preparation was measured using a HapLog®. A dose of most products, excluding Viras (15.4 N) and Sandoz (13.7 N), could be squeezed with a force similar to or weaker than that required for squeezing Lamisil (12.9 N). This may have been related to the rigidity of the container (Figure 5). Using a HapLog®, we detected the intensity of forces on fingers in contact with the container, and successfully assessed the sensor-wearing person's finger contact force while maintaining the free sense of touch at the fingertip (*13*).

Based on the results of this study, it may be important

for pharmacists to understand the pharmaceutical properties of many generic products in comparison with a brand-name drug in order to meet various patient needs. Considering the physicochemical properties of each preparation, an adequate drug must be selected in accordance with individual patients' skin conditions.

Acknowledgements

The authors thank Mr. Yusuke Gokan for providing technical assistance in some parts of experimentation. We also thank Mr. Yukimitsu Suda, Frontier Science Business Division, Shiseido Co., Ltd., for supplying HapLog®.

References

1. 2012 national health care costs overview. Ministry of Health, Labor and Welfare, *http://www.mhlw.go.jp/toukei/saikin/hw/k-iryohi/12/dl/data.pdf* (accessed December 25, 2017). (in Japanese)
2. Promotion of use of generic drugs (generic drugs). Ministry of Health, Labor and Welfare, *http://www.mhlw.go.jp/stf/seisakunitsuite/bunya/kenkou_iryou/iryou/kouhatu-iyaku/* (accessed December 25, 2017). (in Japanese)
3. Wada Y, Nozawa M, Goto M, Shimokawa K, Ishii F. Generic selection criteria for safety and patient benefit [I] Comparing the original drugs and generic ones in pharmaceutical properties. J Comm Pharm Sci. 2014; 6:97-105. (in Japanese)
4. Nozawa M, Wada Y, Yamazaki N, Shimokawa K, Ishii F. Generic selection criteria for safety and patient benefit [II] Physicochemical characteristics of original and generic drugs for three different difluprednate-containing preparations (ointment, cream, and lotion). J Jpn Soc Comm Pharm. 2014; 2:37-48. (in Japanese)
5. Wada Y, Nozawa M, Goto M, Shimokawa K, Ishii F. Generic selection criteria for safety and patient benefit [III] Comparing the pharmaceutical properties and patient usability of original and generic ophthalmic solutions containing timolol maleate. J Jpn Soc Pharm Health Sci. 2015; 41:394-403. (in Japanese)
6. Wada Y, Ami S, Nozawa M, Goto M, Shimokawa K, Ishii F. Generic selection criteria for safety and patient benefit [V]: Comparing the pharmaceutical properties and patient usability of original and generic nasal spray containing ketotifen fumarate. Drug Discov Ther. 2016; 10:88-92.
7. Wada Y, Kihara M, Nozawa M, Shimokawa K, Ishii F. Generic selection criteria for safety and patient benefit [IV] Physicochemical and pharmaceutical properties of brand-name and generic ketoprofen tapes. Drug Discov Ther. 2015; 9:229-233.
8. Wada Y, Takaoka Y, Nozawa M, Goto M, Shimokawa K, Ishii F. Generic selection criteria for safety and patient benefit [VI]: Comparing the physicochemical and pharmaceutical properties of brand-name, generic, and OTC felbinac tapes. Drug Discov Ther. 2016; 10:300-306.
9. Watanabe K, Nakamura S, Shimamoto T, Uramatsu S, Kishi K, Uemura T, Shinike H. Preparation and evaluation of new metronidazole gel using hydroxypropyl methylcellulose. Jpn J Pharm Palliat Care Sci. 2009; 2:39-43. (in Japanese)
10. Yoshida M. Extensibility of beesoften oil cream at various temperatures of 0.3%. Jpn J Med Pharm Sci. 2014; 71:449-454. (in Japanese)
11. Komoda M, Akakuma S, Obara S, Koto A, Aono H, Kurahashi Y, Sugiyama N, Ishi N, Noda Y. Basic examination of bicarbonate sugar ointment neutralized reaction of leakage from gastrostomy fistula. Jpn Soc Par Ent Nutr. 2013; 28:819-825. (in Japanese)
12. Haptic Skill Logger, Kato Tech Co., Ltd. *http://english.keskato.co.jp/* (accessed December 25, 2017).
13. Nakatani M, Kawasoe T. Haptic Skill Logger (HapLog): The wearable sensor for evaluating haptic behaviors. J Robot Soc Jpn. 2012; 30:499-501. (in Japanese)
14. Shibata Y, Ikeda H, Kondou Y, Kihara K. Comparison of pharmaceutical properties of topical non-steroidal anti-inflammatory drug preparations on quality of life. Yakugaku Zasshi. 2005; 125:397-404. (in Japanese)
15. Nishizawa S, Yamaoka K, Yamaoka H, Yoshimura K, Hirabayashi S. Basic pharmaceutical research on formulation of kojic acid ointment for hospitals: *in vitro* releace test and evaluation of permeability. Jpn J Pharm Health Care Sci. 2004; 30:20-26. (in Japanese)
16. Mizoguchi M, Ohara K, Aiba Y, Takado T, Hino H, Matsunaga K, Watanabe S. The pH of the skin. In: Encyclopedia of skin. Asakura Bookstore, Tokyo, 2008; pp. 24. (in Japanese)

(Received December 27, 2017; Revised February 6, 2018; Accepted February 9, 2018)

Original Article

DOI: 10.5582/ddt.2017.01068

Anesthetic activity of plant essential oils on *Cyprinus carpio* (koi carp)

Nattakanwadee Khumpirapang[1,2], Surachai Pikulkaew[3], Songyot Anuchapreeda[4], Siriporn Okonogi[2,5,*]

[1] *Interdisciplinary Program in Nanoscience and Nanotechnology, Graduate School, Chiang Mai University, Chiang Mai, Thailand;*
[2] *Research Center of Pharmaceutical Nanotechnology, Chiang Mai University, Chiang Mai, Thailand;*
[3] *Department of Food Animal Clinic, Faculty of Veterinary Medicine, Chiang Mai University, Chiang Mai, Thailand;*
[4] *Department of Medical Technology, Faculty of Associated Medical Sciences, Chiang Mai University, Chiang Mai, Thailand;*
[5] *Department of Pharmaceutical Sciences, Faculty of Pharmacy, Chiang Mai University, Chiang Mai, Thailand.*

Summary **The aims of this study were to investigate the anesthetic and cytotoxic effects of essential oils (EOs) of *Ocimum basilicum* (OBO), *O. canum* (OCO), and *O. sanctum* (OSO) on *Cyprinus carpio* (koi carp). For anesthetic effect, induction time to surgical anesthesia and recovery time were determined. For cytotoxicity effect, viability of fish peripheral blood nuclear cells (PBMCs) was investigated. Results indicated that increasing oil concentration caused significant ($p < 0.01$) decrease of induction time. OSO at 100, 200, and 300 mg/L gave the induction time of 169.5 ± 10.2, 62.8 ± 2.3, 45.3 ± 2.2 sec, respectively, significantly shorter than OCO, and OBO. The recovery time of anesthetized fish was dose dependent ($p <0.01$). Among them, OCO showed the longest recovery time of 313.0 ± 8.1, 420.7 ± 12.6, 616.6 ± 12.1 sec for concentrations of 100, 200, and 300 mg/L, respectively, followed by OSO and OBO, respectively. Within 10 min contact time of the EOs and fish PBMCs, the fish PBMC viability was higher than 80%. Increase contact time and EO concentration caused an increase in cytotoxicity to fish PBMC. OBO showed less toxic than OSO and OCO. Based on the desired induction and recovery times for anesthetizing koi carp, OBO, OCO, and OSO at 300, 200, and 100 mg/L, respectively were suggested to be the most suitable. It was concluded that OBO, OCO, and OSO can be used as natural anesthetics for fish.**

Keywords: Anesthetic activity, cytotoxicity, *Ocimum basilicum*, *Ocimum canum*, *Ocimum sanctum*

1. Introduction

Stress in fish can be induced by physical, chemical, and perceived factors. These factors can evoke several physiological responses in fish (*1*). Handling, capture, transport, and confinement are the most common physical stress factors. Generally, when fish are subjected to the physical stress they show physiological stress response by escape attempts (*2*). Physical stress can cause many undesirable responses such as the changes in circulating catecholamines and corticosteroids, resulted in a changes in metabolism, haematological features, immune function features, stress protein, osmoregulatory disturbance, reduction of egg quality, spermatocrit, and growth as well as a decrease in disease resistance leading to increase of susceptibility to diseases or illness *(3,4)*.

Normally, anesthetics have been used to immobilize and reduce metabolism in fish, thereby improve stress response of fish (*5*). There are several chemical anesthetics available for aquatic animals, such as tricaine methanesulfonate (MS-222), benzocaine, quinaldine, 2-phenoxyethanol, and metomidate (*6*). These anesthetics involve the central nervous system by either enhancing inhibitory signal or blocking excitatory signals with different target binding (*7*). The choice of anesthetics depends on several factors such as safety,

Released online in J-STAGE as advance publication February 25, 2018.

*Address correspondence to:
Dr. Siriporn Okonogi, Department of Pharmaceutical Sciences, Faculty of Pharmacy, Chiang Mai University, Chiang Mai 50200, Thailand.
E-mail: okng2000@gmail.com

cost, and comfortable use (*8*). However, these chemical anesthetics have a long withdrawal period before human consumption (*9*). MS-222 is currently approved by the United States Food and Drug Administration (*10*), but the fish exposed to MS-222 require a long withdrawal period (21 days) for being released into the environment or sold for human consumption (*11*). Importantly, MS-222 is suspected as a carcinogenic agent in human (*12*). According to these issues, anesthetics from natural sources such as plants, particularly the edible plants, are of increasing interest.

The essential oil (EO) of certain plants has been recognized to have anesthetic activity. Clove oil, an EO from flower buds of clove tree (*Syzygium aromaticum*) is the most common agent used to immobilize fish (*13,14*). The anesthetic activity of clove oil is considered to be due to eugenol and eugenol derivatives existing in the EO (*15*). Literature review on phytochemistry and the related activities demonstrates that eugenol containing plant has anesthetic effect in fish. Moreover, EO from *Ocimum gratissimum* which is rich in eugenol, has been reported to have anesthetic activity in *Rhamdia quelen* (silver catfish) (*16*) and *Paralichthys orbignyanus* (Brazilian flounder) (*17*). Interestingly, the EOs of certain plants in Lamiaceae such as *O. basilicum*, *O. canum*, and *O. sanctum* were reported to contain eugenol and its derivatives (*18-20*). However, they have not yet been studied or used for fish anesthesia. Plants in genus *Ocimum* are found primarily in the tropical regions of Asia, Africa, and central and south America (*21*). *O. basilicum*, *O. canum*, and *O. sanctum* are edible plants and have been historical used as food or food additives in Thai and other Asian cuisines. The use in food remedies of these plants can basically prove their safety for human consumption. They also have been used as Asian folk medicine because they have been reported to exert a variety of biological activities such as anti-proliferative activity against cancer cells, anti-microbial and anti-fungal activities (*22,23*), and anti-oxidative activity (*24*). These plants are widely grown in Thailand and many Asian countries. Their advantages on low cost, safety, ease of raw plant material collecting, and high existing of potential compounds (eugenol and eugenol derivatives) are of most interest for investigation as an alternative fish anesthetics.

Koi carp, the Japanese ornamental carp, became an appreciated and expensive pet worldwide (*25*). Due to their distinctive color and scale patterns, this fish becomes the most popular for outdoor ornamental (*26*). Currently, handling and transportation of this fish is increasing leading to the increase in demand for anesthetics to decrease the fish stress according to these physical processes. Therefore, koi carp was selected to use as a fish model in the present study. This study aimed to investigate the anesthetic efficacy of EO from Thai medicinal plants (*O. basilicum*, *O. canum*, and *O. sanctum*) on this fish and cytotoxic effect of these EOs was also evaluated for safety issue.

2. Materials and Methods

2.1. *Chemicals*

Absolute ethanol and phosphate buffer solution (PBS) were from Merck Millipore (Darmstadt, Germany). Dimethyl sulfoxide (DMSO), 3-(4,5-Dimethylthiazol-2-yl)-2,5-diphenyltetrazolium bromide (MTT), and MS-222 were of Sigma-Aldrich (St Louis, MO, USA). Lymphoprep was from Axis-Shield PoC AS (Oslo, Norway). RPMI 1640, fetal bovine serum, L-glutamine, and penicillin-streptomycin were from GIBCO Invitrogen™ (New York, USA).

2.2. *Fish and rearing conditions*

Healthy juvenile (weight; 9.7 ± 0.1 g and total length; 9.2 ± 0.1 cm) and adult (weight; 251.4 ± 4.6 g and total length; 20.9 ± 2.7 cm) koi carp were purchased from an ornamental fish shop located in Chiang Mai, Thailand. The fish were stocked in a 300 L tank and maintained under laboratory conditions. During acclimatization, the dechlorinated tap water was changed daily (50%). The fish were fed with a commercial pelletized diet (INTEQC Feed, Thailand) and held under natural light condition. After maintenance at these conditions for 2-4 weeks, the fish were starved for 24 h prior to the experiments. The studies were conducted according to a permission obtained by the Animal Care and Committee of the Faculty of Veterinary Medicine, Chiang Mai University (FVM-ACUC) (Process no. R3/2555).

2.3. *Plant materials*

O. basilicum, *O. canum*, and *O. sanctum* were collected from the medicinal plant garden of Chiang Mai University, Chiang Mai, Thailand in December 2015. After identification, the voucher specimens were deposited at the Herbarium, Faculty of Pharmacy, Chiang Mai University, Thailand (collection No. 009802, 009819, and 009810, respectively).

2.4. *Extraction and analysis of EOs*

OBO, OCO, and OSO were obtained from the fresh aerial parts of *O. basilicum*, *O. canum*, *O. sanctum*, respectively by hydro-distillation for 3 h. The obtained EOs of each plant was stored in a light-resistant container at – 20°C for further studies.

Chemical analysis of the obtained EOs was performed using gas chromatography-mass spectrometry (GC-MS) on an Agilent 6890 gas chromatography coupled to electron impact (70 eV) and a Hewlett Packard (HP) mass selective detector (HP 5973-MSD). The HP5-MSI; 30.0 m × 0.25 mm

Table 1. Behavior of *Cyprinus carpio* (koi carp) in various stages of anesthesia and recovery from anesthesia

Stages	Description	Exhibited behavior
0	Normal	Normal
1	Light sedation	Fish are disoriented
2	Excitatory stage	Fish reduced swimming activity and show partial loss of equilibrium
3	Surgical stage	Fish stopped their swimming activity, experienced a total loss of equilibrium, and had no responsiveness
4	Death stag	Death; respiration stopped
Recovery		Retaking of swimming activity, equilibrium, and responsiveness

i.d. × 0.25 µm film thickness (Agilent Technologies Inc, USA) was used as a capillary column for GC-MS. The analytical conditions used were modified from the previous study (*27*). Briefly, the injector temperature was 250°C, the oven temperature conditions were as follows: 3 min isothermal at 70°C, then increased at the rate of 3°C/min to 188°C and then at 20°C/min to 280°C (3 min isothermal), and the detector temperature was 280°C. The EO sample was diluted with dichloromethane to 1:100 (v/v). Injection volume was 1 µL. Identification of the compounds was performed based on comparing their retention times and mass spectra relative to those of spectral peaks available in Wiley and the National Institute of Standards and Technology; NIST mass spectral libraries.

2.5. *In vivo anesthetic activity of EOs*

The anesthetic activity of OBO, OCO, and OSO was studied in juvenile koi carp. MS-222 was used as a positive control. The EO was diluted to 1:10 (v/v) with absolute ethanol. MS-222 was dissolved in deionized water to a concentration of 10 g/L and adjusted to pH 6.5-7.5 by sodium bicarbonate. Two hundred sixty fish were divided into 13 groups, each group contained 20 individual fish in an aquarium containing 7 L of dechlorinated tap water (15 × 30 × 22.5 cm) and used for each EO type and concentration. The tanks (10 × 10 × 15 cm glass aquarium) contained 1 L of dechlorinated water were prepared for anesthesia tanks. The diluted EO or MS-222 stock solution was added to the tank until reaching the final concentrations of 100, 200, and 300 mg/L. A tank contained 0.3% (v/v) absolute ethanol in dechlorinated water was used as a vehicle control. The ethanol concentration of the control tank was the same as the maximum amount used in the anesthetic tank. The fish was placed into the anesthesia tank one by one and each fish was used only once. The anesthetic activity was evaluated by comparing the induction time that the fish required to reach a surgical stage of anesthesia after exposure to the EO. The stages of anesthesia were assessed in accordance with fish behavioural responses adapted from McFarland (*28*) and Zahl *et al*. (*29*) (as described in Table 1). The body part near the caudal fin of the fish was pressed with forceps in order to confirm that the fish reached stage 3 which is a surgical stage of anesthesia. The maximum observation time was 20 min. After reaching at the surgical stage of anesthesia, the fish were immediately transferred to anesthetic free tank to be recovered from the anesthesia. The recovery time was recorded after the fish completely recovered.

2.6. *Cytotoxicity study of EOs*

Determination of normal peripheral blood nuclear cells (PBMCs) was performed using MTT colorimetric assay. This assay is based on the ability of viable cells to metabolize a water-soluble tetrazolium salt into a water-insoluble formazan product. Thirty adult koi carp were placed one by one into the anesthesia tank (20 × 40 × 25 cm) containing 100 mg/L MS-222 in 15 L of dechlorinated tap water in order to be anesthetize to stage 3 of anesthesia. Blood samples (20 mL) from six healthy fish were collected by venipuncture of the caudal vessel and kept in heparin-coated test tubes. The fish blood was diluted (1:1 v/v) with 0.1 M phosphate buffer solution (PBS) and further diluted (3:1 v/v) with Ficoll-Hypaque. The fish PBMCs were collected after centrifuging at 3,000 rpm for 30 min and washed three times with PBS. Complete RPMI 1640 medium (10% FBS, 100 unit/mL of penicillin, 100 µg/mL of streptomycin, and 1 mM of L-glutamine) was used to resuspend PBMCs. The PBMCs (1×10^6 cells) suspension in 100 µL medium were seeded into 96-well plates and incubated for 24 h at 37°C, 5% CO_2 and 95% relative humidity. An exact amount of 100 µL of the fresh medium containing various concentrations (100, 200, 300, 400, and 500 mg/L) of EOs dissolved in DMSO (100 mg/mL) was added into each well and incubated for 10 min, 1, 6, and 12 h. After that, 100 µL of the medium was removed, 15 µL of MTT dye solution (5 mg/L in PBS) was added to each well. After 4 h of incubation, the supernatant was removed and 200 µL DMSO was added to each well to dissolve formazan crystals. Using an AccuReaderTM M965/965+ microplate reader (Metertech Inc., Taiwan), the absorbance was measured at 578 nm and corrected by a reference wavelength of 630 nm. Solution of 1.0% of DMSO in RPMI 1640 complete medium was used as a reference control. All experiments were performed in triplicate. The percent of cell viability was calculated

using the following equation.

$$\text{Cell viability (\%)} \frac{\text{mean absorbance of treatment}}{\text{mean absorbance of reference}} \times 100$$

2.7. *Statistical analysis*

Data are presented as means ± S.E.M. and normality of the data was checked using Kolmogorov-Smirnov's test. The ANOVA followed by Tukey's post hoc test was used to analyze anesthetic activity and cytotoxicity study. The values of $p < 0.05$ were considered as statistically significant.

3. Results

3.1. *Extraction and analysis of EOs*

Hydrodistillation for 3 h of three plants yielded different amount of EOs. The highest yield (0.24%) was from *O. basilicum*. The yields of EOs obtained from *O. canum* and *O. sanctum* were only 0.14% and 0.18%, respectively. OBO appeared as a clear pale yellowish liquid similar to OSO. The outer appearance of OCO was slightly different. It was a clear liquid with intense yellowish orange. GC-MS analysis of OBO showed that there were 20 identifiable components which represented 96.74% of the total compounds in the EO whereas there were 13 compounds presented in OCO and 14 compounds in OSO, which represented 92.09% and 91.27% of the total compounds in OCO and OSO, respectively (Table 2). The major component of OBO was methyl chavicol (78.12%). Other main compounds existing in this EO but far less amount than methyl chavicol were 1,8-cineole (3.54%) and trans-α-bergamotene (3.02%). Eugenol was not found in OBO but methyl eugenol was found instead but at very low amount (0.44%). Major compounds of OCO were E-citral (41.01%) and Z-citral (37.04%) whereas that of OSO were methyl eugenol (46.18%) and eugenol (11.56%).

3.2. *Anesthetic activity of EOs*

It was found that increasing concentration of EO as well as MS-222 significantly ($p < 0.05$) decreased the induction time for fish anesthesia (Figure 1). No

Table 2. Chemical compounds existing in OBO, OCO, and OSO

Retention time (min)	Components	Percentage of chemical compound		
		OBO	OCO	OSO
4.08	α-Pinene	0.09	0.09	0.09
4.39	Camphene	-	-	-
4.93	Sabinene	0.09	0.09	0.09
5.03	β-Pinene	0.17	0.17	0.17
5.33	β-Myrcene	0.29	0.29	0.29
6.43	Limonene	0.19	0.19	0.19
6.60	1,8-Cineole	3.54	3.54	3.54
7.02	1,3,6-Octatriene	2.37	2.37	2.37
8.35	Terpinolene	0.16	0.16	0.16
8.79	Linalool	0.53	0.53	0.53
10.42	L-Camphor	1.49	1.49	1.49
11.23	Borneol	0.57	0.57	0.57
11.32	α Terpineol	-	-	-
13.04	Methyl chavicol	78.12	78.12	78.12
14.74	Z-Citral (Neral)	-	-	-
15.38	Geraniol	-	-	-
16.11	E-Citral (Geranial)	-	-	-
18.66	α-Cubebene	-	-	-
19.23	Eugenol	-	-	-
19.76	α-Copaene	-	-	-
20.55	β-Elemene	0.70	0.70	0.70
21.43	Methyl eugenol	0.44	0.44	0.44
21.81	β-Caryophyllene	-	-	-
22.21	Trans-α-Bergamotene	3.02	3.02	3.02
22.79	β-Selinene	0.34	0.34	0.34
23.08	β-Farnesene	-	-	-
23.90	Germacrene-D	1.36	1.36	1.36
24.10	Trans-β-Farnesene	0.23	0.23	0.23
25.10	β-Bisaboloene	-	-	-
25.66	β-Sesquiphellandrene	0.25	0.25	0.25
26.48	Cis-α-Bisabolene	-	-	-
30.08	δ-Cadinene	2.79	2.79	2.79
Total		96.74	96.74	96.74

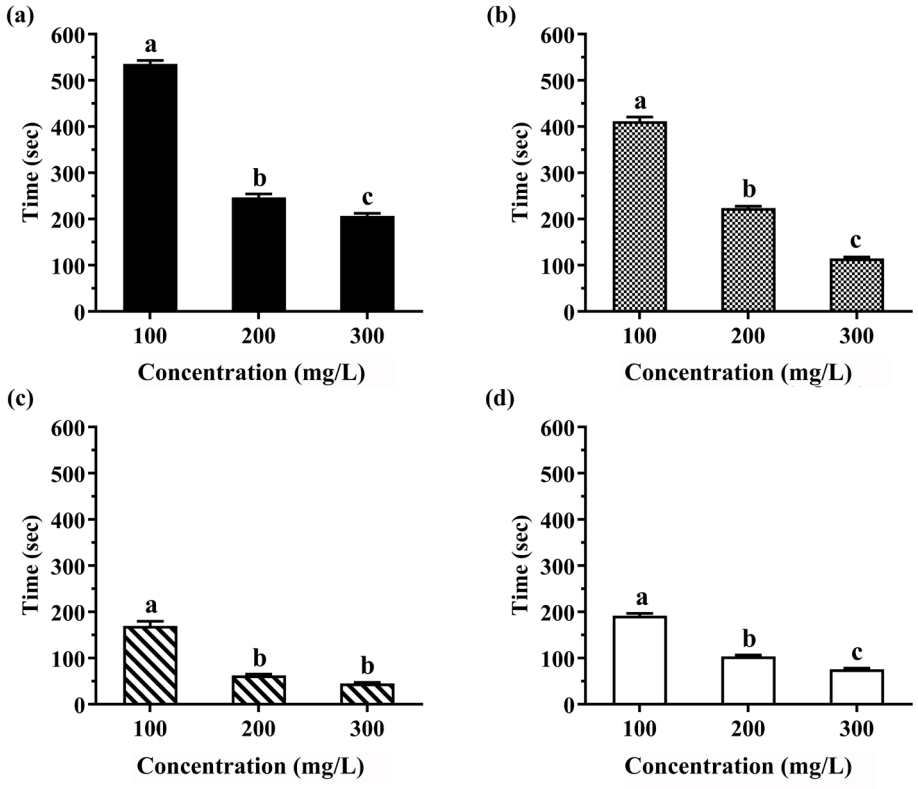

Figure 1. Induction time for koi carp (n = 20) exposed to 100, 200, and 300 mg/L of OBO (a), OCO (b), OSO (c), and MS-222 (d) to reach the surgical anesthesia stage. Data are presented as means ± S.E.M. ($p < 0.001$).

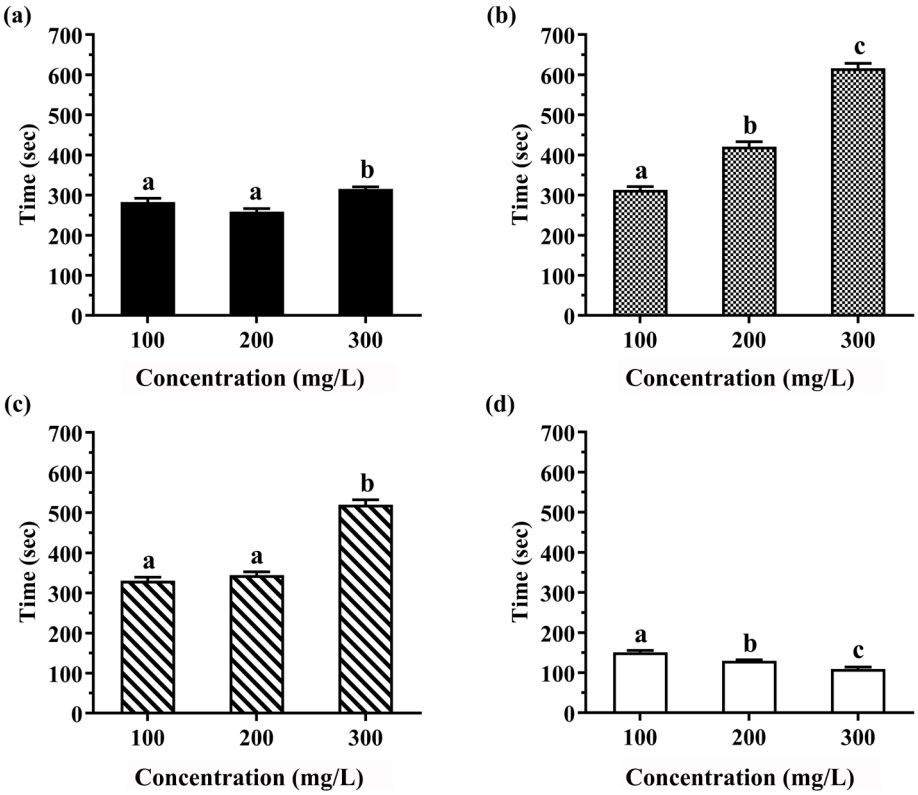

Figure 2. Recovery time for koi carp (n = 20) exposed to 100, 200, and 300 mg/L of OBO (a), OCO (b), OSO (c), and MS-222 (d). Data are presented as means ± S.E.M. ($p < 0.01$).

mortality of the fish was found after receiving the EOs at all tested concentrations (100, 200, and 300 mg/L). Data analysis using two-way ANOVA indicated that not only EO type but also EO concentration played a significant role on anesthetic effect ($p < 0.001$). Moreover, the EO type × EO concentration interaction also showed significant ($p < 0.001$). Within the same final concentration, OSO revealed the shortest induction time of all stages of anesthesia. The induction times for anesthesia (stage 3) caused by OSO at 100, 200, and 300 mg/L were 169.5 ± 10.2, 62.8 ± 2.3, 45.3 ± 2.2 sec, respectively. Moreover, it was found that at these concentrations, the induction time to the surgical anesthesia of the fish caused by OSO was significantly shorter than that caused by MS-222 ($p < 0.05$). OBO at 100, 200, and 300 mg/L showed longest induction times of approximately 535, 250, and 205 sec, respectively. It was observed that after exposure to OBO and OCO, the fish showed slightly mucous secretions.

The EO type and concentration also showed a major effect on the recovery time ($p < 0.001$ (Figure 2). The EO type × concentration interaction showed significant ($p < 0.001$). While ethanol at 0.3% v/v neither sedated the fish nor provided any undesirable side effect to the fish. The recovery time of the fish anesthetized by MS-222 was faster than those anesthetized by the EOs and the effect was not dose dependent. The recovery time of the fish anesthetized by the EOs was dose dependent ($p < 0.01$). The anesthetized fish caused by OCO showed the longest recovery time at concentration of 100, 200, and 300 mg/L (313.0 ± 8.1, 420.7 ± 12.6, 616.6 ± 12.1 sec, respectively), followed by those anesthetized by OSO (330.4 ± 8.5, 344.5 ± 8.1, 520.0 ± 12.3 sec, respectively) and OBO (282.9 ± 9.0, 258.6 ± 7.7, 315.1 ± 5.4 sec, respectively).

3.3. *Cytotoxicity study of EOs*

Direct contact of fish PBMCs to the EOs demonstrated some difference. All tested EOs exhibited concentration and time dependent toxicity to the fish but at different levels ($p < 0.05$) (Figures 3-5). OBO showed the least toxicity among them. More than 80% of fish PBMCs survived after exposure to all concentrations of the EOs (100, 200, 300, 400, and 500 mg/L) for 10 min and those exposed to 100 mg/L OBO for 1, 6, and 12 h. Although an elevation of EO concentration and exposure time increased toxicity to the fish PBMCs, at high concentrations of 300-500 mg/L, OBO showed significantly lower cytotoxic than OCO and OSO.

4. Discussion

Our investigation started with the extraction of EOs from the fresh raw plant materials followed by chemical analysis of the EOs using GC-MS and then the *in vivo* test in koi carp. We found that OBO, OCO, and OSO had strong effect on fish anesthesia. The yield of OBO obtained was similar with that extracted from *O. basilicum* grown in Australia (*30*), whereas the yield of OCO and OSO from *O. canum* and *O. sanctum*, respectively, less than the previous reports (*31,32*). The variation of yield as well as chemical races in the producing plant species are often affected by

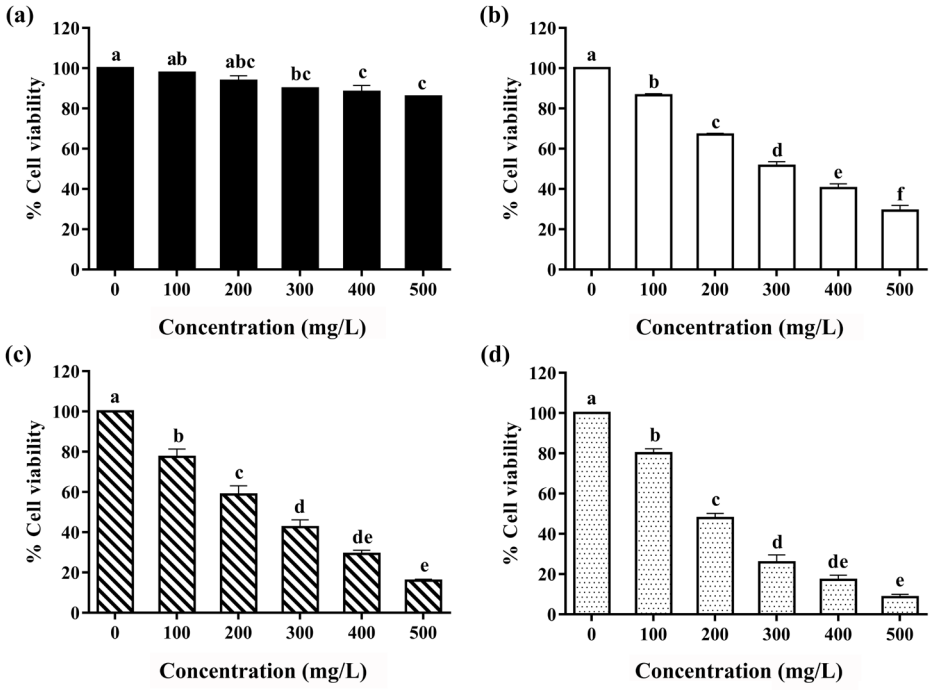

Figure 3. Dose-response curves of viability of koi carp PBMCs exposed to OBO at 10 min (a), 1 h (b), 6 h (c), and 12 h (d). Data are presented as means ± S.E.M. ($p < 0.05$).

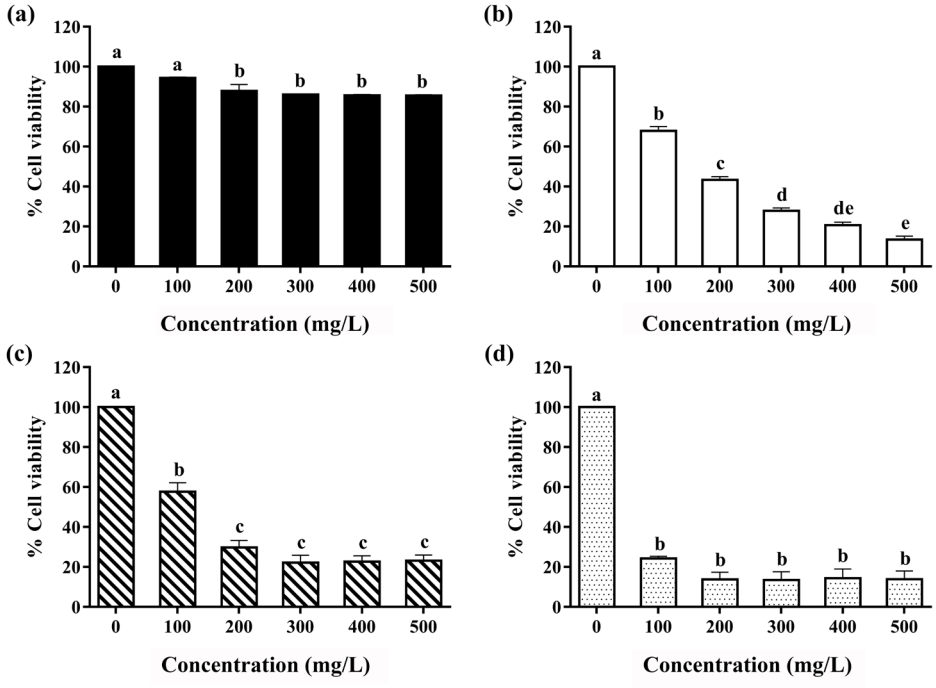

Figure 4. Dose-response curves of viability of koi carp PBMCs exposed to OCO at 10 min (a), 1 h (b), 6 h (c), and 12 h (d). Data are presented as means ± S.E.M. ($p < 0.05$).

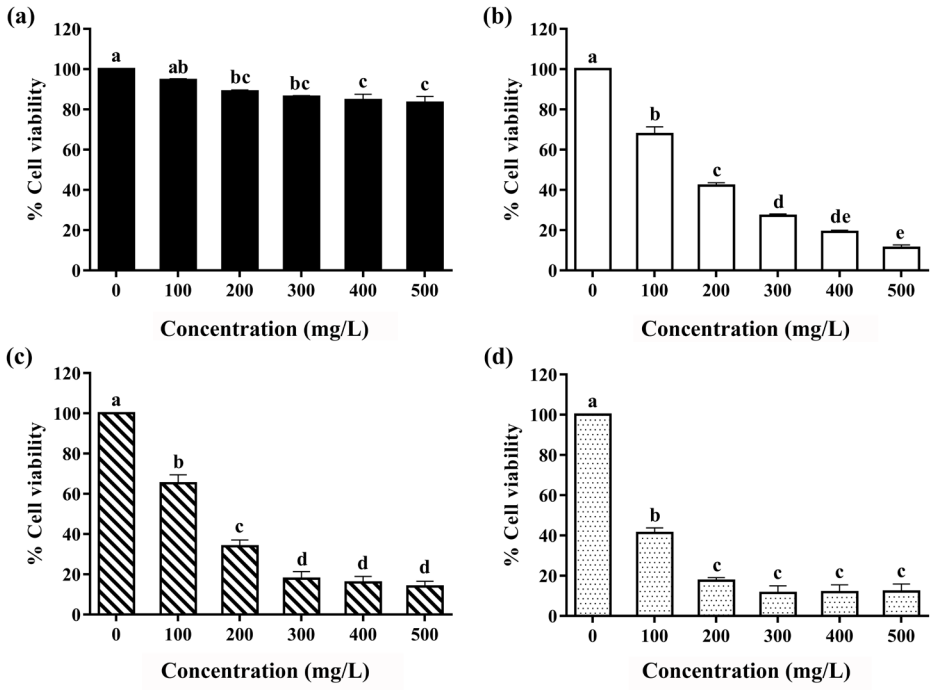

Figure 5. Dose-response curves of viability of koi carp PBMCs exposed to OSO at 10 min (a), 1 h (b), 6 h (c), and 12 h (d). Data are presented as means ± S.E.M. ($p < 0.05$).

environment conditions; geographic variations, genetic factors, and harvest period of plants (*33*). In the present study, chemical analysis of the EOs indicated that compounds existing in OBO contained no eugenol and very low amount of eugenol derivatives (0.44% methyl eugenol). Our study found that methyl chavicol was the major constituent (78.12%) of OBO. This finding was in good agreement with the reports of Grayer *et al*. (*34*) and Hasegawa *et al*. (*35*). From the previous study, methyl chavicol showed the anesthetic activity in rats by direct inhibition of sodium channels, the major cause of excitability blockade (*36*). Therefore,

the fish anesthetic activity of OBO presented in the present study is considered to be mainly due to methyl chavicol.

OCO was previously reported to have different major compounds such as camphor (*37,38*), 1,8-cineole (*39*), citral (*40*), eugenol (*41*), geraniol (*32*), and linalool (*42*). However, in the present study, E-citral (41.01%) and Z-citral (37.04%) were found at the highest level in this EO. Even though, eugenol and its derivatives were not found, OCO showed the anesthetic activity in the fish. It was previously reported that E-citral and Z-citral had the anesthetic activity on white shrimps (*Litopenaeus vannamei*) (*43*) and Wistar rats (*Rattus norvegicus*) (*44*). Therefore, the fish anesthetic activity of OCO as found in the current study is considered to be due to these two isomers of citral. For OSO, eugenol was previously reported to be a major compound existing in this EO (*19,45*). In the current study, methyl eugenol (46.18%) was the most abundant. Eugenol was also existed (11.56%) but significantly lower amount than methyl eugenol. These results are similar to the findings of the other previous reports (*46-48*). Methyl eugenol has been reviewed to have anesthetic activity (*49*). Thus, the fish anesthetic effect of OSO is considered to be mainly due to methyl eugenol and the minor effect of eugenol. Among the three EOs, OSO showed the shortest induction time indicating the highest anesthetic activity, followed by OCO and OBO. The ideal anesthetic agent should meet the major criteria of high capability of rapid induction to surgical anesthesia within 3 or 5 min and the fish should recover within 5 min in anesthetic-free water. The recovery time should not be longer than two-fold of the induction time and no mortality should be occurred (*50*). Based on these criteria, the appropriated concentration for koi carp anesthesia of OBO, OCO, and OSO was 300, 200, and 100 mg/L, respectively.

An ideal fish anesthetic should also be non-toxicity to fish, low cost, causing rapid anesthesia without any side effects (*50*). The EOs used in the present study are easily extracted using simple distillation and the raw plant materials are easily available and low cost. All studied concentrations of OSO (100-300 mg/L) and 300 mg/L OCO showed a short induction time but very long recovery time. The three EOs showed longer recovery time than MS-222. This effects are considered to be due to the accumulation of lipophilic EOs in adipose tissue of the fish (*51,52*). The lipophilicity of plant EOs is higher than that of MS-222, therefore, the clearance and elimination of EOs was slower than MS-222.

Quantitative analysis of cell viability of fish PBMCs after contact with the EOs could indicate the safety or toxicity of the EOs to the fish. However, for direct contact of the fish PBMCs and the EOs, the EOs showed some toxic at different levels. It was found that the toxicity of OCO was almost same as OSO whereas OBO had significantly lower toxicity on fish PBMCs than OCO and OSO, respectively. The secretion found in the fish exposed to OBO and OCO suggesting some minor side effects. Generally, it is regarded as safe when the cell viability is higher than 80% after exposure to the tested sample (*53*). The maximum induction time of all tested EOs was about 300 sec or 5 min. The results demonstrated that direct contact to the EOs up to 10 min, higher than 80% viability of the PBMCs was still obtained. Therefore, it could be confirmed that OBO, OCO, and OSO were safe for fish anesthesia. High viability of fish PBMC (> 80%) after exposed to 100 mg/L OBO for 1, 6, and 12 h, confirming that OBO was safer than the other two EOs. However, higher EO concentration and longer time of the direct exposure caused higher cytotoxicity to the cells. Because some previous studies have been reported that the whole blood concentrations of MS-222 in *Salmo gairdneri* (rainbow trout) was about 74% of the bath administration concentration after losing of reflex (*54*) and 70% of MS-222 in bath administration concentration was found in blood concentration of *Ictalurus punctatus* (catfish) (*55*). Therefore, our results suggested that it should be careful when high dose of these EOs were used for fish anesthesia particularly for a long period of anesthetized time for example in case of fish operation or long distance transportation.

In conclusion, our findings demonstrate that OBO, OCO, and OSO possess effective anesthetic activity to the fish. Their anesthetic efficacy are due to their respective main components; methyl chavichol for OBO, eugenol for OCO, and methyl eugenol and eugenol for OSO. The anesthetic activity and toxicity of OBO, OCO, and OSO is concentration and exposure time dependent. Using an effective dose within 10 min is confirmed for their anesthetic efficacy and safety. It is concluded that OBO, OCO, and OSO are novel promising natural anesthetics for fish.

Acknowledgements

This work was financially supported by the Thailand Research Fund through the Research and Researchers for Industries grant No. PHD56I0040.

References

1. Barton BA. Stress in fishes: A diversity of responses with particular reference to changes in circulating corticosteroids. Integr Comp Biol. 2002; 42:517-525.
2. Barton BA, Iwama GK. Physiological changes in fish from stress in aquaculture with emphasis on the response and effects of corticosteroids. Annu Rev Fish Dis. 1991; 1:3-26.
3. Wagner E, Arndt R, Hilton B. Physiological stress responses, egg survival and sperm motility for rainbow trout broodstock anesthetized with clove oil, tricaine methanesulfonate or carbon dioxide. Aquaculture. 2002; 211:353-366.

4. Bonga SW. The stress response in fish. Physiol Rev. 1997; 77:591-625.
5. Weber RA, Pérez-Maceira JJ, Peleteiro JB, García-Martín L, Aldegunde M. Effects of acute exposure to 2-phenoxyethanol, clove oil, MS-222, and metomidate on primary and secondary stress responses in Senegalese sole (*Solea senegalensis* Kaup 1858). Aquaculture. 2011; 321:108-112.
6. Stoskopf M, Posner L. Anesthesia and restraint of laboratory fish. In: Anesthesia and analgesia in laboratory animals (Fish R, Danneman P, Brown M, *et al*., eds.). Academic Press, New York, USA, 2008; pp. 519-534.
7. Meyer RE, Fish RE. Pharmacology of injectable anesthetics, sedatives, and tranquilizers. In: Anesthesia and analgesia in laboratory animals (Fish RE, Brown MJ, Danneman PJ, *et al*., eds.). Academic Press, San Diego, USA, 2008; pp. 27-82.
8. Iwama G, Ackerman P. Anaesthetics. In: Analytical techniques in biochemistry and molecular biology of fishes (Hochachka P, Mommsen D, eds.). Elsevier Science, Amsterdam, Netherlands, 1994; pp. 1-15.
9. Cho GK, Heath DD. Comparison of tricaine methanesulphonate (MS222) and clove oil anaesthesia effects on the physiology of juvenile chinook salmon *Oncorhynchus tshawytscha* (Walbaum). Aquacult Res. 2000; 31:537-546.
10. Schnick RA, Meyer FP, VanMeter HD. Announcement of compounds registered for fishery uses. Prog Fish-Cult. 1979; 41:36-37.
11. Nochetto CB, Reimschuessel R, Gieseker C, Cheely CS, Carson MC. Determination of tricaine residues in fish by liquid chromatography. J AOAC Int. 2009; 92:1241-1248.
12. Maricchiolo G, Genovese L. Some contributions to knowledge of stress response in innovative species with particular focus on the use of the anaesthetics. Open Mar Biol J. 2011; 5:24-33.
13. Javahery S, Nekoubin H, Moradlu AH. Effect of anaesthesia with clove oil in fish. Fish Physiol Biochem. 2012; 38:1545-1552.
14. Iversen M, Finstad B, McKinley RS, Eliassen RA. The efficacy of metomidate, clove oil, Aqui-S™ and Benzoak® as anaesthetics in Atlantic salmon (*Salmo salar* L.) smolts, and their potential stress-reducing capacity. Aquaculture. 2003; 221:549-566.
15. Cortés-Rojas DF, de Souza CRF, Oliveira WP. Clove (*Syzygium aromaticum*): A precious spice. Asian Pac J Trop Biomed. 2014; 4:90-96.
16. Silva LD, Parodi T V, Reckziegel P, Garcia VD, Burger ME, Baldisserotto B, Malmann CA, Pereira AMS, Heinzmann BM. Essential oil of *Ocimum gratissimum* L.: Anesthetic effects, mechanism of action and tolerance in silver catfish, *Rhamdia quelen*. Aquaculture. 2012; 350:91-97.
17. Benovit SC, Gressler LT, de Lima Silva L, de Oliveira Garcia L, Okamoto MH, dos Santos Pedron J, Sampaio LA, Rodrigues RV, Heinzmann BM, Baldisserotto B. Anesthesia and transport of Brazilian flounder, *Paralichthys orbignyanus*, with essential oils of *Aloysia gratissima* and *Ocimum gratissimum*. J World Aquacult Soc. 2012; 43:896-900.
18. Lee SJ, Umano K, Shibamoto T, Lee KG. Identification of volatile components in basil (*Ocimum basilicum* L.) and thyme leaves (*Thymus vulgaris* L.) and their antioxidant properties. Food Chem. 2005; 91:131-137.
19. Kumar A, Shukla R, Singh P, Dubey NK. Chemical composition, antifungal and antiaflatoxigenic activities of *Ocimum sanctum* L. essential oil and its safety assessment as plant based antimicrobial. Food Chem Toxicol. 2010; 48:539-543.
20. Vyry Wouatsa NA, Misra L, Venkatesh Kumar R. Antibacterial activity of essential oils of edible spices, *Ocimum canum* and *Xylopia aethiopica*. J Food Sci. 2014; 79:972-977.
21. Simon JE, Quinn J, Murray RG. Basil: A source of essential oils. In: Advances in new crops (Janick J, Simon J, eds.). Timber Press, Portland, USA, 1990; pp. 484-489.
22. Viyoch J, Pisutthanan N, Faikreua A, Nupangta K, Wangtorpol K, Ngokkuen J. Evaluation of *in vitro* antimicrobial activity of Thai basil oils and their micro-emulsion formulas against *Propionibacterium acnes*. Int J Cosmet Sci. 2006; 28:125-133.
23. Sinha GK, Gulati BC. Antibacterial and antifungal study of some essential oils and some of their constituents. Indian Perfum. 1990; 34:126-129.
24. Bunrathep S, Palanuvej C, Ruangrungsi N. Chemical compositions and antioxidative activities of essential oils from four Ocimum species endemic to Thailand. J Heal Res. 2007; 21:201-206.
25. Bar I, Kaddar E, Velan A, David L. Melanocortin receptor 1 and black pigmentation in the *Japanese ornamental* carp (*Cyprinus carpio* var. Koi). Front Genet. 2013; 4:1-11.
26. Xu P, Zhang X, Wang X, Li J, Liu G, Kuang Y, Xu J, Zheng X, Ren L, Wang G. Genome sequence and genetic diversity of the common carp, *Cyprinus carpio*. Nat Genet. 2014; 46:1212-1219.
27. Okonogi S, Chaiyana W. Enhancement of anti-cholinesterase activity of *Zingiber cassumunar* essential oil using a microemulsion technique. Drug Discov Ther. 2012; 6:249-255.
28. McFarland WN. A study of the effects of anaesthetics on the behaviour and physiology of fishes. Publ Inst Mar Sci Univ Texas Austin. 1959; 6:23-55.
29. Zahl IH, Samuelsen O, Kiessling A. Anaesthesia of farmed fish: Implications for welfare. Fish Physiol Biochem. 2012; 38:201-218.
30. Lachowicz KJ, Jones GP, Briggs DR, Bienvenu FE, Palmer MV, Ting SS, Hunter M. Characteristics of essential oil from basil (*Ocimum basilicum* L.) grown in Australia. J Agric Food Chem. 1996; 44:877-881.
31. Kicel A, Kurowska A, Kalemba D. Composition of the essential oil of *Ocimum sanctum* L. grown in Poland during vegetation. J Essent Oil Res. 2005; 17:217-219.
32. Ngassoum MB, Ousmaila H, Ngamo LT, Maponmetsem PM, Jirovetz L, Buchbauer G. Aroma compounds of essential oils of two varieties of the spice plant *Ocimum canum* Sims from northern Cameroon. J Food Compost Anal. 2004; 17:197-204.
33. Chalchat JC, Özcan MM. Comparative essential oil composition of flowers, leaves and stems of basil (*Ocimum basilicum* L.) used as herb. Food Chem. 2008; 110:501-503.
34. Grayer RJ, Kite GC, Goldstone FJ, Bryan SE, Paton A, Putievsky E. Infraspecific taxonomy and essential oil chemotypes in sweet basil, *Ocimum basilicum*. Phytochemistry. 1996; 43:1033-1039.
35. Hasegawa Y, Tajima K, Toi N, Sugimura Y.

Characteristic components found in the essential oil of *Ocimum basilicum* L. Flavour Fragr J. 1997; 12:195-200.
36. Silva-Alves KS, Ferreira-da-Silva FW, Peixoto-Neves D, Viana-Cardoso KV, Moreira-Junior L, Oquendo MB, Oliveira-Abreu K, Albuquerque AA, Coelho-de-Souza AN, Leal-Cardoso JH. Estragole blocks neuronal excitability by direct inhibition of Na^+ channels. Braz J Med Biol Res. 2013; 46:1056-1063.
37. Chagonda LS, Makanda CD, Chalchat J. The essential oils of *Ocimum canum* Sims (basilic camphor) and Ocimum urticifolia Roth from Zimbabwe. Flavour Fragr J. 2000; 15:23-26.
38. Selvi MT, Thirugnanasampandan R, Sundarammal S. Antioxidant and cytotoxic activities of essential oil of *Ocimum canum* Sims. from India. J Saudi Chem Soc. 2015; 19:97-100.
39. Zollo PH, Biyiti L, Tchoumbougnang F, Menut C, Lamaty G, Bouchet PH. Aromatic plants of tropical Central Africa. Part XXXII. Chemical composition and antifungal activity of thirteen essential oils from aromatic plants of Cameroon. Flavour Fragr J. 1998; 13:107-114.
40. Ntezurubanza L, Scheffer JJC, Looman A. Composition of the essential oil of *Ocimum canum* grown in Rwanda. Pharm Weekbl. 1985; 7:273-276.
41. Ekundayo O, Laakso I, Hiltunen R. Constituents of the volatile oil from leaves of *Ocimum canum* Sims. Flavour Fragr J. 1989; 4:17-18.
42. Weaver DK, Dunkel F V, Ntezurubanza L, Jackson LL, Stock DT. The efficacy of linalool, a major component of freshly-milled *Ocimum canum Sims* (Lamiaceae), for protection against postharvest damage by certain stored product Coleoptera. J Stored Prod Res. 1991; 27:213-220.
43. Parodi T V, Cunha MA, Heldwein CG, de Souza DM, Martins ÁC, Garcia LdO, Junior WW, Monserrat JM, Schmidt D, Caron BO. The anesthetic efficacy of eugenol and the essential oils of *Lippia alba* and *Aloysia triphylla* in post-larvae and sub-adults of *Litopenaeus vannamei* (Crustacea, Penaeidae). Comp Biochem Physiol C Toxicol Pharmacol. 2012; 155:462-468.
44. Sousa DG, Sousa SD, Silva RE, Silva-Alves KS, Ferreira-da-Silva FW, Kerntopf MR, Menezes IR, Leal-Cardoso JH, Barbosa R. Essential oil of *Lippia alba* and its main constituent citral block the excitability of rat sciatic nerves. Braz J Med Biol Res. 2015; 48:697-702.
45. Laakso I, Seppänen-Laakso T, Herrmann-Wolf B, Kühnel N, Knobloch K. Constituents of the essential oil from the holy basil or tulsi plant, *Ocimum sanctum*. Planta Med. 1990; 56:527-532.
46. Khan A, Ahmad A, Akhtar F, Yousuf S, Xess I, Khan LA, Manzoor N. *Ocimum sanctum* essential oil and its active principles exert their antifungal activity by disrupting ergosterol biosynthesis and membrane integrity. Res Microbiol. 2010; 161:816-823.
47. Ravid U, Putievsky E, Katzir I, Lewinsohn E. Enantiomeric composition of linalol in the essential oils of Ocimum species and in commercial basil oils. Flavour Fragr J. 1997; 12:293-296.
48. Laskar S, Majumdar SG. Variation of major constituents of essential oil of the leaves of *Ocimum sanctum* Linn. J Indian Chem Soc. 1988; 65:301-302.
49. Sell AB, Carlini EA. Anesthetic action of methyleugenol and other eugenol derivatives. Pharmacology. 1976; 14:367-377.
50. Marking L, Meyer F. Are better anesthetics needed in fisheries? Fisheries. 1985;10:2-5.
51. Guénette SA, Uhland FC, Hélie P, Beaudry F, Vachon P. Pharmacokinetics of eugenol in rainbow trout (*Oncorhynchus mykiss*). Aquaculture. 2007; 266:262-265.
52. Hansen MK, Nymoen U, Horsberg TE. Pharmacokinetic and pharmacodynamic properties of metomidate in turbot (*Scophthalmus maximus*) and halibut (*Hippoglossus hippoglossus*). J Vet Pharmacol Ther. 2003; 26:95-103.
53. Anazetti MC, Melo PS, Durán N, Haun M. Comparative cytotoxicity of dimethylamide-crotonin in the promyelocytic leukemia cell line (HL60) and human peripheral blood mononuclear cells. Toxicology. 2003; 188:261-274.
54. Hunn JB, Schoettger RA, Willford WA. Turnover and urinary excretion of free and acetylated MS 222 by rainbow trout, *Salmo gairdneri*. J Fish Res Board Can. 1968; 25:25-31.
55. Hunn JB, Allen JL. Movement of drugs across the gills of fishes. Annu Rev Pharmacol. 1974; 14:47-54.

(Received November 7, 2017; Accepted November 29, 2017)

Original Article

DOI: 10.5582/ddt.2018.01003

Efficacy of anesthetic rice nanogel on pain reduction in human oral cavity

Sakornrat Khongkhunthian[1,2], Thanapat Sastraruji[3], Srikanjana Klayraung[4], Siriporn Okonogi[2,5,*]

[1] *Department of Restorative Dentistry and Periodontology, Faculty of Dentistry, Chiang Mai University, Chiang Mai, Thailand;*
[2] *Research Center of Pharmaceutical Nanotechnology, Chiang Mai University Chiang Mai, Thailand;*
[3] *Dental Research Center, Faculty of Dentistry, Chiang Mai University, Chiang Mai, Thailand;*
[4] *Program in Biotechnology, Faculty of Science, Maejo University, Chiang Mai, Thailand;*
[5] *Department of Pharmaceutical Sciences, Faculty of Pharmacy, Chiang Mai University, Chiang Mai, Thailand.*

Summary **The aim of this study was to determine the efficacy of two local anesthetic rice nanogels (RNG) on pain reduction from needle insertion in oral cavity. Nanogel base was prepared using modified rice as gelling agent. The average particle size of RNG determined by photon correlation spectrophotometer was 485 ± 70 nm. Lidocaine hydrochloride (LH) and prilocaine hydrochloride (PH) were incorporated into RNG to obtain anesthetic RNG containing 5% and 20% LH or PH. Clinical efficacy test of each gel was performed in oral cavity of 100 healthy volunteers (25-60 years old). Evaluation was done by recording different pain measurements after inserting a needle into buccal mucosa after applying 5% and 20% anesthetic RNG. RNG base (placebo) and commercial anesthetic gels were used as negative and positive controls, respectively. It was found that the pain level in the negative control group was significantly higher than those of the anesthetic groups. Moreover, the pain level of the anesthetic RNG groups were lower than that of the commercial groups, especially in 20% anesthetic groups. For patient's satisfaction, most of the volunteers were appreciated with the anesthetic RNG as well as the commercial gels. They preferred to use high drug content RNG more than those with low drug content or placebo. It can be concluded that the anesthetic RNG has potential clinical efficacy in pain reduction during needle insertion in oral cavity.**

Keywords: Nanogel, lidocaine, prilocaine, anesthetic efficacy, pain relief

1. Introduction

Nobody likes going to the dentist, especially for some people, the problems run deeper and form a phobia. The causes of dental phobia can be many and varied but one of those is painful from needle insertion. The anxiety and fear often occurred in preoperative patients (*1*). Especially in children, anxiety and fear caused negative impression to dental treatment and reflecting in avoidance to dental attendance. However, properly dental management could reduce such a fear (*2*). It was reported that the anxiety was increased according to the poor oral hygiene of the patients and related to low quality of life (*3*). In addition, Armfield and his coworkers found that not only children are afraid of dentists but also adults (*4*). The local anesthetic gel is, therefore, introduced to oral mucosa prior to injection in order to reduce the pain from the needles. However, the efficacy of the available anesthetic gels are not high enough, which might be due to the delivery systems are not well suitable.

Nanoparticle delivery systems have been shown to be effective in protecting drugs from degradation, overcoming biological barriers, and controlling the rate and duration of drug release (*5-7*). Various types of nanoparticle systems have been developed using polymer based nanoparticles (*8-10*). Recently, natural polymers such as chitosan and starch have been used

**Address correspondence to:*
Dr. Siriporn Okonogi, Department of Pharmaceutical Sciences, Faculty of Pharmacy, Chiang Mai University, Chiang Mai 50200, Thailand.
E-mail: okng2000@gmail.com

instead of synthetic polymers (*11,12*). Hydrogels are cross-linked networks of hydrophilic polymers containing a large amount of water. This structure can be used for loading and release of drugs and natural bioactives (*13,14*). Nanogel is an advanced formulation of nano-sized hydrogel particles. Nanogel possesses advantage above its original macroscopic hydrogel that it can be injected in the circulation directly to target tissues and can better deliver their payloads for both local and systemic applications (*15*). It has been reported that nanogels not only protect the drugs from degradation and elimination but also participate actively in the delivery process due to their characteristic properties like adhesive, stimuli-responsive behaviour, softness and swelling to help achieve a controlled response at the target tissues (*16-18*).

Lidocaine and prilocaine are amino amide class local anesthetics (*19*). They are nowadays widely used in dental treatment for pain protection and elimination during treatment and minor surgery (*20,21*). Commercial available semisolid products are gel, cream, and ointment. The gels usually contain only lidocaine at various concentrations of 2-10% as hydrochloride salt form. The creams and ointments usually contain lidocaine alone or in the combination with prilocaine as the base form. However, the commercial available anesthetic gels have poor property on mucoadhesion. Moreover, most of gelling agents commonly used in the gels are of chemical synthetic polymers. We previously reported the advantages of modified rice on high mucoadhesive property and suitable for using as filming or gelling agent in drug delivery systems *via* oral mucosa (*22,23*). We have also developed rice nanogel (RNG) using modified rice as gelling agent and found that type of rice affect the properties including drug release behavior of RNG (*24,25*). Importantly, it has been reported that RNG containing local anesthetics causes no toxicity to oral epithelial cells and no inflammatory effect to oral tissues (*26*). We hypothesized that RNG could increase anesthetic efficacy and patient satisfactory during dental treatment. Therefore, in the present study, efficacy of RNG containing lidocaine or prilocaine at different drug concentrations on pain reduction and patient's satisfaction were investigated.

2. Materials and Methods

2.1. *Materials*

Pharmaceutical-grade lidocaine hydrochloride (LH) and prilocaine hydrochloride (PH) were obtained from Gufic Bioscince Ltd. (Mumbai, India). Sodium hydroxide and glacial acetic acid were from RCI Labscan Co., Ltd. (Bangkok, Thailand). Commercial gel A containing 5% LH was from Septodont Ltd. (Kent ME16 0JZ, UK). Commercial gel B containing 20% benzocaine was from Ultradent Products Inc. (South Jordan, USA). Commercial gel C containing combination of 14% benzocaine, 2% butamben, and 2% tetracaine hydrochloride was from Hager Worldwide Inc. (Maidstone, UK). All other chemicals and solvents were of AR grade or the highest grade available unless otherwise stated.

2.2. *Anesthetic RNG preparation*

Modified rice powder was prepared according to the previous method (*24*) and used as gelling agent. RNG base was prepared by mixing suitable amount of modified rice powder with purified water. The particle size of the obtained RNG base was determined using photon correlation spectroscopy (PCS). The anesthetic RNG containing of LH (LH-RNG) or PH (PH-RNG) were prepared according to the method previously described (*25*). Briefly, exact amount of LH or PH was incorporated into certain amount of RNG base and mixed well until the drug was completely dissolved. Subsequently added with NRG base until the desired concentration of drug was reached. The mixture was further triturated until the obviously transparent anesthetic RNG was obtained.

2.3. *Volunteers and ethical considerations*

One hundred healthy volunteers were recruited from Faculty of Dentistry and Faculty of Pharmacy, Chiang Mai University. The exclusion criteria included having a systemic disease, bleeding disorders, drug allergy, pregnancy, breastfeeding, habits of smoking or alcohol consumption, being under medical treatment with drugs or having acute or chronic infection in oral and maxillofacial region. The study was approved by the Human Experiment Committee of the Faculty of Dentistry, Chiang Mai University (Process No. 26/2556). Written informed consent was obtained from all volunteers prior to study.

2.4. *In vivo study of pain reduction*

The study was designed to be double-blind randomized trial. The LH-RNG and PH-RNG were prepared by an independent researcher who was not involved in this *in vivo* research procedure. Both LH-RNG and PH-RNG were similar in appearance. In 5% drug content gel group, RNG and placebo were prepared as a clear gel similar to a commercial gel A whereas in 20% group, RNG and placebo were prepared in the same color as the commercial gels B and C. The pain reduction measurement was performed twice in the same 100 volunteers, the first test was done with the use of 5% anesthesia for 1 week prior to the second test with 20% anesthetic. RNG base (placebo) was used as a negative control. Commercial gel A (5% LH) was used as a positive control in case of 5% anesthetic test whereas

20% commercial gel B and C were used as positive controls in case of 20% anesthetic test. The allocated oral area of the volunteers was divided into four parts, including upper right, upper left, lower right, and lower left buccal vestibules (Figure 1). Neither the dentist nor the volunteers knew which product was applied to each area. Exact amount (0.2 mL) of the anesthetic product was applied on the selected area. After 1 min, the anesthetic product was removed and a sterile dental 27-gauge, 1.5-inch needle was inserted into the mucosa by only one dentist.

The anesthetic efficacy was obtained from each volunteer using visual analogue scale (VAS) and numerical rating scale (NRS) as described by Ferreira-Valente and coworkers (*27*) as well as Wong-Baker faces pain rating scale (WPS) (*28*). Briefly, the VAS is a 100 mm horizontal line; left end (0 mm) represents no pain and right end (100 mm) represents the most imaginable pain. The NRS is a line with 10 score; 0 on the left end represents no pain whereas 10 on the right end represents the most severe pain. The volunteers were asked to check a mark on the line of VAS and NRS and the pain intensity was measured. For WPS, 6 facial expressions reflect 6 pain levels. Level 0 or happiest face represents no pain whereas level 5, the saddest face, represents the highest pain (Figure 2). All variables were recorded and analyzed by the same investigator.

2.5. *Side effects & satisfactory level*

After applying the anesthetic RNG, systemic side effects such as nausea, vomiting, dizziness, and palpitation and local side effects such as erythema, irritation, swelling, and color change of the tissue were recorded. In addition, all volunteers were recalled after 24 h and were asked whether they had any delayed side effects. The responses of volunteers on satisfaction with the use of anesthetic products were evaluated with the help of rating scale of 1-5 for bad, fair, good, very good, and excellent, respectively.

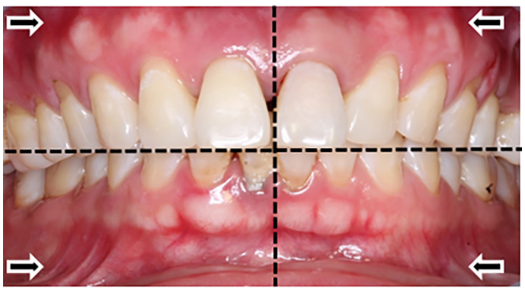

Figure 1. Illustration of the area where the test products were applied.

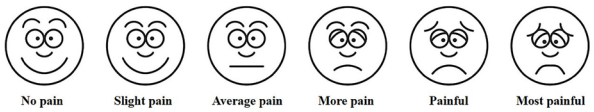

Figure 2. Wong-Baker FACES Pain rating scale.

2.6. Statistical analysis

The VAS and NRS were presented as mean and standard deviation (SD). Statistical analysis was performed by independent *t*-test or a one-way ANOVA with Dunnett C. Kolmogorov-Smirnov's test was used as normality of data evaluation. The statistical significance was considered as p-value < 0.05. The WPS and satisfactory levels were reported as frequencies.

3. Results

3.1. *RNG preparation and characterization*

RNG base was successfully prepared using modified rice powder of approximately 8-10% in water. The outer appearance of RNG was transparent and colorless having average particle size measured by PCS, after 1000-fold water dilution, of 485 ± 70 nm with a polydispersity index (PdI) of approximately 0.3. Incorporation with LH or PH to obtained 5% and 20% of either LH or PH gave the LH-RNG and PH-RNG with the same outer appearance as RNG base.

3.2. *Efficacy of LH-RNG and PH-RNG on pain reduction*

One hundred volunteers were recruited in this study (51 females, 49 males, age ranged between 25-60 years, average age is 37 ± 2.54 years). Significant difference (p < 0.01) in terms of VAS was found between the negative control group and all anesthetic groups as seen in Figure 3. The highest VAS pain score was 3.37 ± 2.41 in negative control group. Comparison among the 5% anesthetic gel groups, it was found that commercial gel A group showed slightly higher VAS than LH-RNG and PH-RNG groups with no significant differences (p = 0.35 and 0.25, respectively). Among 20% anesthetic groups, both RNG groups showed significantly lower VAS values (0.68 ± 1.29 and 0.38 ± 0.72, respectively)

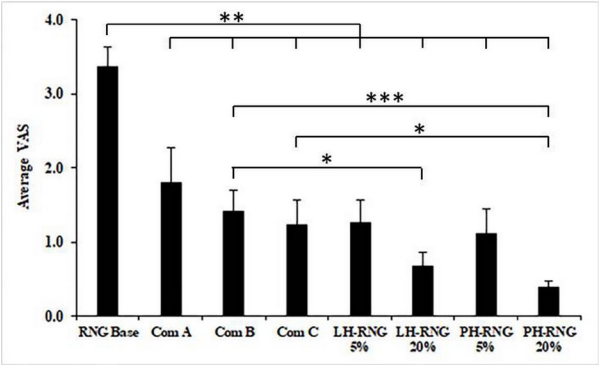

Figure 3. VAS scores between groups; $^{*}p < 0.05$, $^{**}p < 0.01$, $^{***}p < 0.001$.

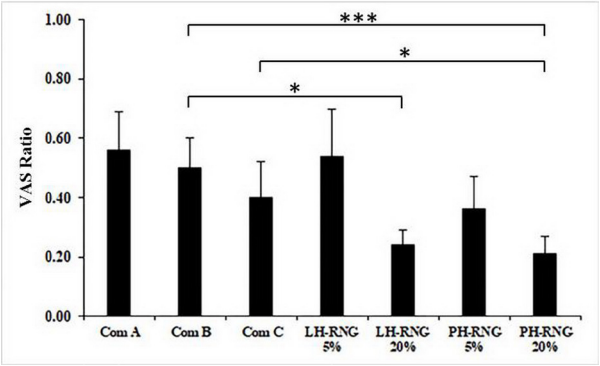

Figure 4. VAS ratio based on VAS placebo group; $^{*}p < 0.05$, $^{***}p < 0.001$.

Table 1. Average numerical rating scale (NRS) of the test products

Drug content	Test products	Average NRS*
5%	Commercial gel A	1.43 ± 0.90d
	LH-RNG	0.97 ± 0.83c
	PH-RNG	0.85 ± 0.74bc
20%	Commercial gel B	0.60 ± 0.65b
	Commercial gel C	0.62 ± 0.68b
	LH-RNG	0.24 ± 0.47a
	PH-RNG	0.21 ± 0.43a
0%	RNG base	2.81 ± 0.73e

*Values are mean ± SD followed by different lowercase letters imply the significant differences ($p < 0.001$) between values in the same column.

than those of commercial products B and C (1.42 ± 1.73 and 1.23 ± 1.28, respectively). Significant difference between 20% LH-RNG and commercial product B was found ($p = 0.03$) whereas 20% PH-RNG showed significant differences from both commercial products B and C ($p < 0.001$ and $p = 0.03$, respectively). However, similar results of LH-RNG and PH-RNG were obtained in both concentrations.

Further data analysis was presented as VAS ratio based on VAS of the negative control group (VAS ratio = VAS anesthetics/VAS placebo). Efficacy of the anesthetics on pain reduction is addressed when the ratio was less than 1 as shown in Figure 4. It was found that all anesthetic products showed effective reduction of pain, particularly 20% LH-RNG and 20% PH-RNG which exhibited significant differences from the commercial products.

The NRS is presented in Table 1. The highest NRS value was found in the negative control group and significant difference from other anesthetic groups was shown ($p < 0.001$). Among 5% anesthetic group, the significant differences between a commercial gel A and both rice gels were presented. Furthermore, 5% LH and PH showed no significant difference. In 20% anesthetic group, NRS scores of LH-RNG and PH-RNG were significantly lower than a commercial gels B and C. No significant difference between LH-RNG and PH-RNG was found in both concentrations. It was noted that higher anesthetic content caused the significant

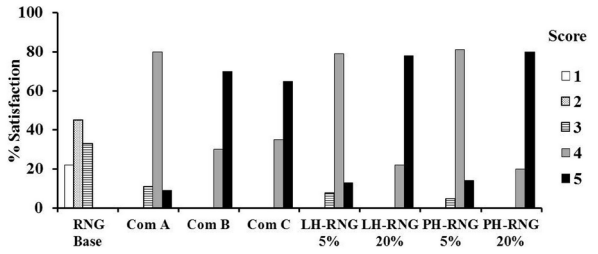

Figure 5. Percentage of satisfaction in each level to the test products.

reduction of pain.

For WPS, the negative control group showed the highest frequency of facial pain expression at level 3 (49%), followed by at level 2 (32%). Considering the 5% anesthetic group, the highest frequency of facial pain expression of the commercial gel was found at level 2 (50%) whereas that of LH-RNG and PH-RNG was found at level 1 (37% and 43%, respectively), followed by level 0 (34% and 36%, respectively). Among the 20% anesthetic group, all gels showed facial pain expression at level 0 but the percentage frequency at this level was different. The extremely high percentage of frequency of facial pain expression at level 0 was found in LH-RNG and PH-RNG (78% and 80%, respectively), whereas that of the commercial gels B and C was only 49% and 47%, respectively.

3.3. *Side effects & satisfactory level*

No sign of side effects was found in all volunteers. The satisfactory results are shown in Figure 5. The number indicates the level of satisfaction, *e.g.*, level 1 represents the least satisfaction whereas level 5 is the highest satisfaction. Higher satisfaction was found with the use of the anesthetic gel than the placebo. Moreover, the volunteers preferred to use 20% to 5% anesthetic gels.

4. Discussion

Nanogel is defined as a three-dimensional hydrogel that possesses particle size in the nanoscale size range (*29*). Many kinds of polymers particularly from natural sources have been used for producing nanogels (*22*). In the present study, the nanogel was prepared from the modified rice starch. The particles size of RNG obtained in this study was 485 ± 70 nm indicating that the nanogel from rice starch could be formed. A polydispersity index (PdI) of approximately 0.3 of the obtained RNG indicates that its particle size distribution is in moderate range. The cross-linked swellable polymer networks in nanogels possess high capacity to hold water (*30,31*), therefore, the outer appearance of the RNG obtained is transparent. For a local anesthetic to be dental use, it should be compatible with the oral mucosal tissues, *e.g.*, not irritating, and its action

should be temporary and completely reversible. It should be effective in doses far below its toxic level, it should be hypoallergenic and have a rapid onset of anesthesia with a duration of action sufficient to complete the dental procedure comfortably (*32*). From our experience, lidocaine and prilocaine are effective local anesthetic with no toxicity to oral epithelial tissues (*26*). LH and PH molecules were used in the study because they have higher hydrophilicity than their base form (lidocain and prilocaine). Both LH and PH can be easily incorporated into RNG to obtained LH-RNG and PH-RNG because the nanogel also possess high hydrophilicity. Moreover, many researches have shown that the desirable features of the nanogels have high loading capacity for hydrophilic therapeutics, and their network protects the encapsulated drug molecules against degradation as enzymes cannot penetrate into the particles (*33-35*). Moreover, nanogel also show high mucoadhesive property (*23*). The commercial dental anesthetic gels that are most commonly used can be divided into 2 groups, one is low drug content and another is high drug content gels. The low drug content gels usually contain 5% LH. For the high drug content group, the gels contain 20% benzocaine and a combination of 14% benzocaine, 2% butamben, and 2% tetracaine hydrochloride are generally used. From the best of our knowledge, there is no 20% LH or PH gel available in the market. Therefore, the commercial products containing 5% LH was used as a positive control for the low drug content group. For the high drug content group, as there is no commercial anesthetic gels containing 20% LH or PH, the gels with other anesthetics having the same drug concentration of 20% were used as positive controls to the main aim of pain reduction and satisfaction of volunteers.

Evaluation of pain is one of the most difficult challenges for researchers. Many measurement tools, including color scales, pain thermometers, VAS, NRS, and WPS have been developed to elicit self-reports of pain from volunteers (*27,28,36*). In the present study, VAS, NRS, and WSP have been selected for evaluation of the favorable results of LH-RNG and PH-RNG on pain reduction. From VAS and NRS, anesthetic gel groups showed significantly less pain than placebo group after needle insertion into buccal mucosa. Both developed RNG could reduce pain in all concentrations. The 5% anesthetic RNG was comparable to commercial product, whereas 20% anesthetic RNG presented superior results over the two commercial gels. Confirming with the VAS ratio analysis, the developed 20% anesthetic gels significantly exhibited the better pain reduction results than the commercial products, especially PH-RNG. However, no significant differences in efficacy between lidocaine and prilocaine for both concentrations was found. The WPS evaluation of patient's satisfaction demonstrate that the anesthetic gels are more preferable than placebo, especially those gels with the higher concentration of anesthesia. Taken together, it can be concluded that the developed anesthetic gels can potentially reduce pain from needle injection in oral cavity. The patient's satisfaction will reflect the attitude of dental procedures which injection is needed. The efficacy of both anesthetic rice gels will not only reduce the pain from injection, but also can reduce patient's dental fear.

Acknowledgements

The authors are thankful for the support from the Agricultural Research Development Agency (ARDA).

References

1. Mitchell M. Anaesthesia type, gender and anxiety. J Perioper Pract. 2013; 23:41-47.
2. Mendoza-Mendoza A, Perea MB, Yañez-Vico RM, Iglesias-Linares A. Dental fear in children: the role of previous negative dental experiences. Clin Oral Investig. 2015; 19:745-751.
3. McGrath C, Bedi R. The association between dental anxiety and oral health-related quality of life in Britain. Community Dent Oral Epidemiol. 2004; 32:67-72.
4. Armfield JM, Spencer AJ, Stewart JF. Dental fear in Australia: Who's afraid of the dentist? Aust Dent J. 2006; 51:78-85.
5. Couvreur P. Nanoparticles in drug delivery: Past, present and future. Adv Drug Deliv Rev. 2013; 65:21-23.
6. Blanco E, Shen H, Ferrari M. Principles of nanoparticle design for overcoming biological barriers to drug delivery. Nat Biotechnol. 2015; 33:941-951.
7. Naksuriya O, van Steenbergen MJ, Torano JS, Okonogi S, Hennink WE. A kinetic degradation study of curcumin in its free form and loaded in polymeric micelles. AAPS J. 2016; 18:777-787.
8. Yokoyama M. Polymeric micelle drug carriers for tumor targeting. Polym Drug Deliv I Part Drug Carriers. 2006; 923:27-39.
9. Naksuriya O, Shi Y, Van Nostrum CF, Anuchapreeda S, Hennink WE, Okonogi S. HPMA-based polymeric micelles for curcumin solubilization and inhibition of cancer cell growth. Eur J Pharm Biopharm. 2015; 94:501-512.
10. Khonkarn R, Mankhetkorn S, Hennink WE, Okonogi S. PEG-OCL micelles for quercetin solubilization and inhibition of cancer cell growth. Eur J Pharm Biopharm. 2011; 79:268-275.
11. Wu Y, Li M, Gao H. Polymeric micelle composed of PLA and chitosan as a drug carrier. J Polym Res. 2009; 16:11-18.
12. Santander-Ortega MJ, Stauner T, Loretz B, Ortega-Vinuesa JL, Bastos-González D, Wenz G, Schaefer UF, Lehr CM. Nanoparticles made from novel starch derivatives for transdermal drug delivery. J Control Release. 2010; 141:85-92.
13. Peppas NA, Hilt JZ, Khademhosseini A, Langer R. Hydrogels in biology and medicine: From molecular principles to bionanotechnology. Adv Mater. 2006; 18:1345-1360.
14. Buwalda SJ, Boere KWM, Dijkstra PJ, Feijen J,

Vermonden T, Hennink WE. Hydrogels in a historical perspective: From simple networks to smart materials. J Control Release. 2014; 190:254-273.
15. Zhang H, Zhai Y, Wang J, Zhai G. New progress and prospects: The application of nanogel in drug delivery. Mater Sci Eng C Mater Biol Appl. 2016; 60:560-568.
16. Motornov M, Roiter Y, Tokarev I, Minko S. Stimuli-responsive nanoparticles, nanogels and capsules for integrated multifunctional intelligent systems. Prog Polym Sci. 2010; 35:174-211.
17. Zha L, Banik B, Alexis F. Stimulus responsive nanogels for drug delivery. Soft Matter. 2011; 7:5908-5916.
18. Kabanov AV, Vinogradov SV. Nanogels as pharmaceutical carriers: Finite networks of infinite capabilities. Angew Chem Int Ed Engl. 2009; 48:5418-5429.
19. Johnson SM, Saint John BE, Dine AP. Local anesthetics as antimicrobial agents: A review. Surg Infect (Larchmt). 2008; 9:205-213.
20. Haase A, Reader A, Nusstein J, Beck M, Drum M. Comparing anesthetic efficacy of articaine versus lidocaine as a supplemental buccal infiltration of the mandibular first molar after an inferior alveolar nerve block. J Am Dent Assoc. 2008; 139:1228-1235.
21. American Society of Regional Anesthesia and Pain Medicine (ASRA), Neal JM, Mulroy MF, Weinberg GL, American Society of Regional A, Pain M. American Society of Regional Anesthesia and Pain Medicine checklist for managing local anesthetic systemic toxicity: 2012 version. Reg Anesth Pain Med. 2012; 37:16-18.
22. Okonogi S, Kaewpinta A, Khongkhunthian S, Yotsawimonwat S. Effect of rice variety on the physicochemical properties of the modified rice powders and their derived mucoadhesive gels. Drug Discov Ther. 2015; 9:221-228.
23. Okonogi S, Khongkhunthian S, Jaturasitha S. Development of mucoadhesive buccal films from rice for pharmaceutical delivery systems. Drug Discov Ther. 2014; 8:262-267.
24. Okonogi S, Kaewpinta A, Khongkhunthian S, Yotsawimonwat S. Effect of rice variety on the physicochemical properties of the modified rice powders and their derived mucoadhesive gels. Drug Discov Ther. 2015; 9:221-228.
25. Okonogi S, Kaewpinta A, Yotsawimonwat S, Khongkhunthian S. Preparation and characterization of lidocaine rice gel for oral application. Drug Discov Ther. 2015; 9:397-403.
26. Khongkhunthian S, Supanchart C, Yotsawimonwat S, Okonogi S. *In vitro* oral epithelium cytotoxicity and *in vivo* inflammatory inducing effects of anesthetic rice gel. Drug Discov Ther. 2017; 11:323-328.
27. Ferreira-Valente MA, Pais-Ribeiro JL, Jensen MP. Validity of four pain intensity rating scales. Pain. 2011; 152:2399-2404.
28. Garra G, Singer AJ, Domingo A, Thode HC. The wong-baker pain FACES scale measures pain, not fear. Pediatr Emerg Care. 2013; 29:17-20.
29. Li D, van Nostrum CF, Mastrobattista E, Vermonden T, Hennink WE. Nanogels for intracellular delivery of biotherapeutics. J Control Release. 2017; 259:16-28.
30. Kersey FR, Merkel TJ, Perry JL, Napier ME, Desimone JM. Effect of aspect ratio and deformability on nanoparticle extravasation through nanopores. Langmuir. 2012; 28:8773-8781.
31. Rolland JP, Maynor BW, Euliss LE, Exner AE, Denison GM, DeSimone JM. Direct fabrication and harvesting of monodisperse, shape-specific nanobiomaterials. J Am Chem Soc. 2005; 127:10096-10100.
32. Giovannitti JA, Rosenberg MB, Phero JC. Pharmacology of local anesthetics used in oral surgery. Oral Maxillofac Surg Clin North Am. 2013; 25:453-465.
33. Soni KS, Desale SS, Bronich TK. Nanogels: An overview of properties, biomedical applications and obstacles to clinical translation. J Control Release. 2016; 240:109-126.
34. Wu HQ, Wang CC. Biodegradable smart nanogels: A new platform for targeting drug delivery and biomedical diagnostics. Langmuir. 2016; 32:6211-6225.
35. Li Y, Maciel D, Rodrigues J, Shi X, Tomás H. Biodegradable polymer nanogels for drug/nucleic acid delivery. Chem Rev. 2015; 115:8564-8608.
36. Abdellatif AM. Pain assessment of two palatal anesthetic techniques and their effects on the child's behavior. Pediatr Dent J. 2011; 21:129-137.

(Received January 21, 2018; Revised February 21, 2018; Accepted February 22, 2018)

Brief Report

DOI: 10.5582/ddt.2017.01062

Welfare analysis of a zero-smoking policy – A case study in Japan

Yuuki Nakamura[1], Kenzo Takahashi[2,*], Marika Nomura[3], Miwako Kamei[4]

[1] *Graduate School of Pharmacy, Nihon University, Chiba, Japan;*
[2] *Graduate School of Public Health, Teikyo University, Tokyo, Japan;*
[3] *Department of International Health and Collaboration, National Institute of Public Health, Saitama, Japan;*
[4] *School of Pharmacy, Nihon University, Chiba, Japan.*

Summary **Smoking cessation efforts in Japan reduce smoking rates. A future zero-smoking policy would completely prohibit smoking (0% rate). We therefore analyzed the social welfare of smokers and non-smokers under a hypothetical zero-smoking policy. The demand curve for smoking from 1990 to 2014 was estimated by defining quantity as the number of cigarettes smoked and price as total tobacco sales/total cigarettes smoked by the two-stage least squares method using the tax on tobacco as the instrumental variable. In the estimation equation (calculated using the ordinary least squares method), the price of tobacco was the dependent variable and tobacco quantity the explanatory variable. The estimated constant was 31.90, the estimated coefficient of quantity was − 0.0061 (both, $p < 0.0004$), and the determinant coefficient was 0.9187. Thus, the 2015 consumer surplus was 1.08 trillion yen (US$ 9.82 billion) (95% confidence interval (CI), 889 billion yen (US$ 8.08 billion) – 1.27 trillion yen (US$ 11.6 billion)). Because tax revenue from tobacco in 2011 was 2.38 trillion yen (US$ 21.6 billion), the estimated deadweight loss if smoking were prohibited in 2014 was 3.31 trillion yen (US$ 30.2 billion) (95% CI, 3.13 trillion yen (US$ 28.5 billion) – 3.50 trillion yen (US$ 31.8 billion)), representing a deadweight loss about 0.6 trillion yen (US$ 5.45 billion) below the 2014 disease burden (4.10-4.12 trillion yen (US$ 37.3-37.5 billion)). We conclude that a zero-smoking policy would improve social welfare in Japan.**

Keywords: Tobacco, zero-smoking policy, welfare analysis, disease burden

1. Introduction

In Japan, smoking cessation is promoted based on the Healthy Japan 21 (second term) health and assessment project, in which the rate for adult smoking is set at 12% and the rate for underage (younger than age 18) smoking is set at 0%. Due to smoking cessation efforts in Japan, smoking rates have declined in recent years (Figure 1). The next step in an anti-smoking policy would be the entire prohibition of smoking to achieve a smoking rate of 0%, namely, a zero-smoking policy. In order to evaluate a zero-smoking policy, the social welfare of both smokers and non-smokers must be considered. Even though a zero-smoking policy has not yet been discussed as actual policy by governments including that of Japan, this paper has examined how such a hypothetical policy would affect the social welfare of both smokers and non-smokers.

Three previous studies have estimated the disease burden due to smoking to be 3.96 (*1*), 7.15 (*2*), and 4.13 (*3*) trillion yen (US$ 36.0, 65.0, and 37.5 billion, respectively, assuming $ 1 = 110 yen (Table 1)). Although these numbers appear to differ substantially, a previous study by the current authors adjusted those numbers by standardizing the population of smokers in 1990 as 45.74 million and the unit cost of the opportunity cost (the willingness to pay for 1 quality-adjusted life year gain (*4*)) as 6 million yen. The resulting numbers were 7.34, 7.35, and 7.33 trillion yen (US$ 66.7, 66.6, and 66.8 billion), respectively (*4*). If the population of smokers in 2014 is assumed to be 25.16 million, then the disease burden of smokers in

Released online in J-STAGE as advance publication February 25, 2018.

**Address correspondence to:*
Dr. Kenzo Takahashi, Teikyo University Graduate School of Public Health, 2-11-1 Kaga, Itabashi-ku, Tokyo 173-8605, Japan.
E-mail: kenzo.takahashi.chgh@med.teikyo-u.ac.jp

Table 1. Estimation of disease burden due to smoking in previous studies in trillions of yen (billions of US dollars)

Index year	1993		1999		2005	
Excess Health Expenditures						
Smoking						
Health Expenditures by Excess Morbidity	1.22 (11.13)	Smoking rate as of 1965.	1.29 (11.76)	• Smoking rate as of 1974. • "Bronchitis or COPD" was included in Emphysema.	1.45 (13.18)	Smoking rate as of 1980.
Health Expenditures by Effects on Embryos	Not calculated		–[a]		–	
Dental Health Expenditures by Excess Morbidity	–		–		0.18 (1.59)	
Passive Smoking						
Health Expenditures by Excess Morbidity	0.01 (0.10)	• Subjects were 45 years of age or older.	0.01 (0.13)	• Subjects were 40 years of age or older.	0.14 (1.30)	• Subjects were 40 years of age or older. • Subjects were individuals from 45 to 75 years of age with breast cancer.
Subtotal	1.23 (11.23)		1.31 (11.90)		1.77 (16.07)	
Labor Force Loss by Smoking-related Diseases						
Smoking						
Hospitalization by Excess Morbidity	0.03 (0.27)	• The total number of hospitalizations was defined as the product of the number of inpatients per day and the average duration of hospitalization. • The unit cost of the opportunity cost was the per capita National Income.	0.34 (3.10)	The unit cost of the opportunity cost was the average compensation for employees.	0.22 (1.97)	The unit cost of the opportunity cost was the per capita Net Domestic Product (NDP).
Excess Mortality	2.63 (23.91)	The unit cost of the opportunity cost was the per capita National Income.	5.38 (48.92)	• The unit cost of the opportunity cost was the average compensation for employees. • Compensation for employees was discounted by 3%.	2.00 (18.17)	• The unit cost of the opportunity cost was the per capita NDP. • Compensation for employees was discounted by 3%.
Passive Smoking						
Hospitalization by Excess Morbidity	–	• The total number of hospitalizations was defined as the product of the number of inpatients per day and the average duration of hospitalization. • Subjects were 45 years of age or older. • The unit cost of the opportunity cost was the per capita National Income.	–	• Subjects were 40 years of age or older. • The unit cost of the opportunity cost was the average compensation for employees.	–	• Subjects were 40 years of age or older. • The unit cost of the opportunity cost was the per capita NDP.
Excess Mortality	0.06 (0.55)	• Subjects were 40 years of age or older. • The unit cost of the opportunity cost was the per capita National Income.	0.11 (1.00)	• Subjects were 40 years of age or older. • The unit cost of the opportunity cost was the average compensation for employees. • Compensation for employees was discounted by 3%.	0.13 (1.17)	• Subjects were 40 years of age or older. • The unit cost of the opportunity cost was the per capita NDP. • Compensation for employees was discounted by 3%.
Labor Force Loss by Fire Due to Smoking						
Hospitalization by Injury	–	The unit cost of the opportunity cost was the per capita National Income.	–	The unit cost of the opportunity cost was the average compensation for employees.	–	The unit cost of the opportunity cost was the per capita NDP.
Death	0.01 (0.07)	The unit cost of the opportunity cost was the per capita National Income.	0.01 (0.08)	• The unit cost of the opportunity cost was the average compensation for employees. • Compensation for employees was discounted by 3%.	0.01 (0.06)	• The unit cost of the opportunity cost was the per capita NDP. • Compensation for employees was discounted by 3%.
Subtotal	2.73 (24.81)		5.85 (53.14)		2.37 (21.51)	
Total	3.96 (36.03)		7.15 (65.04)		4.13 (37.59)	
Source	Institute of Health Economics and Policy, 1997 (*1*)		Aburatani, 2002 (*2*)		Institute of Health Economics and Policy, 2010 (*3*)	

[a] Costs lower than 0.005 trillion yen are shown with a "–".

2014 could be estimated as 4.10-4.12 trillion yen (US$ 37.3-37.5 billion). In any case, smoking poses a huge burden to society.

The disease burden due to tobacco was estimated to be € 21 billion in Germany (*5*), US$ 15.8 billion in California (*6*), US$ 5.03 billion in China (*7*), US$ 3.15-4.58 billion in South Korea (*8*), and US$ 291-336 million in Taiwan (*9*). If these estimates are converted to per capita figures, then the disease burden would be € 286 (assuming € 1 = US$ 1.1), US$ 471.60, US$ 4.05, US$ 68.00-98.90, and US$ 13.00-15.00. The disease burden per capita in Japan is US$ 570, which seems to be larger than that in the countries or regions listed. However, populations, smoking rates, and the unit cost of the opportunity cost may differ by country, so international comparisons should be made with great caution.

Smoking differs from other diseases because smokers decide to smoke of their own free will and because smoking may have some utility for them. Needless to say, the disease burden is a negative externality for them, and thus they do not factor it when they assess smoking's utility. However, smokers are also members of society, so the utility they derive from smoking should not be ignored as long as smoking is evaluated from a societal point of view.

Thus, a zero-smoking policy could be rationalized if the deadweight loss due to the zero-smoking policy proves to be less than the disease burden. If not, a zero-smoking policy would be a welfare loss to society. To the extent known, such a welfare analysis has not been conducted. Therefore, this paper has examined the social welfare resulting from a zero-smoking policy.

2. Methods

A general demand curve for a good in a market is shown in Figure 2. According to basic economics, if tax rate t were imposed on the consumer in this market, consumer surplus would be *abg*, tax revenue would be *gbeh*, and thus deadweight loss should be *bec*, which is the welfare loss due to taxation. If the tax rate rises to t' in Figure 3, demand for this good disappears, and thus consumer surplus and tax revenue must be zero. In this case, the deadweight loss would be *b'e'c*. Hence, a zero-smoking policy reduces social welfare by the amount of this deadweight loss, and thus the additional deadweight loss should be the consumer surplus plus tax revenue before prohibition in Figure 2. However, a society in which smoking is prohibited can earn as much as the disease burden due to smoking. If the deadweight loss is smaller than the disease burden, then the zero-smoking policy would be a welfare gain to society, but if not, the zero-smoking policy would be a welfare loss to society.

To estimate the demand curve for smoking, its quantity is defined as the number of cigarettes smoked, according to the Japan Tobacco Association (http://*www.tioj.or.jp/data/index.html*), and its price is defined as the total amount of tobacco sales divided by the number of cigarettes smoked, deflated by the Consumer Price Index.

The demand curve for tobacco estimated was using the ordinal least squares method, with the price of tobacco serving as the dependent variable and the quantity of tobacco serving as an explanatory variable. The period studied was from 1990 to 2014. The price and the quantity of cigarettes smoked were determined simultaneously, and the two-stage least squares method was used with the tax on tobacco as the instrumental variable.

This study involved no ethical concerns since only previously published data were used.

3. Results and Discussion

Figure 4 shows the observed quantity and price as dots and the fitted line according to the two-stage least

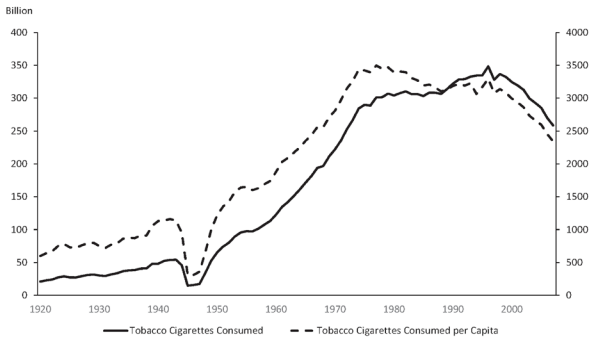

Figure 1. Tobacco use in Japan. The solid line represents the number of cigarettes smoked according to the Japan Tobacco Association (*http://www.tioj.or.jp/data/index.html*), and this number is scaled on the left-hand axis. The dashed line represents the number of cigarettes smoked per capita, which is divided by the population over 15 years, as was cited from *http://www.health-net.or.jp/tobacco/product/pd070000.html*. This number is scaled on the right-hand axis. The authors created this figure from the data mentioned above.

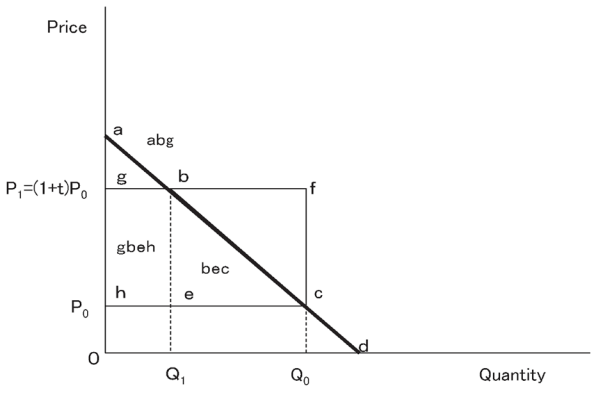

Figure 2. Demand curve for tobacco. In this market, the pyramid-shaped *area* of abg indicates consumer surplus, the square area of *gbeh* indicates tax revenue, and the pyramid-shaped area of *bec* indicates deadweight loss. The authors created this figure.

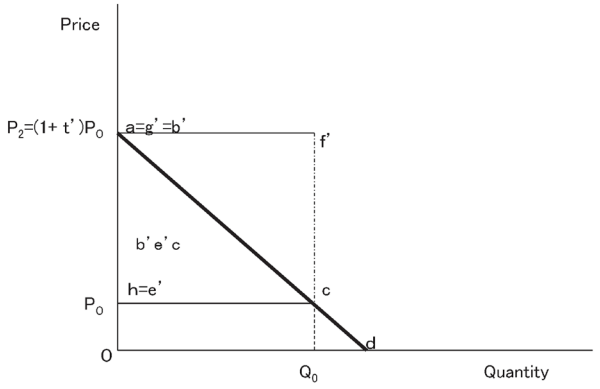

Figure 3. Deadweight loss due to a zero-smoking policy. If the tax rate rises to t', the quantity should be zero. In this case, deadweight loss would be the pyramidal shape of *b'e'c*. The authors created this figure

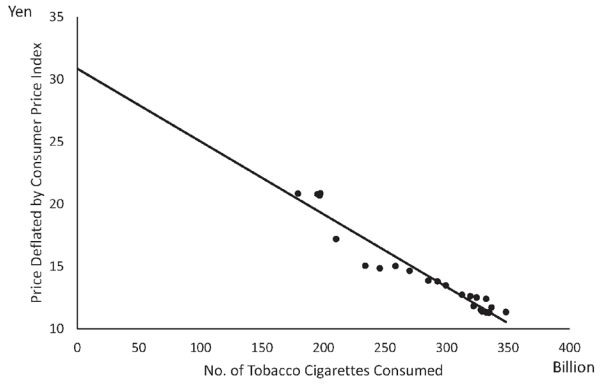

Figure 4. Plot of the price and quantity of tobacco in Japan and a fitted line. Dots indicate the price and quantity of tobacco from 1990 to 2014 according to the Japan Tobacco Association (*http://www.tioj.or.jp/data/index.html*). The line represents the fitted line as a result of estimating two-stage least squares. The authors created this figure from the data mentioned above.

squares method. The estimated constant term was 31.90, and the estimated coefficient of quantity was − 0.0061. The *p*-values for both were less than 0.0004. The determinant coefficient was 0.9187.

On the basis of these results, the consumer surplus in 2015 was calculated to be 932 billion yen (US$ 8.48 billion) with a 95% confidence interval (CI) ranging from 746 billion yen (US$ 6.788 billion) to 1.20 trillion yen (US$ 10.2 billion). Because tax revenue from the tobacco tax in 2011 was 2.38 trillion yen (US$ 21.6 billion), the deadweight loss if smoking were prohibited in 2014 was estimated to be 3.31 trillion yen (US$ 30.2 billion) with its 95% CI ranging from 3.13 trillion yen (US$ 28.5 billion) to 3.50 trillion yen (US$ 31.8 billion).

If smoking were prohibited in 2014, the deadweight loss, which was estimated as 3.31 trillion yen (US$ 30.2 billion), would be about 0.8 trillion yen (US$ 7.27 billion) less than the disease burden in 2014, which was 4.10-4.12 trillion yen (US$ 37.3-37.5 billion). Therefore, a zero-smoking policy would improve social welfare in Japan.

The estimated demand curve implies that the price elasticity of tobacco was about 0.85 when evaluated using the average price and quantity with a 95% CI ranging from 0.73 to 0.92. Studies in countries other than Japan such as India (*10,11*), China (*12*), the U.S. (*13*), and Jordan (*14*) have examined the price elasticity of tobacco, yielding figures ranging from 0.212 in India to 1.15 in Jordan. In comparison, the price elasticity in the current study was moderate. Japanese studies have estimated the price elasticity of tobacco to be 0.1 to 0.3 (*15,16)*, so the current result seems high in comparison. In general, a higher price elasticity implies greater consumer surplus, and thus the additional deadweight loss due to a zero-smoking policy would be greater and might exceed the disease burden. A more accurate value for the price elasticity is needed to reach a definitive conclusion.

Moreover, the specified demand curve for tobacco seems somewhat simpler than that in previous studies. Other factors, such as total population or income, need to be taken into account when specifying the equation with which to estimate the demand curve. In this sense, a limitation of this study is that estimates should be evaluated as an average with other factors excluded. Therefore, conclusions should be similarly evaluated. The other excluded factors might strongly affect this study's estimates and conclusions. More detailed specification of the estimation equation is beyond the scope of this paper and represents a topic for further study.

The disease burden may not have been sufficiently specified. Estimates in three previous studies (*1-3*) did not consider the disutility of smoking to non-smokers. More detailed specification of the disease burden is also a topic for the future.

Even though this study only considered price controls on smoking, in principle, other methods of reducing smoking, such as limiting the areas in which smoking is allowed, could have the same impact on the utility of smoking to smokers if these methods also reduce the rate of smoking. However, price controls only lead to deadweight costs according to the overall welfare analysis, especially when certain externalities are taken into consideration. Therefore, this paper does not mean to suggest that price controls are the only way to reduce smoking.

In conclusion, social welfare due to a zero-smoking policy in Japan was estimated based on available data. The deadweight loss was smaller than the disease burden in 2014, leading to the conclusion that a zero-smoking policy would improve social welfare. This conclusion can be buttressed by further studies that consider other factors, such as price controls.

Acknowledgements

This study was partially funded by a Research Grant

from the Ministry of Health, Labor, and Welfare (grant no. H27-Jyunkankitou-Ippan-006).

References

1. Institute of Health Economics and Policy. Report of a study involving a cost-benefit analysis of smoking policies. Institute for Health Economics and Policy. 1997. (in Japanese)
2. Aburatani Y. Report of a study of the effects of increasing the tobacco tax. Institute for Health Economics and Policy. 2002. (in Japanese)
3. Institute of Health Economics and Policy. Report of a study of an anti-smoking policy – Estimated costs of smoking. Institute for Health Economics and Policy. 2010. (in Japanese)
4. Ohkusa Y. Empirical research for the critical value of expenditure per QALY. Health and Society. 2003; 13:121-130. (in Japanese)
5. Neubauer S, Welte R, Beiche A, Koenig HH, Buesch K, Leidl R. Mortality, morbidity and costs attributable to smoking in Germany: Update and a 10-year comparison. Tob Control. 2006; 15:464-471.
6. Max W, Rice DP, Sung HY, Zhang X, Miller L. The economic burden of smoking in California. Tob Control. 2004; 13:264-267.
7. Sung HY, Wang L, Jin S, Hu TW, Jiang Y. Economic burden of smoking in China, 2000. Tob Control. 2006; 15(Suppl 1):i5-i11.
8. Kang HY, Kim HJ, Park TK, Jee SH, Nam CM, Park HW. Economic burden of smoking in Korea. Tob Control. 2003; 12:37-44.
9. Lee CH, Ko YC, Goggins W, Huang JJ, Huang MS, Kao EL, Wang HZ. Lifetime environmental exposure to tobacco smoke and primary lung cancer of non-smoking Taiwanese women. Int J Epidemiol. 2000; 29:224-231.
10. Selvaraj S, Srivastava S, Karan A. Price elasticity of tobacco products among economic classes in India, 2011-2012. BMJ Open. 2015; 5:e008180.
11. Kostova D, Dave D. Smokeless tobacco use in India: Role of prices and advertising. Soc Sci Med. 2015; 138:82-90.
12. Verguet S, Gauvreau CL, Mishra S, MacLennan M, Murphy SM, Brouwer ED, Nugent RA, Zhao K, Jha P, Jamison DT. The consequences of tobacco tax on household health and finances in rich and poor smokers in China: An extended cost-effectiveness analysis. Lancet Glob Health. 2015; 3:e206-e216.
13. Goodchild M, Perucic AM, Nargis N. Modelling the impact of raising tobacco taxes on public health and finance. Bull World Health Organ. 2016; 94:250-257.
14. Sweis NJ, Cherukupalli R. Cigarette demand is responsive to higher prices: Findings from a survey of university students in Jordan. Tob Control. 2016; 25:631-633.
15. Yoshida Y, Atoda N. An analysis of tobacco tax revenue in light of the effects of an increase in the Tobacco Tax on smoking. Bulletin of Konan Women's University. 2010; 47:69-76. (in Japanese)
16. Ito Y, Nakamura M. The effect of increasing tobacco tax on tobacco sales in Japan. Nihon Koshu Eisei Zasshi. 2013; 60:613-618. (in Japanese)

(Received November 15, 2017; Revised December 22, 2017; Accepted January 25, 2018)

Brief Report

DOI: 10.5582/ddt.2018.01001

Assessment of rectal feces storage condition by a point-of-care pocket-size ultrasound device for healthy adult subjects: A preliminary study

Koichi Yabunaka[1,2], Masaru Matsumoto[1,2], Mikako Yoshida[1,2], Shiho Tanaka[3], Yuka Miura[4], Takuya Tsutaoka[1,5], Mayumi Handa[1,6], Gojiro Nakagami[2,3], Junko Sugama[4], Shingo Okada[7], Hiromi Sanada[2,3,*]

[1] *Department of Imaging Nursing Science, Graduate School of Medicine, The University of Tokyo, Tokyo, Japan;*
[2] *Global Nursing Research Center, Graduate School of Medicine, The University of Tokyo, Tokyo, Japan;*
[3] *Department of Gerontological Nursing/Wound Care Management, Graduate School of Medicine, The University of Tokyo, Tokyo, Japan;*
[4] *Institute for Frontier Science Initiative, Kanazawa University, Kanazawa, Ishikawa, Japan;*
[5] *Imaging Technology Center, Research & Development Management Headquarters, Fujifilm Corporation, Tokyo, Japan;*
[6] *Marketing Planning Group, Ultrasound Promotion Department, Fujifilm Medical Corporation, Tokyo, Japan;*
[7] *Department of Surgery, Kitamihara Clinic, Hakodate city, Hokkaido, Japan.*

Summary **The aim of this study was to assess rectal feces storage condition by a pocket-size ultrasonography (PUS) in healthy adults so as to define normal rectal defecation desire. Participants were first assessed rectum by PUS imaging immediately after defecation desire (pre-defecation). Nurses checked the amount and quality of the participants' feces using King's Stool Chart and Bristol stool scale. Finally, PUS was performed for defecation with no defecation desire (post-defecation). Pre-defecation PUS detected high echo area in all patients. All of the post-defecation PUS did not detect high echo area (perfectly no recognizable high echo area in 54.5%, high echo line in 36.4%, and low echo of entire circumference in 9.1% of the patients). Average diameter of rectal crescent was 4.22 ± 0.8 cm. Bristol Stool Scale 1 or 2 (indicating hard stool) of pre-defecation PUS indicated high echo area and acoustic shadow in 100% of the patients. This study showed that healthy adult with defecation desire had high average rectal echo area of 4.0 cm in diameter. PUS may be able to define the rectum diameter for defecation desire of elderly people. PUS is capable of assessing fecal retention of the rectum for point-of-care examinations in home care.**

Keywords: Ultrasonography, Constipation, Defecation care, Rectal diameter

1. Introduction

Chronic idiopathic constipation is a common functional gastrointestinal disorder in communities (*1*). Elderly patients complain mainly of difficulty in defecating, hard feces, and a feeling of incomplete evacuation (*2*). In addition, constipation degrades quality of life and causes economic burdens for patients and healthcare providers (*3,4*). Therefore, it is very important for healthcare providers to make efforts to prevent chronic constipation and to initiate appropriate assessment to manage the condition in the case of it. For diagnostic tests for constipation, colonic transit, anorectal manometry, balloon expulsion parameters, and various imaging studies (plain abdominal radiography, barium enema, colonoscopy, defecography, abdominal computed tomography, magnetic resonance imaging) are widely recommended as physiologic tests (*5*). However, these procedures have a number of limitations. Plain abdominal radiography, barium enemas, defecography, and computed tomography scanning expose patients to radiation. Colonoscopy is often poorly tolerated by

**Address correspondence to:*
Dr. Koichi Yabunaka, Department of Imaging Nursing Science, Graduate School of Medicine, The University of Tokyo, 7-3-1 Hongo, Bunkyo-ku, Tokyo, 113-0033, Japan.
E-mail: kyabunaka-tky@umin.ac.jp

patients. Magnetic resonance imaging and defecography are costy and lack standardization (*6*).

On the other hand, transabdominal ultrasonography (US) could be a practical test in primary and point-of-care ultrasonography since it is low cost and fast, and the follow-up test is noninvasive (*7*). Furthermore, point-of-care examinations have come to be used more in home care and bedside by the spread of the pocket-size ultrasonography (PUS) (*8*). Several recent studies have reported cases for which a US technique was used to diagnose constipation for measuring the rectal diameter in children. US images show a fecal mass in the rectum as a crescent-shaped acoustic shadow (*9-14*). Several authors have proposed the use of US as a first-line clinical imaging and initial diagnostic technique for colon (*15,16*). In particular, rectal defecation care for chronic-constipation patients is important in home care setting since the high rate of recurrence of constipation with rectal outlet problems in elderly contributes to complications such as fecal impaction (*17*).

However, there is little information available on sonographic visualization of rectal feces storage condition in adults including elderly people. Since defecation desire of elderly with dementia are unclear, PUS needs to be performed to confirm normal rectal feces storage condition in healthy adults prior to investigation of defecation situation of constipation patients in home care and bedside. The objective of this study is to assess rectal feces storage condition by PUS in healthy adults so as to define normal rectal feces storage condition.

2. Materials and Methods

2.1. *Patients*

Fourteen healthy adult volunteers (6 men and 8 women; mean age 37.6 ± 10.8 years) underwent rectal US. The subjects had no history of abdominal surgery, irritable bowel syndrome, organic disease, feeling of unsatisfied defecation were excluded. The Ethical Review Board of The University of Tokyo approved the study protocol (#11521). The researchers obtained written informed consent from all volunteers for participation in the study. All participants were free to retract their consent at any time and were encouraged to report any pain or discomfort during the PUS examination.

2.2. *Ultrasound technique*

For all of the participants, rectum was assessed by PUS imaging immediately after defecation desire (pre-defecation). Nurses checked the amount and quality of the participants' feces using King's Stool Chart and Bristol stool scale. Finally, PUS was performed after defecation with no defecation desire (post-defecation). PUS was scanned on the abdominal skin approximately 2 cm above the symphysis with the supine position. The resulting PUS imaging was performed with behind a full or partially filled bladder at an angle of approximately 15 degrees downward from the transverse plane (*10*). The sonographic examinations lasted for a total of approximately 5 min. All of the PUS was performed by nurses who had received sufficient PUS training. A PUS system (SONOSITE iViz: PUD-A, Sonosite, Bothwell, WA, USA) with a curvedarray (5 MHz) probe was used. The iViz offers twodimensional imaging and allows adjustments of global gain and depth. Images were compressed and stored for review.

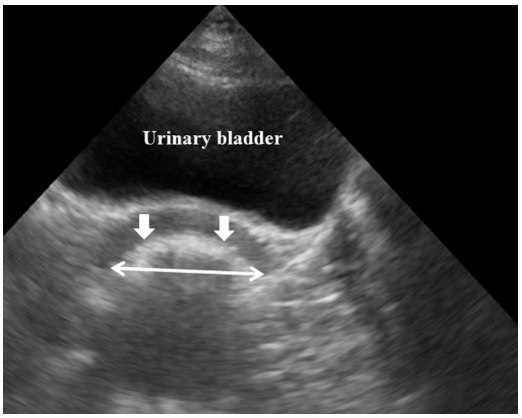

Figure 1. Presence of feces US image showing a crescent shaped high echoes area in transverse sections (arrows). Measured rectal crescent (seen behind the urinary bladder).

2.3. *Data analysis*

Image J software was used for image analysis and processing. For all of the ultrasound images, transverse rectal diameter from the outer to outer rectum wall was then measured at the level of high echo area three times by two certified sonographers (Figure 1). Two independent certified sonographers evaluated the ultrasound images to ensure inter-rater reliability. All images were evaluated under blind conditions. The relations between the rectal diameters were assessed by Cohen's kappa statistic to establish agreement between the two certified sonographers. All statistical analyses were conducted using SPSS for Windows version 22.0 software (SPSS Inc., Chicago, Illinois, USA). The following variables were recorded: age, gender, amount of defecation after constipation by King's Stool Chart and Bristol stool scale.

3. Results and Discussion

Participant characteristics are shown in Table 1. Among the 14 eligible participants, 3 participants were excluded for their feeling of unsatisfied defecation after defecation; thus the final analysis was performed for 11 patients (5 men, 6 women; mean age, 40.1 years; range,

Table 1. Clinical characteristics of the participants (n = 11)

ID	Age	Sex	Bristol Stool Scale	kings stool chart (g)	Measuring rectal crescent (cm)	Pre-defecation US findings	AS	Post-defecation US findings
1	60	F	1	Less than100	3.615	High echo area	+	High echo line
2	32	F	2	100-200	3.935	High echo area	+	High echo line
3	32	F	2	Less than100	4.185	High echo area	+	Low echo of all circumference
4	30	F	3	Over 200	3.881	High echo area	-	Low echo of all circumference
5	43	M	3	100-200	2.832	High echo area	-	High echo line
6	53	M	4	100-200	4.099	High echo area	-	Low echo of all circumference
7	32	M	4	Less than100	4.394	High echo area	-	High echo line
8	30	M	4	100-200	4.490	High echo area	-	Low echo of all circumference
9	55	M	4	Over 200	4.861	High echo area	-	High echo line
10	54	F	4	100-200	4.565	High echo area	+	Low echo of all circumference
11	31	F	4	Over 200	4.980	High echo area	-	High echo line

AS, acoustic shadows.

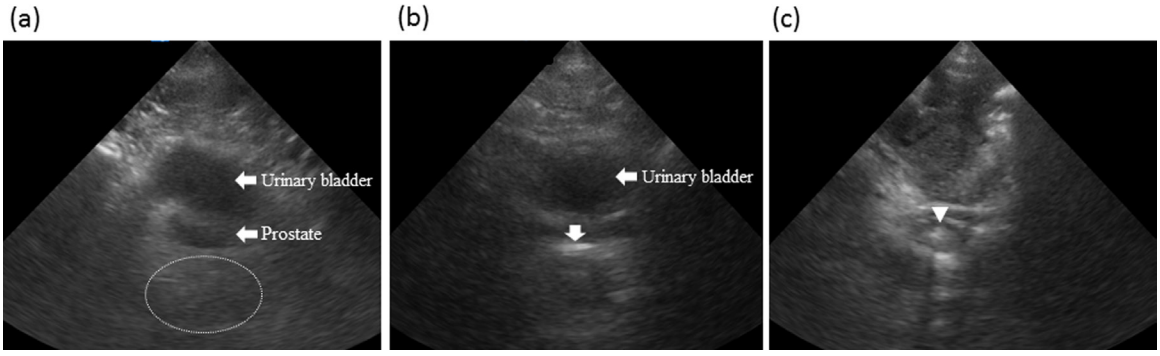

Figure 2. Absence of feces: (a) US image showing perfectly no recognizable high echo area (circle). (b) US image showing high echo line in transverse sections (arrow). (c) US image showing low echo of all circumference (arrowhead).

Table 2. Comparison of Bristol Stool Scale and pre-defecation PUS findings (n = 11)

Pre-defecation PUS findings	Bristol stool form scale			
	1 (n = 1)	2 (n = 2)	3 (n = 2)	4 (n = 6)
High echo area				
+	1 (100.0%)	2 (100.0%)	2 (100.0%)	6 (100.0%)
-	0 (0.0%)	0 (0.0%)	0 (0.0%)	0 (0.0%)
AS				
+	1 (100.0%)	2 (100.0%)	0 (0.0%)	1 (16.7%)
-	0 (0.0%)	0 (0.0%)	2 (100.0%)	5 (83.3%)

30-60 years). All of pre-defecation PUS detected high echo area with defecation desire in 100% (11/11). All of post-defecation PUS did not detect high echo area with no defecation desire, perfectly no recognizable high echo area in 54.5% (6/11), high echo line in 36.4% (4/11), and low echo of all circumference in 9.1% (1/11) (Figure 2). Average diameter of the measured rectal high echo areas was 4.22 ± 0.8 cm (Mean ± SD). Table 2 shows comparison of Bristol Stool Scale and pre-defecation PUS findings. Bristol Stool Scale 1 or 2 of pre-defecation PUS findings indicated high echo area and AS in 100%. Intra class correlations (95% CI) for the measured rectal diameters were: inter-rater reliability (r = 0.99).

The present study assessed normal rectal feces storage condition for pre-defecation PUS and post-defecation PUS in healthy adults. The normal rectal with defecation desire indicated high echo area with average 4 cm in diameter, and hard stool correlated with AS since the deep AS indicated loading of hard feces in the colon (*15*). Moreover, all of post-defecation PUS did not detect high echo area with no defecation desire, indicating no residual feces in rectum.

The pelvic US was used in similar studies to evaluate rectal diameter in children (*9-11,13,14*). Children with normal defecation patterns in the studies by Joensson *at al*. (*9*) and Singh *et al*. (*11*) had an average rectal diameter of 2.1 cm and 2.4 cm, respectively. However, US increased the rectal diameter with age in both the patient and healthy groups (healthy

age group were: ≤ 3 years 2.7 cm, 3.1-6.0 years 2.92 cm, 6.1-12.0 years 3.28 cm, and > 12.0 years 3.18 cm) (*12*). Therefore, US of an enlarged rectal diameter cannot be the sole predictor to determine whether a child is constipated (*9*). Moreover, the fecal retention was defined to be present when a stool mass was palpable on digital rectal examination (*14*). However, it is difficult to define fecal retention on digital rectal examination since defecation desire is unclear in children. In this study, PUS detected average 4 cm rectal diameter in healthy adults with defecation desire. In a healthy subject, it may be possible to define defecation desire that represents fecal retention of the rectum. However, elderly people with dementia have difficulty in expressing defecation desire as well as infants. Therefore, rectum diameter greater than 4 cm may be defined as defecation desire of elderly people. In the next step, we have to investigate rectum diameter in elderly people with defecation desire.

US for rectal may be more appropriate for children than for adults because of less attenuation of the ultrasonic beam by subcutaneous fat and muscle, both of which are thinner in pediatric subjects (*18*). Several studies have used high-performance device or portable laptop type ultrasound equipment which can clearly visualize colon of fecal loading in adults (*15,16*). In our study, the authors have found that PUS is capable of clearly visualizing fecal retention of the rectum. We presume that PUS for defecation care tools will someday become an integral part of the physical assessment and be used as frequently as the stethoscope is (*7*) since the elderly population with chronic constipation which require home health care will be increasing (*17*).

The design of this study had some obvious limitations. First, the number of subjects was small. Future studies with large numbers of healthy subjects are required to further examine the use of US for determining the causes of normal rectal defecation status. Second, an additional consideration needs to be given to the dependence of the efficacy of US on operator skill and technique. Finally, PUS evaluation of the colon did not include sigmoid colon since it is difficult to perform a sigmoid colon located in the pelvis due to gastrointestinal gas and complex arrangement (*19*).

In conclusions, this study shows that healthy adult with defecation desire had a rectal diameter greater than 4.0 cm and PUS may be able to define rectum diameter for defecation desire of elderly people. PUS is capable of assessing fecal retention of the rectum for point-of-care examinations in home care.

Conflict of Interest

This was a joint research program with FUJIFILM Corporation, and the study was conducted under the sponsorship of this organization.

Acknowledgements

The authors are deeply grateful to the study participants, all of whom greatly contributed to this study.

References

1. Bharucha AE, Pemberton JH, Locke GR. American Gastroenterological Association technical review on constipation. Gastroenterology. 2013; 144:218-238.
2. Harari D, Gurwitz JH, Avorn J, Bohn R, Minaker KL. How do older persons define constipation? Implications for therapeutic management. J Gen Inter Med. 1997; 12:63-66.
3. Dennison C, Prasad M, Lloyd A, Bhattacharyya SK, Dhawan R, Coyne K. The health-related quality of life and economic burden of constipation. Pharmacoeconomics. 2005; 23:461-476.
4. Zeitoun JD, de Parades V. Chronic constipation in adults. Presse Med. 2013; 42:1176-1185.
5. Remes-Troche JM, Rao SS. Diagnostic testing in patients with chronic constipation. Curr Gastroenterol Rep. 2006; 8:416-424.
6. Rao SS, Ozturk R, Laine L. Clinical utility of diagnostic tests for constipation in adults: A systematic review. Am J Gastroenterol. 2005; 100:1605-1615.
7. Moore CL, Copel JA. Point-of-care ultrasonography. N Engl J Med. 2011; 364:749-757.
8. Andersen GN, Graven T, Skjetne K, Mjolstad OC, Kleinau JO, Olsen O, Haugen BO, Dalen H. Diagnostic influence of routine point-of-care pocket-size ultrasound examinations performed by medical residents. J Ultrasound Med. 2015; 34:627-636.
9. Joensson IM, Siggaard C, Rittig S, Hagstroem S, Djurhuus JC. Transabdominal ultrasound of rectum as a diagnostic tool in childhood constipation. J Urol. 2008; 179:1997-2002.
10. Klijn AJ, Asselman M, Vijverberg MA, Dik P, de Jong TP. The diameter of the rectum on ultrasonography as a diagnostic tool for constipation in children with dysfunctional voiding. J Urol. 2004; 172:1986-1988.
11. Singh SJ, Gibbons NJ, Vincent MV, Sithole J, Nwokoma NJ, Alagarswami KV. Use of pelvic ultrasound in the diagnosis megarectum in children with constipation. J Pediatr Surg. 2005; 40:1941-1944.
12. Bijoś A, Czerwionka-Szaflarska M, Mazur A, Romanczuk W. The usefulness of ultrasound examination of the bowel as a method of assessment of functional chronic constipation in children. Pediatr Radiol. 2007; 37:1247-1252.
13. Karaman A, Ramadan SU, Karaman I, Gokharman D, Erdogan D, Kacar M, Cavusoglu YH, Kosar U. Diagnosis and follow-up in constipated children: Should we use ultrasound? J Pediatr Surg. 2010; 45:1849-1855.
14. Hatori R, Tomomasa T, Ishige T, Tatsuki M, Arakawa H. Fecal retention in childhood: Evaluation on ultrasonography. Pediatr Int. 2017; 59:462-466.
15. Yabunaka K, Matsuo J, Hara A, Takii M, Nakagami G, Gotanda T, Sanada H. Sonographic visualization of fecal loading in adults: Comparison with computed tomography. J Diagn Med Sonog. 2015; 31:86-92.

16. Yabunaka K, Nakagami G, Komagata K, Sanada H. Ultrasonographic follow-up of functional chronic constipation in adults: A report of two cases. SAGE Open Med Case Rep. 2017; 5:2050313X17694234.
17. Gallegos-Orozco JF, Foxx-Orenstein AE, Sterler SM, Stoa JM. Chronic constipation in the elderly. Am J Gastroenterol. 2012; 107:18-25.
18. Taniguchi DK, Martin RW, Myers J, Silverstein FE. Measurement of the ultrasonic attenuation of fat at high frequency. Acad Radiol. 1994; 2:114-120.
19. Yabunaka K, Sanada S, Fukui H, Tamate S, Fujioka M. Transabdominal sonographic appearance of adult colonic polyps. J Med Ultrason (2001). 2006; 33:231-237.

(Received January 8, 201; Revised February 4, 2018; Accepted February 21, 2018)

Case Report

DOI: 10.5582/ddt.2018.01000

Atypical presentation of pyogenic iliopsoas abscess in two cases

Sudeshna Ghosh, Himanshu Narang, Pawan Goel, Prabhat Kumar*, Manish Soneja, Ashutosh Biswas

Department of Medicine, All India Institute of Medical Science, New Delhi, India.

Summary **Iliopsoas abscess (IPA) is an uncommon diagnosis in medical wards. Herein, we present two unusual cases of IPA. First patient was an elderly diabetic patient who had gas-forming bilateral IPA caused by *Escherichia coli*. This infection proved fatal and patient succumbed on third day of hospital admission. Second patient was a young boy who had right sided sacroilitis with IPA. *Staphylococcus aureus* was isolated from the pus culture and patient was successfully treated without any sequelae.**

Keywords: Gas-forming iliopsoas abscess, pyogenic sacroiliitis, immunosuppression

1. Introduction

Iliopsoas abscess (IPA) was first described in year 1881 by Mynter. Since then a large number of case series and reports have been published in medical literature. The psoas muscle arises from the lateral borders and transverse processes of the 12th thoracic to the 5th lumbar vertebrae. The fibres of iliacus muscle which originates in the iliac fossa of pelvis blend with psoas muscle to form iliopsoas tendon which inserts into lesser trochanter of femur. Nerve supply of psoas muscle is from lumbar plexus (L1-L3) and iliacus is supplied by femoral nerve (L2-L4). This iliopsoas muscle is the strongest flexor of the hip joint. The iliopsoas muscle is related closely to various important anatomical structures like hip joint, sigmoid colon, vertebral bodies, appendix and abdominal aorta (*1*). It is also surrounded by rich venous plexus and retroperitoneal lymph nodes, which could explain the increased risk of hematogenous infections in this muscle.

Once IPA was considered always secondary to tuberculosis, but due to availability of effective treatment of tuberculosis, pyogenic IPA have become more common. Pyogenic gas-forming IPA is a rare entity with only few reported cases so far (*2-6*). Also, IPA which is secondary to sacroilitis is unusual (*7-10*). We present these two cases of IPA in this report.

2. Case Report

2.1. *Case 1*

A 61-year old diabetic and hypertensive male patient presented to the emergency department on 11th of November 2017 with complaints of high grade fever for 10 days and bilateral flank pain for 4 days. The fever was high grade with chills and pain was dull aching, persistent without any radiation. He also gave history of intermittent low back pain for last two weeks which was non-radiating and used to aggravate on standing. He was also a known case of coronary artery disease and chronic obstructive pulmonary disease, for which he was on regular medications. On examination, he was febrile and drowsy. His blood pressure was 130/80 mm of Hg, pulse rate-110/minute and respiratory rate 22/minute. Abdominal examination showed bilateral flank fullness and tenderness. Rest of the systemic examination was essentially normal.

Blood investigations showed significant neutrophilic leukocytosis, anemia, high procalcitonin levels, mildly deranged renal parameters and normal blood sugar levels (Table 1). A non-contrast computed tomography (NCCT) of abdomen was done which showed bilateral iliopsoas abscess with air pockets and diskitis at L4-L5 level (Figure 1). There was no evidence of any involvement of intra-abdominal organs. A computed tomography (CT) guided pigtail catheter insertion was done on the left side and about a litre of frank pus was drained out. He was empirically started on intravenous

Released online in J-STAGE as advance publication February 25, 2018.

**Address correspondence to:*
Dr. Prabhat Kumar, Department of Medicine, Teaching Block, All India Institute of Medical Science, New Delhi 110029, India.
E-mail: drkumar.prabhat@gmail.com

Table 1. Blood investigations of case 1 showing marked leukocytosis

Test name	Day 1	Day 2	Day 3
Hemoglobin	7.9 gm/dL	7.6 gm/dL	6.6 g m/dL
Total leukocyte count	43,100/mcL	45,300/mcL	50,229/mcL
Neutrophil	80%	70%	88%
Platelet	210,000/mcL	252,000/mcL	170,000/mcL
Urea	86 mg/dL	54 mg/dL	59 mg/dL
Creatinine	1.6 mg/dL	0.6 mg/dL	1.1 mg/dL
Procalcitonin	3.07 ng/mL		8.4 ng/mL

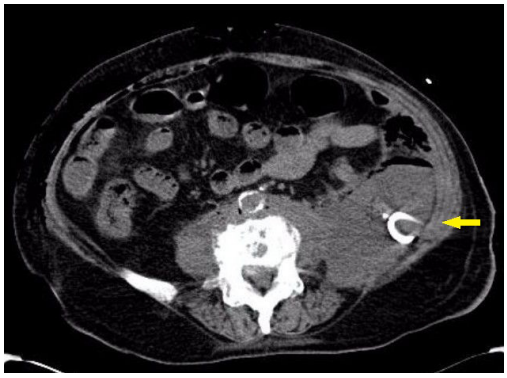

Figure 1. NCCT abdomen showing bilateral psoas abscess with pigtail in situ on left side (arrow).

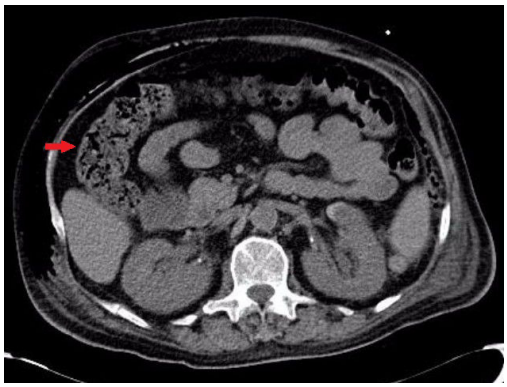

Figure 2. Air pockets in anterior abdominal wall on CT imaging (arrow).

cefoperazone-sulbactam along with teicoplanin. Another pigtail was inserted on the right side which too showed frank pus. The patient showed minimal improvement after admission. But from day 2 of admission, he started complaining of sharp chest pain on the right side. On examination, there was palpable crepitus over the abdomen extending up to the right chest wall. A repeat imaging done showed multiple pockets of air in both the psoas abscesses which had extended into the subcutaneous tissue to involve the whole of abdomen and right side of anterior chest wall (Figure 2). Meanwhile, gram negative bacilli (*Escherichia coli*) was isolated from the pus which was sensitive to third generation cephalosporins, penems, and aminoglycoside. Tests for *Mycobacterium tuberculosis* and fungal elements were negative. He continued to deteriorate, developed septic shock, metabolic acidosis and eventually succumbed on 3rd day of admission, in spite of timely drainage of abscess and appropriate antibiotics.

2.4. *Case 2*

A 15-year old boy presented in first week of November 2017 with complaints of pain in his right buttock for a week, which was sudden in onset, severe in intensity, non-radiating, associated with high grade fever and restriction of movement around right hip joint. There was no recent history of trauma. For these complaints he received some over-the-counter medications, but his symptoms gradually worsened. On physical examination, he was febrile and was lying with both hips extended. His blood pressure was 110/70 mm Hg and pulse rate was 110/min. There was severe limitation of movement around right hip joint. Right posterior superior iliac spine and right hip joint was significantly tender.

Blood investigation showed leukocytosis with high levels of acute phase reactants (Table 2). Magnetic resonance imaging (MRI) of sacroiliac joint was also done immediately. There were articulate surface irregularities with marrow edema in the right SI joint along with a large collection beneath the iliopsoas muscle, tracking down the lateral pelvic wall and exiting through the ipsilateral obturator foremen to form an intramuscular septated collection (Figures 3 and 4). There were small pockets of collection in the iliopsoas, pelvic and gluteal muscles. A CT guided aspiration was done. The patient was empirically started on piperacillin-tazobactum along with vancomycin. Patient responded within 24 hours of antibiotics. Gram stain showed gram positive cocci which later proved to be methicillin sensitive *Staphylococcus aureus* (MSSA). He received intravenous vancomycin for two weeks. A repeat imaging at this juncture showed significant reduction in abscess size and resolution of right sacroilitis. His CRP and ESR levels were also normal after two weeks of antibiotics. He subsequently received amoxicillin-clavulanic acid for a month. After six weeks of therapy, patient was asymptomatic and had no limitation of movements.

3. Discussion

Based on pathogenesis, IPA can be divided into primary and secondary. Primary IPA occurs due to distant hematogenous or lymphatic spread of

Table 2. Blood investigations of case 2 showing raised acute phase reactants with leukocytosis

Test name	Day 1	Day 7	Day 14
Hemoglobin	12.2 gm/dL	11.8 gm/dL	11.3 gm/dL
Total leukocyte count	15,000/mcL	15,700/mcL	8,800/mcL
Neutrophil	80%	67%	58 %
Platelets	239,000/mcL	600,000/mcL	608,000/mcL
Urea	30 mg/dL	42 mg/dL	33 mg/dL
Creatinine	0.78 mg/dL	0.4 mg/dL	0.4 mg/dL
Procalcitonin	2.04 ng/mL		0.08 ng/mL
ESR(first hour)	40	12	20
CRP	121 mg/L	43 mg/L	4.01 mg/L

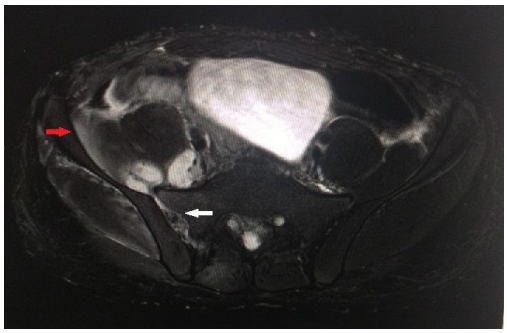

Figure 3. MRI showing right sided sacroilitis (white arrow) along with iliopsoas abscess (red arrow).

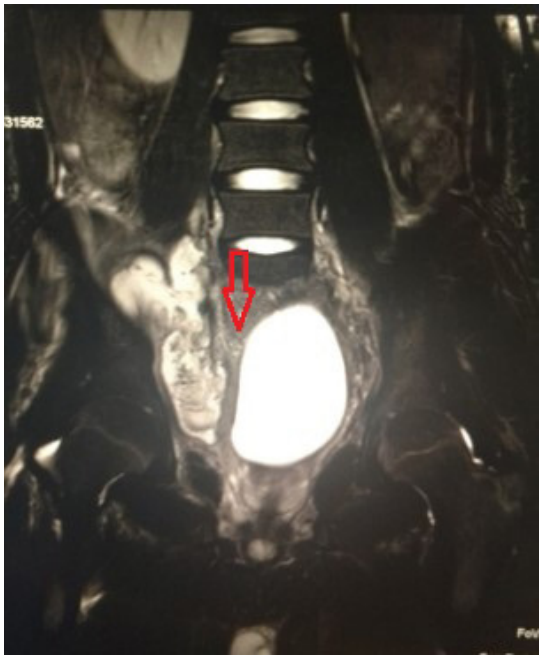

Figure 4. MRI (coronal section) showing a collection of about 11*4*3 cm along the anterior border of right SI joint beneath the psoas muscle, tracking along the lateral pelvic wall indenting the lateral wall of bladder (arrow) and exiting through the ipsilateral obturator foramen.

infection (*11*). Risk factors are intravenous drug abuse, immunocompromised states like diabetes, hematological malignancies, alcoholism and HIV infection (*12*). Young adults and children in tropical countries are more susceptible for primary infection. Secondary IPA occurs after direct extension of infection from an adjacent structure like vertebral bodies, genitourinary tract, gastrointestinal tract, aorta and hip joint (*13*). Primary and secondary IPA of skeletal origin are invariably monomicrobial and most common organism isolated is *S. aureus* (methicillin sensitive more common than methicillin resistant) (*14*). Gram negative bacilli are predominantly seen in secondary psoas abscess of gastrointestinal and genitourinary tract origin, *Escherichia coli* being the most common isolate (*15*). *M. tuberculosis* is still prevalent in developing countries like India. Other causative organisms include *Brucella*, *Klebsiella*, *Bacteroides*, *Proteus*, *Clostridium* and *Salmonella*.

Gas-forming psoas abscess is rarely reported and most commonly caused by gram negative bacilli (*2*). Diabetic patients are predisposed to this infection and have high mortality rate (*3*). In a study by Hsieh *et al*., 88 patients of psoas abscess were analyzed retrospectively and 27 patients (31%) among these had gas-forming psoas abscess. Gram negative bacilli (51.9%) was the most common gas-forming pathogen isolated from pus, followed by gram positive cocci (44.4%) and anaerobes (33.3%). In this study, *E. coli* was the most common gas-forming gram negative bacilli isolated (5 patients) (*4*). Apart from this series, all other reported cases of gas-forming psoas abscess are due to *K. pneumoniae* (*2,3,5,6*). Rapid catabolism along with impaired transport of end products from the site of inflammation leads to gas formation (*16*). The high glucose levels and impaired immunity in diabetic patient provide microbes a favorable environment for sustained growth (*17*). The common gases found in gas abscess are hydrogen, oxygen, carbon dioxide and nitrogen. Psoas abscess is generally treated with antibiotics and image guided percutaneous drainage. However, gas-forming psoas abscess carries an unfavorable outcome, so an early surgical intervention is recommended in these patients (*4*). Our first patient had bilateral gas-forming psoas abscess with spondlyodiscitis, caused by *E. coli*. Surgical intervention was deferred as patient's general condition was poor and instead percutaneous drainage was done. However, the outcome was no favorable in this case.

Secondary IPA occurs due to direct spread of infection from surrounding structures. Extension

of skeletal infection is the most common cause of secondary psoas abscess, with vertebral bodies being the most common site. Pyogenic sacroilitis (PSI) causing psoas abscess is rarely reported in literature (*7-10*). The sacroiliac joint is closely related to iliopsoas muscle, hence infection from sacroiliac joint can easily extend to iliopsoas muscle too (*10*). The most common reported symptom of PSI is lumbogluteal pain. MRI is the preferred imaging modality for diagnosing PSI. The microbiological diagnosis of pyogenic scaroilitis can be done by culture of blood and joint fluid aspirate. The most common causative organism is *S. aureus*, however other organisms like *E. coli*, *Pseudomonas*, *Salmonella*, *Streptococcus* and *M. tuberculosis* have been also implicated (*18*). Treatment of PSI remains drainage of abscess by minimally invasive technique along with appropriate antibiotics. The duration of intravenous antibiotic is generally two weeks, followed by oral antibiotics for 4-6 weeks depending on CRP levels, clinical improvement and radiological clearing of lesion (*18*). The prognosis is favorable if treated appropriately and repeat MRI after successful treatment may show irregular cortical bones with subchondral sclerosis but without any edema. The second case here had right sided PSI with multiple abscesses in ilopsoas, gluteal and pelvic muscles. Methicillin sensitive *S. aureus* was isolated and patient improved significantly after six weeks of antibiotics.

To conclude, pyogenic IPA can have varied clinical manifestations. Bilateral gas forming IPA is rare and carries poor prognosis if treatment is delayed. Sacroilitis causing IPA is also unusual, but has a favorable outcome. These cases can be seen in medical wards too, hence, treating physicians should be aware about these presentations of IPA.

References

1. Schuenke M, Schulte E, Schumacher U. Thieme Atlas of Anatomy: Latin Nomenclature: General Anatomy and Musculoskeletal System. New York, USA, 2006;pp. e470-71.
2. Jang TN, Juang GD, Fung CP. Fulminating gas-forming psoas muscle abscess due to *Klebsiella pneumoniae* following a deep neck infection. J Formos Med Assoc. 1997; 96:134-136.
3. Chang CM, Ko WC, Lee HC, Chen YM, Chuang YC. *Klebsiella pneumoniae* psoas abscess: Predominance in diabetic patients and grave prognosis in gas-forming cases. J Microbiol Immunol Infect. 2001; 34:201-206.
4. Hsieh MS, Huang SC, Loh el-W, Tsai CA, Hung YY, Tsan YT, Huang JA, Wang LM, Hu SY. Features and treatment modality of iliopsoas abscess and its outcome: A 6-year hospital-based study. BMC Infect Dis. 2013; 13:578.
5. Liao PY, Chiang WC, Chen SY, Su CP, Wang JT, Hsueh PR. Rapidly fatal gas-forming pyogenic psoas abscess caused by *Klebsiella pneumoniae*. Clin Infect Dis. 2007; 44:1253-1255.
6. Cheng SP, Chang WW, Tsao YT. Gas-forming iliopsoas abscess: A *Klebsiella pneumoniae*-mediated invasive syndrome. J Emerg Med. 2016; 5:e127-e128.
7. Assalia A, Volpin G, Hashmonai M, Angel A, Stein H, Schein M. Psoas muscle abscess associated with pyogenic sacroiliitis. Eur J Surg. 1996; 162:415-417.
8. Osman A, Govender S. Septic sacroiliitis. Clin Orthop Relat Res. 1995; 313:214-219.
9. Gorgulu S, Komurcu M, Silit E, Kocak I. Psoas abscess as a complication of pyogenic sacroiliitis: Report of a case. Surg Today. 2002; 32:443-445.
10. Hanson P, Delaere B, Nisolle J, Deltombe T. Pyrexia due to pyogenic sacroiliitis with iliopsoas abscess after spinal cord injury. Spinal Cord. 2004; 42:649-651.
11. Mückley T, Schütz T, Kirschner M, Potulski M, Hofmann G, Bühren V. Psoas abscess: The spine as a primary source of infection. Spine (Phila Pa 1976). 2003; 28:e106-113.
12. Mallick IH, Thoufeeq MH, Rajendran TP. Iliopsoas abscesses. Postgrad Med J. 2004; 80:459-462.
13. Adelekan MO, Taiwo SS, Onile BA. A review of psoas abscess. Afr J Clin Exp Microbiol. 2004; 5:55-63.
14. Santaella RO, Fishman EK, Lipsett PA. Primary *vs* secondary iliopsoas abscess. Presentation, microbiology, and treatment. Arch Surg. 1995; 130:1309-1313.
15. Navarro López V, Ramos JM, Meseguer V, Pérez Arellano JL, Serrano R, García Ordóñez MA, Peralta G, Boix V, Pardo J, Conde A, Salgado F, Gutiérrez F; GTI-SEMI Group. Microbiology and outcome of iliopsoas abscess in 124 patients. Medicine (Baltimore). 2009; 88:120-130.
16. Yang WH, Shen NC. Gas-forming infection of the urinary tract: An investigation of fermentation as a mechanism. J Urol. 1990; 143:960-964.
17. Rayfield EJ, Ault MJ, Keusch GT, Brothers MJ, Nechemias C, Smith H. Infection and diabetes: The case for glucose control. Am J Med. 1982; 72:439-450.
18. Kucera T, Brtkova J, Sponer P, Ryskova L, Popper E, Frank M, Kucerova M. Pyogenic sacroiliitis: Diagnosis, management and clinical outcome. Skeletal Radiol. 2015; 44:63-71.

(Received January 5, 2018; Revised January 31, 2018; Accepted February 5, 2018)

Case Report

DOI: 10.5582/ddt.2017.01069

Long-term use of ipragliflozin improved cardiac sympathetic nerve activity in a patient with heart failure: A case report

Shunsuke Kiuchi*, Shinji Hisatake, Takayuki Kabuki, Takahiro Fujii, Takashi Oka, Shintaro Dobashi, Hidenobu Hashimoto, Takanori Ikeda

Department of Cardiovascular Medicine, Toho University Faculty of Medicine, Tokyo, Japan.

Summary **Ipragliflozin is the first SGLT2 inhibitor approved in Japan. Reported here is a case where long-term administration of ipragliflozin decreased the rate of re-hospitalization due to heart failure (HF). An 83-year-old man with chronic HF and diabetes mellitus (DM) was hospitalized four times in the last five years. He was discharged six months after his last hospitalization, but he continued to have class III HF according to the New York Heart Association classification (NYHA), and his DM was also not properly managed. Therefore, he received ipragliflozin. One year after initiation of ipragliflozin, he lost weight (body weight (BW): 79.0 to 76.2 kg), his levels of brain natriuretic peptide (BNP) decreased (191.4 to 122.5 mg/dL), and the class of his HF improved (class III to class II). The management of DM also improved (fasting blood glucose: 100 to 110 mg/dL; hemoglobin A1C: 6.8 to 6.6%). In addition, cardiac sympathetic nerve function evaluated with ^{123}I-metaiodobenzylguanidine cardiac-scintigraphy (^{123}I-MIBG) also improved (the average of the heart-to-mediastinum ratio in early and delayed phases; 1.44 to 2.17 in the early phase, 1.41 to 1.92 in the delayed phase, washout rate; 43.3 to 35.6). The patient was not re-hospitalized due to HF two years after administration of ipragliflozin started. A reduction in cardiac sympathetic nerve hyperactivity by an SGLT2 inhibitor might be one of the mechanisms of its cardio-protective effect, but clinical studies need to be conducted to verify this finding.**

Keywords: Ipragliflozin, cardiac sympathetic nerve activity, heart failure, diabetes mellitus

1. Introduction

Diabetes mellitus (DM) is known to increase the incidence of macrovascular complications, including coronary artery disease, and cardiovascular mortality (*1,2*). One of the goals of DM treatments is to prevent these complications and improve cardiovascular mortality. However, previous studies have revealed that no DM treatments demonstrably reduce these cardiovascular complications or improve the cardiovascular prognosis for patients until the approved of sodium-glucose linked transporter (SGLT) 2 inhibitors. In the EMPA-REG Outcome trial in 2015, a SGLT 2 inhibitor, empagliflozin, reduced the mortality rate from cardiovascular complications in patients with DM for the first time (*3*). Although the EMPA-REG Outcome trial investigated the secondary prevention of cardiovascular complications, the CVD-REAL trial indicated the effect of an SGLT 2 inhibitor as part of primary prevention (*4*). Therefore, an SGLT 2 inhibitor may alleviate cardiovascular complications in all diabetics, but the mechanisms by which is does so are still unclear.

Ipragliflozin, another SGLT 2 inhibitor, was approved and marketed in 2014 in Japan as a DM treatment. Reported here is a case where long-term administration of ipragliflozin reduced cardiac sympathetic nerve activity and the rate of re-hospitalization rate due to heart failure (HF). This case report was performed in accordance with the Declaration of Helsinki and was

Released online in J-STAGE as advance publication February 25, 2018.

**Address correspondence to:*
Dr. Shunsuke Kiuchi, Department of Cardiovascular Medicine, Toho University Faculty of Medicine, 6-11-1 Omori-nishi, Ota-ku, Tokyo 143-8541, Japan.
E-mail: syunnsuke@med.toho-u.ac.jp

approved by the Ethics Committee of Toho University's Omori Medical Center (24-123).

2. Case Report

The patient was an 83-year-old man with HF caused by moderate mitral regurgitation (MR) with left atrium (LA) enlargement, atrial fibrillation (AF), DM, and chronic kidney disease. His HF was severe, and he was hospitalized due to HF four times in the last five years. He was discharged six months after his last hospitalization, but his HF at discharge was class III according to the New York Heart Association classification (NHYA). His HF continued to be class III, so he received oxygen at home. In addition, he had hyperuricemia, dyslipidemia, and peripheral artery disease, and he was taking the following medications: rabeprazole 10 mg, warfarin 3 mg, febuxostat 20 mg, pitavastatin 2 mg, bisoprolol 5 mg, azosemide 15 mg, perindopril 2 mg, sitagliptin 50 mg, beraprost 40 μg, pimobendan 2.5 mg, and tolvaptan 15 mg/day. Laboratory results at discharge were a creatinine level of 1.03 mg/dL, an estimated glomerular filtration rate (eGFR) of 53.0 mL/min/1.73m^2, a fasting plasma glucose (FPG) level of 100 mg/dL, a hemoglobin A1C (HbA1C) of 6.8%, and a brain natriuretic peptide (BNP) level of 191.4 pg/mL. There were no major abnormalities in other laboratory results (data not shown). A chest X-ray at discharge revealed a substantial increase in the cardiothoracic ratio (CTR) (69.2%, Figure 1A). Electrocardiography revealed AF and a complete right bundle branch block (QRS duration: 166 msec) (data not shown). Transthoracic echocardiography at discharge revealed MR on one side with LA enlargement, left ventricular (LV) enlargement (LV diastolic/systolic diameter (LVDd/Ds): 72.6/51.4 mm), and a preserved ejection fraction (EF = 54.5%) (Figure 2A). Class III HF and hyperglycemia persisted, so administration of ipragliflozin was started.

One year after initiation of ipragliflozin, BNP levels and glycemic control improved (BNP 122.5 pg/mL, FPG 110 mg/dL, HbA1C 6.6%). Renal function diminished slightly (creatinine: 1.27 mg/dL, eGFR: 41.9 mL/min/1.73m^2). Cardiac size was slightly smaller (CTR 66.3%, Figure 1B, LVDd/Ds 69.2/48.2mm), and EF was 60.5% (Figure 2B). Moreover, body weight decreased (79.0 to 76.2 kg) and symptoms also improved (NHYA III to II). Blood pressure was maintained (104/75 to 125/74 mmHg). In addition, cardiac sympathetic nerve function was evaluated with ^{123}I-metaiodobenzylguanidine cardiac-scintigraphy (^{123}I-MIBG). Cardiac sympathetic nerve function was evaluated based on the ratio of the average region of interest (ROI) in the heart (H) to the average ROI in the mediastinum (M) (the H/M ratio) in early and delayed images, and the washout rate (WR) was calculated with the formula: WR (%) = (early image H/M – late image H/M)/early image H/M × 100 (*5*). In the stable period prior to the patient's last hospitalization, cardiac sympathetic nerve hyperactivity (early H/M: 1.44, delayed H/M: 1.41, WR: 43.3, Figure 3A) was evident. After administration of ipragliflozin, H/M rose and WR declined, indicating improvement in cardiac sympathetic nerve activity (early H/M: 2.17, delayed H/M: 1.92, WR: 35.6, Figure 3B). Improved parameters as a result of ipragliflozin treatment are summarized in Table 1. Oral medications besides ipragliflozin were not

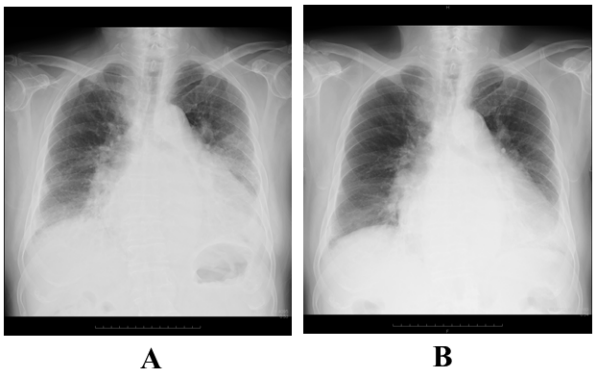

Figure 1. Chest X ray at discharge (A) and one year after initiation of ipragliflozin (B). The increase in the cardiothoracic ratio one year after initiation of ipragliflozin was smaller than at discharge.

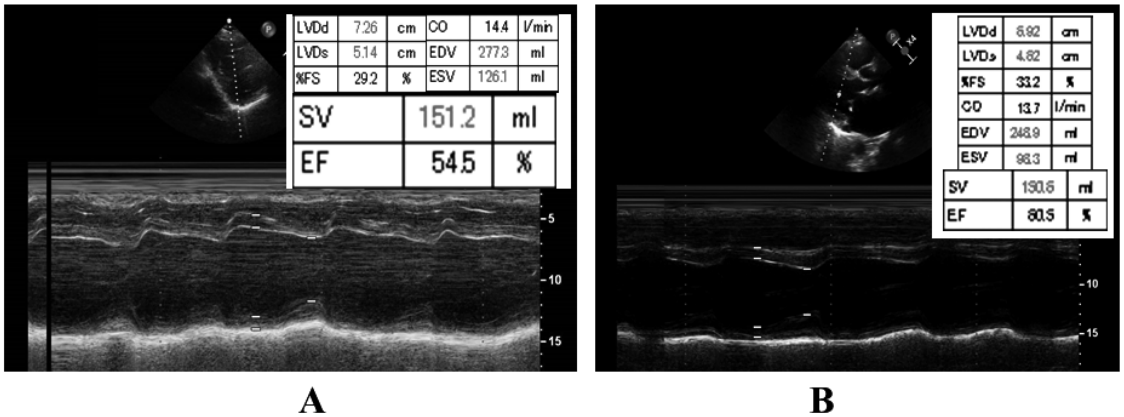

Figure 2. Transthoracic echocardiography at discharge (A) compared with one year after initiation of ipragliflozin (B). Cardiac size was slightly smaller after one year. Ejection fraction was preserved.

changed. The patient was not re-hospitalized due to HF two years after initiation of ipragliflozin.

3. Discussion

In the current case, findings were presumably influenced by ipragliflozin alone since oral medications besides ipragliflozin were not changed. Large-scale clinical trials have reported the cardio-protective effect of SGLT-2 inhibitors. The CANVAS trial reported the cardio-protective effect of canagliflozin (*6*), and the EMPA-REG Outcome trial reported the cardio-protective effect of empagliflozin (*3*). Small-scale clinical trials have reported that other SGLT2 inhibitors have cardio-protective effects, so the cardio-protective effect of SGLT2 inhibitors is presumably not a drug effect but a class effect. Sub-analyses of those trials revealed that SGLT2 inhibitors had a reno-protective effect (*7,8*), but these mechanisms of organ protection by SGLT2 inhibitors are still unclear. SGLT2 inhibitors are reported to have cardio-protective effects through reno-protection, lowering of blood pressure, and a reduction in plasma volume (*9-11*). SGLT2 inhibitors increase blood ketone bodies, and they may cause a shift in renal and myocardial fuel metabolism away from fat and glucose oxidation to more energy-efficient fuel like ketone bodies, thus leading to organ protection. However, SGLT2 inhibitors may also act directly on the heart (*12*). In mice, hyperglycemia increases cardiac oxidative stress, which an SGLT2 inhibitor then reduces (*13*). In addition, SGLT2 inhibitors cause a shift from b-oxidation of free fatty acids to glycolysis in the myocardium, possibly mitigating the potential pro-arrhythmic effects of free fatty acid metabolites (*14*). A study of diabetics has reported that oxidative stress and sympathetic nerve function in the heart are related (*15*). A reduction in oxidative stress might decrease cardiac sympathetic nerve hyperactivity. That said, another study has reported that cardiac sympathetic hyperactivity, evaluated with ^{123}I-MIBG, is useful in evaluating the prognosis for HF (*16*). Therefore, a reduction in cardiac sympathetic nerve hyperactivity by an SGLT2 inhibitor might be a mechanism of its cardio-protective effect.

In conclusion, this case report indicated that long-term use of an SGLT2 inhibitor reduced cardiac sympathetic hyperactivity. Clinical studies need to be conducted to verify this finding.

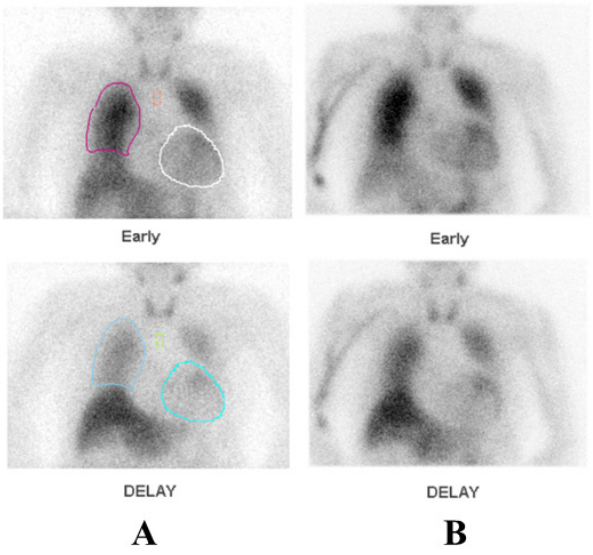

Figure 3. ^{123}I-MIBG cardiac-scintigraphy at discharge (A) and one year after initiation of ipragliflozin (B). After administration of ipragliflozin, cardiac sympathetic nerve function improved.

References

1. Haffner SM, Lehto S, Rönnemaa T, Pyörälä K, Laakso M. Mortality from coronary heart disease in subjects with type 2 diabetes and in nondiabetic subjects with and without prior myocardial infarction. N Engl J Med. 1998; 339:229-234.
2. Baena-Díez JM, Peñafiel J, Subirana I, *et al*. Risk of cause-specific death in individuals with diabetes: A competing risks analysis. Diabetes Care. 2016; 39:1987-1995.
3. Zinman B, Wanner C, Lachin JM, Fitchett D, Bluhmki E, Hantel S, Mattheus M, Devins T, Johansen OE, Woerle HJ, Broedl UC, Inzucchi SE; EMPA-REG OUTCOME Investigators. Empagliflozin, cardiovascular outcomes, and mortality in type 2 diabetes. N Engl J Med. 2015; 373:2117-2128.
4. Kosiborod M, Cavender MA, Fu AZ, Wilding JP, Khunti K, Holl RW, Norhammar A, Birkeland KI, Jørgensen ME, Thuresson M, Arya N, Bodegård J, Hammar N, Fenici P; CVD-REAL Investigators and Study Group. Lower risk

Table 1. Improvement in parameters with ipragliflozin treatment

Items	Before administration of ipragliflozin	After administration of ipragliflozin
body weight (kg)	79.0	76.2
brain natriuretic peptide	191.4	122.5
New York Heart Association classification	III	II
fasting blood glucose	100	110
hemoglobin A1C	6.8	6.6
average of the heart-to-mediastinum ratio in early MIBG	1.44	2.17
average of the heart-to-mediastinum ratio in delayed MIBG	1.41	1.92
washout rate in MIBG	43.3	35.6

MIBG: ^{123}I-metaiodobenzylguanidine cardiac-scintigraphy.

of heart failure and death in patients initiated on sodium-glucose cotransporter-2 inhibitors versus other glucose-lowering drugs: The CVD-REAL Study (Comparative Effectiveness of Cardiovascular Outcomes in New Users of Sodium-Glucose Cotransporter-2 Inhibitors). Circulation. 2017; 136:249-259.
5. Kiuchi S, Hisatake S, Kabuki T, Oka T, Dobashi S, Fujii T, Ikeda T. Azelnidipine is a useful medication for the treatment of heart failure preserved ejection fraction. Clin Exp Hypertens. 2017; 39:350-354.
6. Neal B, Perkovic V, de Zeeuw D, Mahaffey KW, Fulcher G, Stein P, Desai M, Shaw W, Jiang J, Vercruysse F, Meininger G, Matthews D. Rationale, design, and baseline characteristics of the Canaglyflozin Cardiovascular Assessment Study (CANVAS) – A randomized placebo-controlled trial. Am Heart J. 2013; 166:217-223.
7. Wanner C, Inzucchi SE, Lachin JM, Fitchett D, von Eynatten M, Mattheus M, Johansen OE, Woerle HJ, Broedl UC, Zinman B; EMPA-REG OUTCOME Investigators. Empagliflozin and progression of kidney disease in type 2 diabetes. N Engl J Med. 2016; 375:323-334.
8. Neal B, Perkovic V, Mahaffey KW, Fulcher G, Erondu N, Desai M, Shaw W, Law G, Walton MK, Rosenthal N, de Zeeuw D, Matthews DR; CANVAS Program Collaborative Group. Optimizing the analysis strategy for the CANVAS Program: A prespecified plan for the integrated analyses of the CAMVAS and CANVAS-R trials. Diabetes Obes Metab. 2017; 19:926-935.
9. Martens P, Mathieu C, Verbrugge FH. Promise of SGLT2 inhibitors in heart failure: Diabetes and beyond. Curr Treat Options Cardiovasc Med. 2017; 19:23.
10. Tikkanen I, Narko K, Zeller C, Green A, Salsali A, Broedl UC, Woerle HJ; EMPA-REG BP Investigators. Empagliflozin reduces blood pressure in patients with type 2 diabetes and hypertension. Diabetes Care. 2015; 38:420-428.
11. Lytvyn Y, Bjornstad P, Udell JA, Lovshin JA, Cherney DZ. Sodium glucose cotransporter-2 inhibition in heart failure: Potential mechanisms, clinical applications, and summary of clinical trials. Circulation. 2017; 136:1643-1658.
12. Bonner C, Kerr-Conte J, Gmyr V, Queniat G, Moerman E, Thévenet J, Beaucamps C, Delalleau N, Popescu I, Malaisse WJ, Sener A, Deprez B, Abderrahmani A, Staels B, Pattou F. Inhibition of the glucose transporter SGLT2 with dapagliflozin in pancreatic alpha cells triggers glucagon secretion. Nat Med. 2015; 21:512-517.
13. Lin B, Koibuchi N, Hasegawa Y, Sueta D, Toyama K, Uekawa K, Ma M, Nakagawa T, Kusaka H, Kim-Mitsuyama S. Glycemic control with empagliflozin, a novel selective SGLT2 inhibitor, ameliorates cardiovascular injury and cognitive dysfunction in obese and type 2 diabetic mice. Cardiovasc Diabetol. 2014; 26:148.
14. Taegtmeyer H, McNulty P, Young ME. Adaptation and maladaptation of the heart in diabetes: Part I: general concepts. Circulation. 2002; 105:1727-1733.
15. Matyal R, Sakamuri S, Huang T, Owais K, Parikh S, Khabbaz K, Wang A, Sellke F, Mahmood F. Oxidative stress and nerve function after cardiopulmonary bypass in patients with diabetes. Ann Thorac Surg. 2014; 98:1635-1643.
16. Narula J, Gerson M, Thomas GS, Cerqueira MD, Jacobson AF. ^{123}I-MIBG imaging for prediction of mortality and potentially fatal events in heart failure: The ADMIRE-HFX study. J Nucl Med. 2015; 56:1011-1018.

(Received December 14, 2017; Revised January 30, 2018; Accepted February 4, 2018)

Case Report

DOI: 10.5582/ddt.2018.01005

First things first: Importance of eosinophil count in diagnosing occult parasites

Nitin Gupta[1], Animesh Ray[2,*], Sudeshna Ghosh[2], Sundeep Malla[3], Surabhi Vyas[3]

[1] *Departments of Medicine and Microbiology, All India Institute of Medical Sciences, New Delhi, India;*
[2] *Department of Medicine, All India Institute of Medical Sciences, New Delhi, India;*
[3] *Department of Radiology, All India Institute of Medical Sciences, New Delhi, India.*

Summary **Tropical pulmonary eosinophilia (TPE) is a rare allergic manifestation to the filarial nematode. A 38-year old male and a 15-year old female presented with cough and breathlessness. Their complete blood count showed eosinophilia. This finding was overshadowed by the radiological findings suggestive of tuberculosis. The diagnosis of TPE was confirmed by filarial antigen detection test and both the patients were successfully treated with diethylcarbamazine. TPE presents with cough and breathlessness and can be often confused with tuberculosis, especially in endemic settings. An important clue in differentiating the two entities is the presence of eosinophilia in the former.**

Keywords: Tropical pulmonary eosinophilia, filariasis, tuberculosis

1. Introduction

Indian subcontinent is endemic for the filarial nematode, Wuchereria bancrofti and Brugia malayi. The adult filarial worm resides in the lymphatics and releases microfilariae into the peripheral circulation. These microfilariae are trapped in lungs. In less than 0.5% of cases, there may be an exaggerated immune response against microfilariae causing eosinophilic inflammation of lower airways (*1*). This syndrome is called as tropical pulmonary eosinophilia (TPE), where patients present with cough, with or without breathlessness and eosinophilia. It is an easily treatable but a commonly missed entity. We present two cases of TPE who were referred to us with a provisional diagnosis of tuberculosis (TB).

2. Case Report

2.1. *Case 1*

A 38-year-old male patient, resident of Bihar with no prior co-morbidities presented with complaints of cough with expectoration and dyspnea on exertion for one year. He was apparently asymptomatic one year back when he started to have insidious onset cough with mucoid expectoration. This cough would worsen at night and was relieved only temporarily with anti-tussive agents. He also complained of breathlessness on exertion which initially started with strenuous activities like walking up the stairs and gradually progressed in a span of six to seven months, into dyspnea at rest. His brother, who was residing in the same house was diagnosed with pulmonary tuberculosis five years back and was successfully treated with six months of anti-tubercular therapy. There was no associated fever, hemoptysis, chest pain or palpitation. He was not a smoker or an alcoholic. There was no history of tuberculosis. A pulmonary function test was done which revealed severe obstruction with no significant reversibility (FVC-57% of predicted, FEV1-40% of predicted, FEV1/FVC-69% of predicted). He was initially treated with inhalational steroids and inhalational beta-agonists for around four months but there was no response. His serum ACE level was 45 mcg/L (Normal < 40 mcg/L). His Mantoux test was positive with an induration of 25 × 20 mm. Ziehl Neelsen staining and GeneXpert for sputum was negative. A contrast enhanced computed tomography (CECT) scan of chest revealed centrilobular nodules in bilateral lungs with some enlarged subcarinal nodes with foci of calcification

**Address correspondence to:*
Dr. Animesh Ray, Department of Medicine, Teaching block, 3rd floor, All India Institute of Medical Sciences, New Delhi, India.
E-mail: doctoranimeshray@gmail.com

(Figures 1 and 2). With a suspicion of tuberculosis/ sarcoidosis, he was referred to us to initiate anti-tubercular therapy or steroids or both. On examination, there was diffuse wheezing bilaterally. Rest of the systemic examination was normal. On review of records, it was found that he had a total leucocyte count (TLC) of 12,800/cu.mm with an eosinophil of 9.6% (Absolute Eosinophil count or AEC-1229/cu.mm). A repeat complete blood count (CBC) was ordered which revealed a TLC of 31,300/cu.mm with 75% eosinophils (AEC-23475/cu.mm). IgE levels were found to be > 2,500. IgG immunodiffusion test against *Aspergillus fumigatus* was negative. Microscopic examination of stool for parasite detection was negative (thrice). Peripheral blood smear and quantitative buffy coat for malaria or filariasis was negative. Circulating filarial antigen and filarial IgM antibody was found to be positive. With a provisional diagnosis of tropical pulmonary eosinophilia, he was started on diethylcarbamazine (DEC), 100 mg TDS for 21 days. There was a dramatic response after initiation of therapy. During the follow up, one month after initiation of treatment, the patient was completely asymptomatic. His TLC reduced to 8,800/μL with an eosinophil count of 10.6% (AEC-933). There was some improvement in PFT parameters (FVC-64%, FEV1-61%, FEV1/FVC-99%) also.

2.2. *Case 2*

A 14-year old female from Delhi with no prior comorbidities presented with cough and dyspnea on exertion for one year. She was apparently asymptomatic one year back, when she had cough with whitish expectoration which would increase at night time and decrease only with antitussive agents. The severity of cough was mostly static through-out the year. She also had dyspnea on exertion which initially started with strenuous activities like running on the playground and gradually progressed to dyspnea on walking on plain ground for more than two minutes. There was no history of orthopnoea or paroxysmal nocturnal dyspnoea. She had no associated fever, hemoptysis or chest pain. There was no history of allergy in the family or contact with tuberculosis. She was a non-smoker and non-

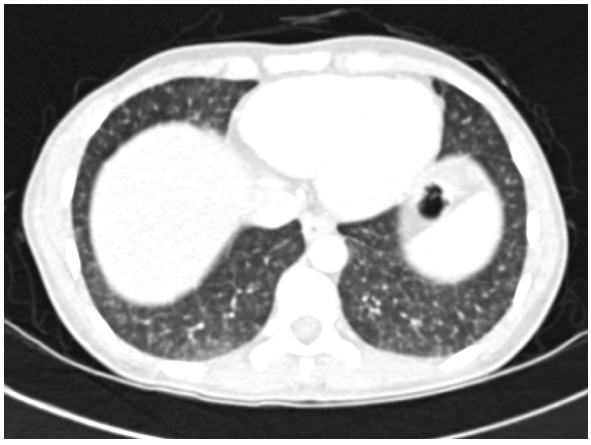

Figure 1. Contrast enhanced computed tomography (CECT) axial lung window image shows centrilobular and random nodules with areas of ground glass opacity in bilateral lungs predominantly in basal location.

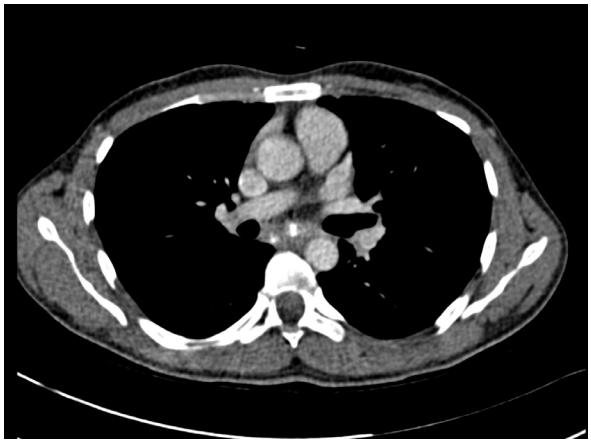

Figure 2. CECT axial mediastinal window image shows calcified sub-carinal nodes.

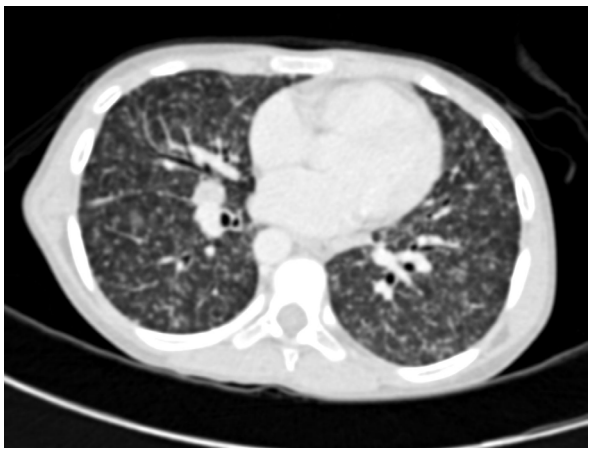

Figure 3. CECT axial lung window image shows diffuse randomly distributed nodules in bilateral lung fields.

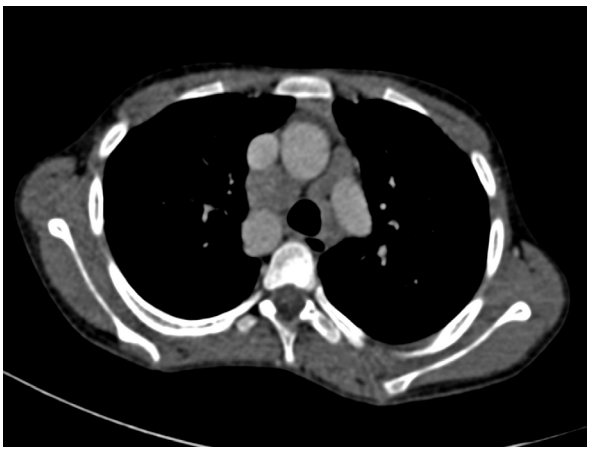

Figure 4. CECT axial mediastinal window image shows multiple enlarged homogenous nodes in right para-tracheal and aortopulmonary location.

alcoholic. On examination, she had mild pallor and bilateral sub-centimetric cervical lymph nodes. The chest examination revealed bilateral diffuse rhonchi. Her Chest X-ray showed bilateral infiltrates. PFT showed restrictive pattern (FVC-51%, FEV1-48%, FEV1/FVC-95%). She was started on inhalational steroids and was referred to us with a suspicion of tuberculosis. Her sputum for AFB was negative and mantoux test was negative (0 mm). CECT chest showed multiple bilateral nodules and enlarged mediastinal (aorto-pulmonary and right paratracheal) lymph nodes (Figures 3 and 4). Her complete blood count was traced and was found to have leukocytosis with eosinophilia (TLC-16,500/cu.mm, Eosinophil-53%, AEC- 8745/cu.mm). The repeat total count was 30,300/cu.mm with eosinophil being 71.8% (AEC-21,755/cu.mm). Peripheral blood smear and quantitative buffy coat for filariasis was negative. The circulating filarial antigen came out to be positive. With a diagnosis of TPE, she was started on DEC, 100 mg TDS for 21 days. The patient responded well with complete resolution of symptoms at follow up. Her chest auscultation was clear with normal vesicular sounds. The TLC reduced to 10,000/cu.mm with an eosinophil count of 35% (AEC- 3,500/cu.mm) after 28 days of therapy. There was some improvement in PFT parameters (FVC-79%, FEV1-76%, FEV1/FVC-92%) also.

3. Discussion

TPE usually presents as dry nocturnal cough only. Dyspnea on exertion is relatively uncommon. Chest findings are usually absent but wheezing may be occasionally found. Initially the wheezing is due to bronchospasm but later on it is due to alveolitis and involvement of lower airways. PFTs commonly demonstrate restrictive pattern with or without superadded obstruction (*1*). Increased eosinophil count (> 3,000/mcl) and IgE levels (> 1,000 U/mL) due to type 1 hypersensitivity is common (*1*). Radiography of chest sometime shows interstitial shadows, miliary mottling and mediastinal lymphadenopathy (*2*).

The patients were initially managed as a case of airway disease but there was no history of smoking and there was no improvement with inhalational steroids. The history of contact, the positive mantoux test in the first patient and the radiology features in both the patients led to the possible diagnosis of tuberculosis. However, their sputum for ZN staining was negative. A large number of Indian population has latent TB and therefore mere positivity of mantoux test is never taken as indicative of active TB (*3*). There are few reports, where TPE was misdiagnosed as TB (*2*). The non-necrotic hilar lymph nodes and the raised ACE levels raised the suspicion of sarcoidosis in the first patient but ACE levels have been shown to have insufficient specificity for sarcoidosis (*4*).

The diagnosis of TPE was missed initially in both the cases as the CBC which is usually the most basic and often, the most informative investigation, was overlooked. In these cases, the primary care physicians concentrated on initially the PFT report and later on the CECT report. Prompt detection and evaluation of eosinophilia would have alleviated the patient of significant morbidity. Eosinophilia can be seen with other causes such as other helminthic infection or Allergic bronchopulmonary aspergillosis (ABPA) but stool for parasites and immunodiffusion test was negative (*5*).

TPE should be suspected in patients residing in endemic area and presenting with nocturnal cough and breathlessness, infiltrates in Chest X-ray and peripheral eosinophil count of 3,000 cells/µl (*6,7*). The diagnosis can be confirmed by presence of filarial antigen and antibody (*1,7*). Clinical response to DEC also points towards the diagnosis of TPE (*6*). It should be noted that the antigen can be absent in 50% of cases (*8*). DEC is the treatment of choice often requiring supplementation with doxycycline or albendazole (*1*). The response to DEC can often be dramatic but frequent relapses are reported. Therefore, the treatment might need repetition in few cases. There is decrease in eosinophilia with the treatment but the PFT values rarely returns to normal.

We report these cases to highlight the need for performing basic investigations first before moving on to expensive/complicated/invasive tests. The cases although rare, the presentation even rarer, could have been easily diagnosed with a simple blood investigation.

References

1. Mullerpattan JB, Udwadia ZF, Udwadia FE. Tropical pulmonary eosinophilia-a review. Indian J Med Res. 2013; 138:295-302.
2. Ray S, Kundu S, Goswami M, Maitra S. Tropical pulmonary eosinophilia misdiagnosed as miliary tuberculosis: A case report and literature review. Parasitol Int. 2012; 61:381-384.
3. Pai M, Rodrigues C. Management of latent tuberculosis infection: An evidence-based approach. Lung India. 2015; 32:205-207.
4. Ungprasert P, Carmona EM, Crowson CS, Matteson EL. Diagnostic utility of angiotensin converting enzyme in sarcoidosis: A population-based study. Lung. 2016; 194:91-95.
5. O'Connell EM, Nutman TB. Eosinophilia in infectious diseases. Immunol Allergy Clin North Am. 2015; 35:493-522.
6. Vijayan VK. Tropical pulmonary eosinophilia: pathogenesis, diagnosis and management. Curr Opin Pulm Med. 2007; 13:428-433.
7. Ottesen EA, Nutman TB. Tropical pulmonary eosinophilia. Annu Rev Med. 1992; 43:417-424.
8. Lal RB, Paranjape RS, Briles DE, Nutman TB, Ottesen EA. Circulating parasite antigen(s) in lymphatic filariasis: Use of monoclonal antibodies to phosphocholine for immunodiagnosis. J Immunol. 1987; 138:3454-3460.

(Received January 25, 2018; Revised February 20, 2018; Accepted February 22, 2018)

DD&T
Drug Discoveries & Therapeutics

Guide for Authors

1. Scope of Articles

Drug Discoveries & Therapeutics welcomes contributions in all fields of pharmaceutical and therapeutic research such as medicinal chemistry, pharmacology, pharmaceutical analysis, pharmaceutics, pharmaceutical administration, and experimental and clinical studies of effects, mechanisms, or uses of various treatments. Studies in drug-related fields such as biology, biochemistry, physiology, microbiology, and immunology are also within the scope of this journal.

2. Submission Types

Original Articles should be well-documented, novel, and significant to the field as a whole. An Original Article should be arranged into the following sections: Title page, Abstract, Introduction, Materials and Methods, Results, Discussion, Acknowledgments, and References. Original articles should not exceed 5,000 words in length (excluding references) and should be limited to a maximum of 50 references. Articles may contain a maximum of 10 figures and/or tables.

Brief Reports definitively documenting either experimental results or informative clinical observations will be considered for publication in this category. Brief Reports are not intended for publication of incomplete or preliminary findings. Brief Reports should not exceed 3,000 words in length (excluding references) and should be limited to a maximum of 4 figures and/or tables and 30 references. A Brief Report contains the same sections as an Original Article, but the Results and Discussion sections should be combined.

Reviews should present a full and up-to-date account of recent developments within an area of research. Normally, reviews should not exceed 8,000 words in length (excluding references) and should be limited to a maximum of 100 references. Mini reviews are also accepted.

Policy Forum articles discuss research and policy issues in areas related to life science such as public health, the medical care system, and social science and may address governmental issues at district, national, and international levels of discourse. Policy Forum articles should not exceed 2,000 words in length (excluding references).

Case Reports should be detailed reports of the symptoms, signs, diagnosis, treatment, and follow-up of an individual patient. Case reports may contain a demographic profile of the patient but usually describe an unusual or novel occurrence. Unreported or unusual side effects or adverse interactions involving medications will also be considered. Case Reports should not exceed 3,000 words in length (excluding references).

News articles should report the latest events in health sciences and medical research from around the world. News should not exceed 500 words in length.

Letters should present considered opinions in response to articles published in Drug Discoveries & Therapeutics in the last 6 months or issues of general interest. Letters should not exceed 800 words in length and may contain a maximum of 10 references.

3. Editorial Policies

Ethics: Drug Discoveries & Therapeutics requires that authors of reports of investigations in humans or animals indicate that those studies were formally approved by a relevant ethics committee or review board.

Conflict of Interest: All authors are required to disclose any actual or potential conflict of interest including financial interests or relationships with other people or organizations that might raise questions of bias in the work reported. If no conflict of interest exists for each author, please state "There is no conflict of interest to disclose".

Submission Declaration: When a manuscript is considered for submission to Drug Discoveries & Therapeutics, the authors should confirm that 1) no part of this manuscript is currently under consideration for publication elsewhere; 2) this manuscript does not contain the same information in whole or in part as manuscripts that have been published, accepted, or are under review elsewhere, except in the form of an abstract, a letter to the editor, or part of a published lecture or academic thesis; 3) authorization for publication has been obtained from the authors' employer or institution; and 4) all contributing authors have agreed to submit this manuscript.

Cover Letter: The manuscript must be accompanied by a cover letter signed by the corresponding author on behalf of all authors. The letter should indicate the basic findings of the work and their significance. The letter should also include a statement affirming that all authors concur with the submission and that the material submitted for publication has not been published previously or is not under consideration for publication elsewhere. The cover letter should be submitted in PDF format. For example of Cover Letter, please visit http://www.ddtjournal.com/downcentre.php (Download Centre).

Copyright: A signed JOURNAL PUBLISHING AGREEMENT (JPA) must be provided by post, fax, or as a scanned file before acceptance of the article. Only forms with a hand-written signature are accepted. This copyright will ensure the widest possible dissemination of information. A form facilitating transfer of copyright can be downloaded by clicking the appropriate link and can be returned to the e-mail address or fax number noted on the form (Please visit Download Centre). Please note that your manuscript will not proceed to the next step in publication until the JPA form is received. In addition, if excerpts from other copyrighted works are included, the author(s) must obtain written permission from the copyright owners and credit the source(s) in the article.

Suggested Reviewers: A list of up to 3 reviewers who are qualified to assess the scientific merit of the study is welcomed. Reviewer information including names, affiliations, addresses, and e-mail should be provided at the same time the manuscript is submitted online. Please do not suggest reviewers with known conflicts of interest, including participants or anyone with a stake in the proposed research; anyone from the same institution; former students, advisors, or research collaborators (within the last three years); or close personal contacts. Please note that the Editor-in-Chief may accept one or more of the proposed reviewers or may request a review by other qualified persons.

Language Editing: Manuscripts prepared by authors whose native language is not English should have their work proofread by a native English speaker before submission. If not, this might delay the publication of your manuscript in Drug Discoveries & Therapeutics.

The Editing Support Organization can provide English proofreading, Japanese-English translation, and Chinese-English translation services to authors who want to publish in Drug Discoveries & Therapeutics and need assistance before submitting a manuscript. Authors can visit this organization directly at http://www.iacmhr.com/iac-eso/support.php?lang=en. IAC-ESO was established to facilitate manuscript preparation by researchers whose native language is not English and to help edit works intended for international academic journals.

4. Manuscript Preparation

Manuscripts should be written in clear, grammatically correct English and submitted as a Microsoft Word file in a single-column format. Manuscripts must be paginated and typed in 12-point Times New Roman font with 24-point line spacing. Please do not embed figures in the text. Abbreviations should be used as little as possible and should be explained at first mention unless the term is a well-known abbreviation (*e.g.* DNA). Single words should not be abbreviated.

Title page: The title page must include 1) the title of the paper (Please note the title should be short, informative, and contain the major key words); 2) full name(s) and affiliation(s) of the author(s), 3) abbreviated names of the author(s), 4) full name, mailing address, telephone/fax numbers, and e-mail address of the corresponding author; and 5) conflicts of interest (if you have an actual or potential conflict of interest to disclose, it must be included as a footnote on the title page of the manuscript; if no conflict of interest exists for each author, please state "There is no conflict of interest to disclose"). Please visit Download Centre and refer to the title page of the manuscript sample.

Abstract: The abstract should briefly state the purpose of the study, methods, main findings, and conclusions. For article types including Original Article, Brief Report, Review, Policy Forum, and Case Report, a one-paragraph abstract consisting of no more than 250 words must be included in the manuscript. For News and Letters, a brief summary of main content in 150 words or fewer should be included in the manuscript. Abbreviations must be kept to a minimum and non-standard abbreviations explained in brackets at first mention. References should be avoided in the abstract. Key words or phrases that do not occur in the title should be included in the Abstract page.

Introduction: The introduction should be a concise statement of the basis for the study and its scientific context.

Materials and Methods: The description should be brief but with sufficient detail to enable others to reproduce the experiments. Procedures that have been published previously should not be described in detail but appropriate references should simply be cited. Only new and significant modifications of previously published procedures require complete description. Names of products and manufacturers with their locations (city and state/country) should be given and sources of animals and cell lines should always be indicated. All clinical investigations must have been conducted in accordance with Declaration of Helsinki principles. All human and animal studies must have been approved by the appropriate institutional review board(s) and a specific declaration of approval must be made within this section.

Results: The description of the experimental results should be succinct but in sufficient detail to allow the experiments to be analyzed and interpreted by an independent reader. If necessary, subheadings may be used for an orderly presentation. All figures and tables must be referred to in the text.

Discussion: The data should be interpreted concisely without repeating material already presented in the Results section. Speculation is permissible, but it must be well-founded, and discussion of the wider implications of the findings is encouraged. Conclusions derived from the study should be included in this section.

Acknowledgments: All funding sources should be credited in the Acknowledgments section. In addition, people who contributed to the work but who do not meet the criteria for authors should be listed along with their contributions.

References: References should be numbered in the order in which they appear in the text. Citing of unpublished results, personal communications, conference abstracts, and theses in the reference list is not recommended but these sources may be mentioned in the text. In the reference list, cite the names of all authors when there are fifteen or fewer authors; if there are sixteen or more authors, list the first three followed by *et al*. Names of journals should be abbreviated in the style used in PubMed. Authors are responsible for the accuracy of the references. Examples are given below:

Example 1 (Sample journal reference):
Nakata M, Tang W. Japan-China Joint Medical Workshop on Drug Discoveries and Therapeutics 2008: The need of Asian pharmaceutical researchers' cooperation. Drug Discov Ther. 2008; 2:262-263.

Example 2 (Sample journal reference with more than 15 authors):
Darby S, Hill D, Auvinen A, *et al*. Radon in homes and risk of lung cancer: Collaborative analysis of individual data from 13 European case-control studies. BMJ. 2005; 330:223.

Example 3 (Sample book reference):
Shalev AY. Post-traumatic stress disorder: Diagnosis, history and life course. In: Post-traumatic Stress Disorder, Diagnosis, Management and Treatment (Nutt DJ, Davidson JR, Zohar J, eds.). Martin Dunitz, London, UK, 2000; pp. 1-15.

Example 4 (Sample web page reference):
World Health Organization. The World Health Report 2008 – primary health care: Now more than ever. *http://www.who.int/whr/2008/whr08_en.pdf* (accessed September 23, 2010).

Tables: All tables should be prepared in Microsoft Word or Excel and should be arranged at the end of the manuscript after the References section. Please note that tables should not in image format. All tables should have a concise title and should be numbered consecutively with Arabic numerals. If necessary, additional information should be given below the table.

Figure Legend: The figure legend should be typed on a separate page of the main manuscript and should include a short title and explanation. The legend should be concise but comprehensive and should be understood without referring to the text. Symbols used in figures must be explained.

Figure Preparation: All figures should be clear and cited in numerical order in the text. Figures must fit a one- or two-column format on the journal page: 8.3 cm (3.3 in.) wide for a single column, 17.3 cm (6.8 in.) wide for a double column; maximum height: 24.0 cm (9.5 in.). Please make sure that artwork files are in an acceptable format (TIFF or JPEG) at minimum resolution (600 dpi for illustrations, graphs, and annotated artwork, and 300 dpi for micrographs and photographs). Please provide all figures as separate files. Please note that low-resolution images are one of the leading causes of article resubmission and schedule delays. All color figures will be reproduced in full color in the online edition of the journal at no cost to authors.

Units and Symbols: Units and symbols conforming to the International System of Units (SI) should be used for physicochemical quantities. Solidus notation (*e.g.* mg/kg, mg/mL, mol/mm^2/min) should be used. Please refer to the SI Guide www.bipm.org/en/si/ for standard units.

Supplemental data: Supplemental data might be useful for supporting and enhancing your scientific research and Drug Discoveries & Therapeutics accepts the submission of these materials which will be only published online alongside the electronic version of your article. Supplemental files (figures, tables, and other text materials) should be prepared according to the above guidelines, numbered in Arabic numerals (*e.g.*, Figure S1, Figure S2, and Table S1, Table S2) and referred to in the text. All figures and tables should have titles and legends. All figure legends, tables and supplemental text materials should be placed at the end of the paper. Please note all of these supplemental data should be provided at the time of initial submission and note that the editors reserve the right to limit the size and length of Supplemental Data.

5. Submission Checklist

The Submission Checklist will be useful during the final checking of a manuscript prior to sending it to Drug Discoveries & Therapeutics for review. Please visit Download Centre and download the Submission Checklist file.

6. Online submission

Manuscripts should be submitted to Drug Discoveries & Therapeutics online at http://www.ddtjournal.com. The manuscript file should be smaller than 5 MB in size. If for any reason you are unable to submit a file online, please contact the Editorial Office by e-mail at office@ddtjournal.com

7. Accepted manuscripts

Proofs: Galley proofs in PDF format will be sent to the corresponding author *via* e-mail. Corrections must be returned to the editor (proof-editing@ddtjournal.com) within 3 working days.

Offprints: Authors will be provided with electronic offprints of their article. Paper offprints can be ordered at prices quoted on the order form that accompanies the proofs.

Page Charge: A page charge of $140 will be assessed for each printed page of an accepted manuscript. The charge for printing color figures is $340 for each page. Under exceptional circumstances, the author(s) may apply to the editorial office for a waiver of the publication charges at the time of submission.

(Revised February 2013)

Editorial and Head Office:

Pearl City Koishikawa 603
2-4-5 Kasuga, Bunkyo-ku
Tokyo 112-0003
Japan
Tel: +81-3-5840-9697
Fax: +81-3-5840-9698
E-mail: office@ddtjournal.com

DD&T
Drug Discoveries & Therapeutics

JOURNAL PUBLISHING AGREEMENT (JPA)

Manuscript No.:

Title:

Corresponding author:

The International Advancement Center for Medicine & Health Research Co., Ltd. (IACMHR Co., Ltd.) is pleased to accept the above article for publication in Drug Discoveries & Therapeutics. The International Research and Cooperation Association for Bio & Socio-Sciences Advancement (IRCA-BSSA) reserves all rights to the published article. Your written acceptance of this JOURNAL PUBLISHING AGREEMENT is required before the article can be published. Please read this form carefully and sign it if you agree to its terms. The signed JOURNAL PUBLISHING AGREEMENT should be sent to the Drug Discoveries & Therapeutics office (Pearl City Koishikawa 603, 2-4-5 Kasuga, Bunkyo-ku, Tokyo 112-0003, Japan; E-mail: office@ddtjournal.com; Tel: +81-3-5840-9697; Fax: +81-3-5840-9698).

1. Authorship Criteria

As the corresponding author, I certify on behalf of all of the authors that:

1) The article is an original work and does not involve fraud, fabrication, or plagiarism.
2) The article has not been published previously and is not currently under consideration for publication elsewhere. If accepted by Drug Discoveries & Therapeutics, the article will not be submitted for publication to any other journal.
3) The article contains no libelous or other unlawful statements and does not contain any materials that infringes upon individual privacy or proprietary rights or any statutory copyright.
4) I have obtained written permission from copyright owners for any excerpts from copyrighted works that are included and have credited the sources in my article.
5) All authors have made significant contributions to the study including the conception and design of this work, the analysis of the data, and the writing of the manuscript.
6) All authors have reviewed this manuscript and take responsibility for its content and approve its publication.
7) I have informed all of the authors of the terms of this publishing agreement and I am signing on their behalf as their agent.

2. Copyright Transfer Agreement

I hereby assign and transfer to IACMHR Co., Ltd. all exclusive rights of copyright ownership to the above work in the journal Drug Discoveries & Therapeutics, including but not limited to the right 1) to publish, republish, derivate, distribute, transmit, sell, and otherwise use the work and other related material worldwide, in whole or in part, in all languages, in electronic, printed, or any other forms of media now known or hereafter developed and the right 2) to authorize or license third parties to do any of the above.

I understand that these exclusive rights will become the property of IACMHR Co., Ltd., from the date the article is accepted for publication in the journal Drug Discoveries & Therapeutics. I also understand that IACMHR Co., Ltd. as a copyright owner has sole authority to license and permit reproductions of the article.

I understand that except for copyright, other proprietary rights related to the Work (*e.g.* patent or other rights to any process or procedure) shall be retained by the authors. To reproduce any text, figures, tables, or illustrations from this Work in future works of their own, the authors must obtain written permission from IACMHR Co., Ltd.; such permission cannot be unreasonably withheld by IACMHR Co., Ltd.

3. Conflict of Interest Disclosure

I confirm that all funding sources supporting the work and all institutions or people who contributed to the work but who do not meet the criteria for authors are acknowledged. I also confirm that all commercial affiliations, stock ownership, equity interests, or patent-licensing arrangements that could be considered to pose a financial conflict of interest in connection with the article have been disclosed.

Corresponding Author's Name (Signature):

Date: